

11-14-2007

# Surface Mean Flow and Turbulence Structure in Tropical Cyclone Winds

Bo Yu

*Florida International University*, [enviyub2@hotmail.com](mailto:enviyub2@hotmail.com)

**DOI:** 10.25148/etd.FI08081552

Follow this and additional works at: <https://digitalcommons.fiu.edu/etd>

---

## Recommended Citation

Yu, Bo, "Surface Mean Flow and Turbulence Structure in Tropical Cyclone Winds" (2007). *FIU Electronic Theses and Dissertations*. 25.  
<https://digitalcommons.fiu.edu/etd/25>

This work is brought to you for free and open access by the University Graduate School at FIU Digital Commons. It has been accepted for inclusion in FIU Electronic Theses and Dissertations by an authorized administrator of FIU Digital Commons. For more information, please contact [dcc@fiu.edu](mailto:dcc@fiu.edu).

FLORIDA INTERNATIONAL UNIVERSITY

Miami, Florida

SURFACE MEAN FLOW AND TURBULENCE STRUCTURE  
IN TROPICAL CYCLONE WINDS

A dissertation submitted in partial fulfillment of the

requirements for the degree of

DOCTOR OF PHILOSOPHY

in

CIVIL ENGINEERING

by

Bo Yu

2007

To: Interim Dean Amir Mirmiran  
College of Engineering and Computing

This dissertation, written by Bo Yu, and entitled Surface Mean Flow and Turbulence Structure in Tropical Cyclone Winds, having been approved in respect to style and intellectual content, is referred to you for judgment.

We have read this dissertation and recommend that it be approved.

---

Fang Zhao

---

Emil Simiu

---

Amir Mirmiran

---

George S. Dulikravich

---

Forrest James Masters

---

Arindam Gan Chowdhury, Major Professor

Date of Defense: November 14, 2007

The dissertation of Bo Yu is approved.

---

Interim Dean Amir Mirmiran  
College of Engineering and Computing

---

Dean George Walker  
University Graduate School

Florida International University, 2007

© Copyright 2007 by Bo Yu

All rights reserved.

## ACKNOWLEDGMENTS

I would like to thank my dissertation committee members: Dr. Fang Zhao, Dr. Emil Simiu, Dr. Amir Mirmiran, Dr. George Dulikravich, Dr. Forrest Masters, and Dr. Arindam Chowdhury, for their firm guidance and direction.

I highly appreciate my committee member Professor Fang Zhao's constant support and encouragement during the entire course of my graduate study at Florida International University. Getting her positive attitude toward life is a gift I hope to carry with me throughout my life.

Dr. Emil Simiu deserves thanks for his advising ability. I sincerely appreciate his involvement and participation throughout my work. I am grateful for his valuable discussions, suggestions and reviews. His expertise and valuable guidance in wind engineering helped me in seeking to achieve the best possible results in my research.

I thank Dr. Amir Mirmiran and Dr. George Dulikravich for serving on my committee and evaluating my research efforts, in spite of their extremely busy schedules.

Dr. Forrest Masters was particularly helpful in guiding me while learning techniques for analyzing stochastic signals and in providing hurricane wind data from the Florida Coastal Monitoring Program (FCMP). I deeply thank Dr. Masters for learning so much from him, and for financial support while I faced a major unforeseen crisis in 2005. I would like to thank Dr. Masters for aiding my early dissertation work.

Special thanks go to my major professor, Dr. Arindam Gan Chowdhury. He had confidence in my abilities to not only complete a degree, but to do so in a way that would significantly advance the state of the art. The discussions I had with Dr. Chowdhury were a great source of learning for me. I am truly thankful for his patience, support and

valuable career advice. I could not have completed this research without his support and help.

I wish to acknowledge with thanks the Department of Civil and Environmental Engineering, Florida International University, and Dr. Stephen Leatherman and Mrs. Carolyn Robertson, International Hurricane Research Center, for financial support.

I would like to thank the following Florida University colleagues for their assistance at various levels of my research: Ivan Canino, Jimmy Erwin, Roy Liu, Collette Blessing, Walter Conklin, Steven Hungler, Phil Gonzalez, Natalie Defraene, and Donya Bernard. Thank you for making this experience in Miami such an unforgettable time.

I would also like to take to thank Dr. Zhenmin Chen in Department of Statistics at Florida International University and Dr. Wolfgang Rogge in University of California, Merced for their valuable help.

Finally, my deep thanks go to my family for their constant love and support.

ABSTRACT OF THE DISSERTATION  
SURFACE MEAN FLOW AND TURBULENCE STRUCTURE  
IN TROPICAL CYCLONE WINDS

by

Bo Yu

Florida International University, 2007

Miami, Florida

Professor Arindam Gan Chowdhury, Major Professor

Hurricanes are one of the deadliest and costliest natural hazards affecting the Gulf coast and Atlantic coast areas of the United States. An effective way to minimize hurricane damage is to strengthen structures and buildings. The investigation of surface level hurricane wind behavior and the resultant wind loads on structures is aimed at providing structural engineers with information on hurricane wind characteristics required for the design of safe structures. Information on mean wind profiles, gust factors, turbulence intensity, integral scale, and turbulence spectra and co-spectra is essential for developing realistic models of wind pressure and wind loads on structures. The research performed for this study was motivated by the fact that considerably fewer data and validated models are available for tropical than for extratropical storms.

Using the surface wind measurements collected by the Florida Coastal Monitoring Program (FCMP) during hurricane passages over coastal areas, this study presents comparisons of surface roughness length estimates obtained by using several estimation methods, and estimates of the mean wind and turbulence structure of hurricane winds over coastal areas under neutral stratification conditions. In addition, a program has been

developed and tested to systematically analyze Wall of Wind (WoW) data, that will make it possible to perform analyses of baseline characteristics of flow obtained in the WoW. This program can be used in future research to compare WoW data with FCMP data, as gust and turbulence generator systems and other flow management devices will be used to create WoW flows that match as closely as possible real hurricane wind conditions.

Hurricanes are defined as tropical cyclones for which the maximum 1-minute sustained surface wind speeds exceed 74 mph. FCMP data include data for tropical cyclones with lower sustained speeds. However, for the winds analyzed in this study the speeds were sufficiently high to assure that neutral stratification prevailed. This assures that the characteristics of those winds are similar to those prevailing in hurricanes. For this reason in this study the terms tropical cyclones and hurricanes are used interchangeably.

## TABLE OF CONTENTS

CHAPTER	PAGE
I. GENERAL INTRODUCTION .....	1
1. Hurricane Hazards .....	1
2. Current Surface Wind Measuring System .....	2
3. Current Observations on Cyclone Flow.....	4
4. Thesis Organization .....	5
References.....	7
II. EVALUATION OF METHODS FOR ESTIMATING SURFACE ROUGHNESS LENGTHS OVER COASTAL AREAS DURING HURRICANE PASSAGES .....	9
Abstract.....	9
1. Introduction.....	10
2. Surface Roughness Length Estimation Methods .....	11
3. Hurricane Wind Data Measurements.....	18
4. Estimation of Surface Roughness Lengths and Other Parameters .....	19
5. Conclusions.....	24
Appendix A. Comparison of Two Methods for Estimating Friction Velocity .....	26
Table Captions .....	27
Figure Captions.....	27
References.....	28
III. GUST FACTORS AND TURBULENCE INTENSITIES FOR HURRICANE WINDS .....	40
Abstract.....	40
1. Introduction.....	40
2. Methods for Gust Factor and Turbulence Intensity Estimation.....	43
3. Hurricane Wind Data Measurements.....	44
4. Basic Mean Wind Characteristics.....	46
5. Estimation of Surface Roughness Lengths .....	47
6. Estimation and Comparison of Normalized Standard Deviation.....	49
7. Peak Factor Estimation and Comparisons .....	51
8. Gust Factor Estimation, Comparisons, and Variability .....	51
9. Conclusions.....	56
Appendix A. Corrections to Gust Factor Estimates.....	58
Table Captions .....	61
Figure Captions.....	61
References.....	62

IV. HURRICANE WIND POWER SPECTRA, CO-SPECTRA, AND INTEGRAL LENGTH SCALES.....	79
Abstract.....	79
1. Introduction.....	79
2. Turbulence on the Micrometeorological Scale: Fundamentals.....	81
3. Hurricane Wind Data Measurements.....	83
4. Basic Mean Wind Speeds .....	85
5. Estimation of Surface Roughness Lengths .....	86
6. Estimation of Integral Length Scales.....	87
7. Power Spectra and Co-Spectra: Estimation and Variability .....	89
8. Conclusions.....	94
Appendix A. Coefficients of Power Spectra and Cospectra of Hurricane Winds Based on FCMP Dataset.....	95
Table Captions .....	97
Figure Captions.....	97
Reference .....	98
V. WALL OF WIND .....	116
Abstract.....	116
1. Wall of Wind Facility .....	116
2. System Control and Data Acquisition .....	117
3. Program Development and Example .....	119
4. Conclusions.....	120
Appendix A. Basic Formulas.....	121
Appendix B. Time Histories of the Wind from WoW Experiments .....	124
Table Captions .....	125
Figure Captions.....	125
References.....	126
VI. GENERAL CONCLUSIONS AND FUTURE WORK.....	136
1. General Conclusions.....	136
2. Recommendations for Future Research.....	140
VITA.....	141

## LIST OF NOTATIONS AND ACRONYMS

$A, B, \alpha, \beta$	coefficients and exponents for power spectral and co-spectral equations
$C_D$	drag coefficient
$C_{uw}$	$u$ - $w$ co-spectrum
$Cov_{uv}$	$u$ - $v$ covariance
$E[ ]$	expected value
$f$	reduced frequencies
$GF$	gust factor
$g$	peak factor
$h$	structure height
$k$	wave number ( $k = 2\pi/\lambda$ )
$L_a^i$	integral length scale of turbulence, ( $i = x, y, z, \quad a = u, v, w$ )
$N$	sample size ( $N = T/t$ )
$n$	Frequency
$p_i, q_i$	coefficients for power spectra and co-spectra ( $i = 1, 2, 3$ )
$R_{aa}$	correlation (covariance) function ( $a = u, v, w$ )
$S_{aa}$	power spectra ( $a = u, v, w$ )
$T$	record length
$t$	gust duration
$TI_a$	turbulence intensity of wind component ( $a = u, v, w$ )
$U, V, W$	mean values of the longitudinal, lateral and vertical wind component
$u, v, w$	longitudinal, lateral and vertical wind components
$u', v', w'$	longitudinal, lateral, and vertical wind fluctuation components
$u_{\max}$	maximum wind speed
$u_z$	horizontal mean wind speed at the height $z$
$u_*$	friction velocity
$x$	fetch distance upwind from the location of interest
$z$	observational heights

$z_d$	displacement distance
$z_0$	surface roughness length
$z_{0rougher}$	surface roughness length over the rougher upwind terrain
$\varepsilon$	energy dissipation rate
$\tau$	time lag
$\lambda$	wave length
$\kappa$	von Karman constant (0.4)
$\varphi$	Kolmogorov constant
$\sigma_a$	standard deviation of wind component, ( $a = u, v, w$ )
$\rho_{aa}$	autocorrelation coefficient functions, ( $a = u, v, w$ )
$\sqrt{\beta}$	ratio of $\sigma_u$ to friction velocity $u_*$
$\delta(x)$	height of an internal boundary layer

ASCE	American Society of Civil Engineers
ASOS	Automated Surface Observing Systems
CW	clockwise
CCW	counter-clockwise
FCMP	Florida Coastal Monitoring Program
FFT	Fast Fourier Transforms
FIU	Florida International University
FSU	flat, smooth and uniform terrain.
IBL	internal boundary layer
IHRC	International Hurricane Research Center
OBL	outer boundary layer
RR	roughness regimes
TKE	turbulent kinetic energy
WoW	Wall of Wind

# **I. GENERAL INTRODUCTION**

## **1. Hurricane Hazards**

Hurricanes are one of the deadliest and costliest natural hazards affecting the Gulf coast and Atlantic coast areas of the United States. The high winds, severe storm surges, and inland floods resulting from torrential rains are primary causes of hurricane-induced loss of life and property damage. For example, Hurricane Katrina in 2005 initially impacted the United States as a Saffir-Simpson Category 1 storm near Miami, Florida, then as a Category 4 storm along the eastern Louisiana-western Mississippi coastlines, resulting in severe storm surge damage along the Louisiana-Mississippi-Alabama coasts, wind damage, and the failure of parts of the levee system in New Orleans (Lott and Ross, 2006). Hurricane Katrina killed at least 1500 people and was responsible for at least 81 billion dollars of property damage. These impacts make Katrina the costliest hurricane in U.S. history and one of the five deadliest hurricanes to ever strike the United States (Blake et. al., 2007).

According to the United States Census Bureau, coastal population within the Southeast region increased 58 percent between 1980 and 2003. Florida shows the greatest percent population change between 1980 and 2003, reaching nearly 75 percent (Crossett et. al., 2004). The rising coastal population has increased the potential damage and loss of life inflicted by hurricanes in the United States.

The effort to reduce hurricane damage is of particular importance in coastal areas vulnerable to extreme wind events. An effective way to minimize hurricane damage is to strengthen structures and buildings. Structural engineers need information of hurricane wind characteristics to design safe structures in hurricane-prone areas (Peterka et al.,

1996). The investigation of surface level hurricane wind behavior and the resultant wind loads on low-rise structures is necessary for this reason. Gust factor, turbulence intensity and integral scale are important factors for evaluating the wind pressure and wind loads on structures (Kareem et al. 1987; Li and Melbourne, 1995, 1999; Ahmad et al. 1997; Nakamura et al. 1998). For example, the turbulence within an incoming flow will affect the separation and reattachment points of the flow around a bluff body and, consequently, the pressures and wind loads acting on the body. Therefore, there is a strong interest in improved knowledge of hurricane wind characteristics and turbulence structure.

## **2. Current Surface Wind Measuring System**

There are various platforms to measure the surface level wind velocities in United States. Automated Surface Observing System (ASOS) operated by National Weather Service (NWS) is one of the primary sources for surface wind measurement. Nearly all ASOS stations are located at airports. At offshore and coastal sites, National Data Buoy Center (NDBC) sets the data buoys and Coastal Marine Automated Network (C-MAN) to obtain information of surface wind conditions (Sparks, 2003).

Although these stations provide useful information for weather forecast and assessment of flight conditions, they are not reliable under strong wind conditions even if one station happens to be in the path of the cyclone. The system often breaks down during the evacuation process, and due to loss of electrical power support or destruction by windborne debris. It can therefore not provide wind engineers with reliable, continuous, high resolution data on surface wind velocities during extreme wind events.

In addition to the surface wind measuring stations, reconnaissance aircraft flying at upper level provide measurements to determine conditions in tropical cyclones. The National Hurricane Center (NHC) assumes that maximum sustained winds averaged over 1-min at 10m above the surface are 90% of the speeds measured at 700 mb, 80 % of those at 850mb, and 85% of those measured at 450m (Pasch et al., 1999). However, this is only a rough assumption estimates of wind speeds based on it are unreliable.

Wind data were also collected by fixed instrumented towers (Tamura et al., 1993; Xu et al., 2001). Since the fixed instrumented towers cannot be moved, only those instrumented towers that happen to be in the path of the cyclone can provide wind data.

Recently, two university research programs, the Wind Engineered Mobile Tower Experiment (WEMITE) and the Florida Coastal Monitoring Program (FCMP), have provided a powerful way to collect wind data during hurricane passage. Sponsored by the Florida Department of Community Affairs, FCMP is focusing on investigating surface-level hurricane wind behavior and the resultant loads on low-rise structures (Masters, 2004).

The FCMP measuring system for the analysis of surface wind characteristics and turbulence structures has the following features: (1) sampling rate of 10 Hz, which is high enough to capture dynamic wind effects; (2) mobile instrumented towers over various terrains provide the opportunity to investigate the effect of effective roughness length on wind characteristics; (3) multi-level of measurement for each tower makes it possible to investigate the variations of some parameters with height; (4) simultaneous measurements from three or four towers during the same cyclone passage provide the opportunity to analyze spatial correlations.

### 3. Current Observations on Cyclone Flow

Increasing evidence indicates that the wind characteristics and turbulence behavior within tropical cyclones flow differ from those of non-cyclone flows.

According to Tamura et al. (1993) and Sharma et al. (1999), values of gust factor and turbulence intensity associated with tropical cyclone winds are higher than those associated with non-cyclone winds. Sharma et al. (1999) also showed that the wind turbulence energy spectrum of tropical cyclone winds is not be adequately described by the Engineering Sciences Data Unit (ESDU) model.

Xu et al. (2001) showed that horizontal turbulence intensities of strong typhoon winds were significantly higher than those from seasonal trade winds. Using three-elevation wind data (9, 15 and 25 m respectively) from a marine tower, Smedman et al. (2003) showed that the wind spectrum, particularly in the low-frequency portion, differed considerably from the standard reference data from the Kansas experiment (Kaimal et al. 1972), when the waves gradually changed from pure wind seas to strong swell under near-neutral atmospheric conditions.

Based on the high resolution wind speed data from Wind Engineering Mobile Instrumented Tower Experiment (WEMITE), Schroeder and Smith (2003) have observed higher wind gust factors during one hurricane passage in United States. For that hurricane passage they also found that there was more low-frequency energy in the longitudinal power spectral density (PSD) than indicated by spectral models for non-hurricane winds, for example the Kaimal model (Kaimal et al., 1972) based on the Kansas experiment or the Tieleman flat-smooth-uniform (FSU) model (Tieleman, 1995).

While much research has been performed on turbulence structure, knowledge of wind turbulence features in hurricanes, particularly those affecting the Gulf and Atlantic coasts, is still incomplete. The major reason for this state of affairs is that few reliable wind data obtained during cyclone passages were available. Owing to the availability of FCMP data a thorough investigation of hurricane wind speed records became possible, and is the focus of this study.

#### **4. Thesis Organization**

The current dissertation presents results of hurricane wind speeds analyses with a view to improving current understanding of their gust factors, turbulence intensities, turbulence spectra and co-spectra, and integral turbulence scales. The dissertation presents information on the Wall of Wind (WoW) in its current stage of development and the data acquisition system.

Chapter 2 presents a comparison of surface roughness length estimates obtained by using several estimation methods. This chapter also estimates surface drag coefficients over coastal areas under strong hurricane winds. In this chapter, the fetch over which the surface roughness may be considered to be uniform for the angular sector being considered is sufficiently long that the logarithmic law may be applied at least up to the elevations at which the wind measurements were performed.

Chapter 3 presents the estimated peak gust factors of hurricane wind speeds over sea surface and open flat terrain in coastal areas. The estimates are affected by errors due to the anemometer response characteristics, which are such that high-frequency components of the turbulence are filtered out. These errors are estimated in the Appendix

to this chapter. In addition, this chapter presents results on the effect on the magnitude of the gust factor of observational height, wind speed, and surface roughness length. Finally, the study presents FCMP-based estimates of turbulence intensities and their variability.

Chapter 4 presents estimates of power spectra and co-spectra, and of integral length scales for hurricane wind speeds over sea surface and over open flat terrain in coastal areas. In addition, Chapter 4 also examines the variability of the turbulent flow features from hurricane to hurricane or, within the same hurricane, from record to record. This information is needed for structural reliability studies.

Chapter 5 presents information on the 6-fan Phase II Wall of Wind (WoW) in its current stage of development and the data acquisition system.

Chapter 6 presents the general conclusions of this work and recommendations for future research.

## References

- Ahmad, S., Islam, N., Ali, A., 1997. Wind-induced response of a tension leg platform, *Journal of Wind Engineering and Industrial Aerodynamics* 72, 225-240.
- Blake, E. S., Rappaport, E. N., Landsea, C. W., 2007. The Deadliest, Costliest, and Most Intense United States Tropical Cyclones from 1851 to 2006 (and Other Frequently Requested Hurricane Facts). *NOAA Tech. Memo NWS TPC-5*.
- Crossett, K. M., Culliton, T. J., Wiley, P. C., Goodspeed, T. R., 2004. *Population Trends Along the Coastal United States, 1980-2008*, National Oceanic and Atmospheric Administration Coastal Trends Report Series.
- Kaimal, J. C., Wyngaard, I. Y., Coté O. R., 1972. Spectral Characteristics of Surface-Layer Turbulence, *Quart. J. Roy. Meteorol. Soc.* 98, 563–598.
- Kareem, A., 1987. *Journal of Wind Engineering and Industrial Aerodynamics* 30, 233-241.
- Li, Q. S., Melbourne, W. H., 1995. An experimental investigation of the effects of free-stream turbulence on streamwise surface pressures in separated and reattaching flows. *Journal of Wind Engineering and Industrial Aerodynamics* 51–52, 313–323.
- Li, Q. S., Melbourne, W. H., 1999. The effects of large scale turbulence on pressure fluctuations in separated and reattaching flows, *Journal of Wind Engineering and Industrial Aerodynamics* 83, 159–169.
- Lott, N., Ross, T., 2006. Tracking and evaluating U.S. billion dollar weather disasters, 1980-2005. *Forum on Environmental Risk and Impacts on Society: Successes and Challenges*, American Meteorological Society.
- Masters, F. J., 2004. Measurement, modeling and simulation of ground-level tropical cyclone winds. PhD dissertation, University of Florida.
- Nakamura, Y., Ohya, Y., Ozono, S., 1988. *Journal of Wind Engineering and Industrial Aerodynamics* 28, 251-259.
- Pasch, R. J., Kimberlain, T. B., Stewart, S. R., 1999. Hurricane Floyd 7–17 September, 1999. Preliminary Report, National Hurricane Center, Miami.
- Peterka, J. A., Cochran, L. S., Pielke, R. A. Nicholls, M.E., 1996. Progress in Modeling External Flows Around Buildings, American Society of Mechanical Engineers, Fluids Division Summer Meeting, San Diego, California, USA, July 7- 11.
- Schroeder, J. L., Smith, D. A., 2003. Hurricane Bonnie wind flow characteristics as determined from WEMITE, *Journal of Wind Engineering and Industrial Aerodynamics* 91, 767–789.

- Sharma, R. N., Richards, P. J., 1999. A re-examination of the characteristics of tropical cyclone winds. *Journal of Wind Engineering and Industrial Aerodynamics* 83, 21-33.
- Smedman, A. S., Högström, U., Sjöblom, A., 2003. A Note on Velocity Spectra in the Marine Boundary Layer, *Boundary-Layer Meteorology* 109, 27–48.
- Sparks, P. R., 2003. Wind speeds in tropical cyclones and associated insurance losses, *Journal of Wind Engineering and Industrial Aerodynamics* 91, 1731-1751.
- Tamura, Y., Shimada, K., Hibi, K., 1993. Wind response of a tower (typhoon observation at the Nagasaki Huis Ten Bosch Domtoren), *Journal of Wind Engineering and Industrial Aerodynamics* 50, 309-318.
- Tieleman, H. W., 1995. Universality of velocity spectra, *Journal of Wind Engineering and Industrial Aerodynamics* 56, 55-69.
- Xu, Y., Pan, Y., Sun A., 1997. Spectral Characteristics and Multi-Scale Structure of the Boundary-Layer Wind Field during Cold Front Passages Over East China, *Boundary-Layer Meteorology* 85: 423–446.
- Xu, Y. L., Zhan, S., 2001. Field measurements of Di Wang Tower during Typhoon York, *Journal of Wind Engineering and Industrial Aerodynamics* 89, 73-93.

## II. EVALUATION OF METHODS FOR ESTIMATING SURFACE ROUGHNESS LENGTHS OVER COASTAL AREAS DURING HURRICANE PASSAGES

A Paper submitted to the Journal of Wind Engineering and Industrial Aerodynamics

Bo Yu<sup>a</sup>, Arindam Gan Chowdhury<sup>b</sup>, and Forrest James Masters<sup>c</sup>

### Abstract

Using high-resolution surface hurricane wind data collected over coastal areas by the Florida Coastal Monitoring Program (FCMP), a comparison is presented of surface roughness lengths estimates obtained by using several estimation methods. The wind directions being considered are those for which the fetch is sufficiently long that the logarithmic law is applicable up to at least the elevations at which the wind speed measurements were performed. The accuracy of the various methods was evaluated in light of the estimates being obtained. This study also estimates surface drag coefficients for hurricane wind conditions over coastal terrains.

**KEYWORDS:** Surface roughness length; Drag coefficient; Coastal area;

Hurricane wind speeds

---

<sup>a</sup> Grad. Research Assistant, Dept. of Civil and Environmental Engineering, Florida International University, Miami, Florida, USA

<sup>b\*</sup> Author for correspondence, Assistant Prof., Dept. of Civil and Environmental Engineering, Florida International University, Miami, Florida, USA

<sup>c</sup> Assistant Prof., Dept. of Civil and Coastal Engineering, University of Florida, Gainesville, Florida, USA.

## 1. Introduction

In wind engineering applications, surface roughness estimates are required for the accurate estimation of mean wind profiles and turbulence characteristics such as gust factors, turbulence intensity, turbulent integral length scales, and power spectra (Barlow et al., 1999). Such estimates are also needed for the simulation of wind flows in the laboratory. The Jensen number, that is, the ratio of the structure height  $h$  to the surface roughness length  $z_0$ , is one of the principal scaling parameters in wind tunnel modeling (Bottema, 1996). Based on wind tunnel data and analytical modeling, Bottema (1996) investigated local diffusion properties as functions of urban terrain roughness with a view to achieving street design (i.e., configuration of and spacing between buildings) resulting in optimal air pollutant removal properties. MacDonald et al. (1998) developed an improved method for the estimation of surface roughness length corresponding to obstacle arrays in the wind tunnel. The model accounts for the dependence of roughness on type of array. Using standing sticks for modeling standing vegetation, Dong et al. (2001) measured wind velocity distributions above vegetation-covered surfaces in wind tunnel, and derived from them drag coefficients and roughness lengths, as well as relations between these parameters and the structural parameters of standing vegetation.

Roughness analyses based on three-year field observations were presented by Barthelmie et al. (1993). These researchers compared sets of roughness lengths for the same site using various methods, and found that the respective roughness length estimates exhibited considerable variations. Indeed, as roughness estimation methods are still under development, no one method can be considered as definitive (Wieringa, 1993;

Grimmond et al., 1998). In the present state of the art an evaluation of existing methods is therefore needed. Such an evaluation is presented in this work.

Since 1998, the Florida Coastal Monitoring Program (FCMP) has collected high resolution (10 Hz) wind data during hurricane passages (Masters, 2004). FCMP is focusing on investigating surface level hurricane wind behavior and the resultant wind loads on low-rise structures. This study uses selected FCMP surface wind measurements during hurricane passages with a view to obtaining, by a variety of methods, estimates of surface roughness lengths and drag coefficients over coastal areas under strong hurricane winds, for which it may be assumed that the stratification is neutral. The accuracy and applicability of the methods were evaluated on the basis of those estimates. In this paper, the fetch over which the surface roughness may be considered to be uniform for the angular sector being considered is sufficiently long so that the logarithmic law may be applied at least up to the elevations at which the wind measurements were performed.

## **2. Surface Roughness Length Estimation Methods**

Methods for estimating surface roughness lengths are based on (1) mean wind measurements at multiple-levels (Profile Method), (2) mean and fluctuating wind measurements at a single-level (Turbulence-Intensity Method, Friction-Velocity Method, Gust-Factor Method), (3) mean and fluctuating wind measurements at multiple-levels (Hybrid Method), or (4) morphometric information (Terrain Method). These methods are described in Sections 2.1 through 2.6 for the case of homogeneous terrain with sufficiently long fetch. Section 2.7 is concerned with the estimation of drag coefficients

and sea surface roughness lengths. Section 2.8 describes the influence of terrain roughness changes on wind characteristics.

### 2.1 Profile Method

The local surface mean wind speed is a function of the oncoming wind speed, the terrain roughness upwind of the location of interest, elevation above ground, and atmospheric stability. The mean wind profile of a homogenous and stationary flow in the surface layer under neutral stability conditions can be described by the logarithmic law,

$$\frac{u_z}{u_*} = \frac{1}{\kappa} \ln[(z - z_d)/z_0] \quad (1)$$

where,  $u_z$  is the horizontal mean wind speed at the measurement height  $z$ ,  $u_*$  is the friction velocity,  $z_0$  is the surface terrain roughness length,  $z_d$  is the displacement distance, and  $\kappa = 0.4$  is the von Karman constant. With the assumption that the logarithmic law is valid for heights  $z_1$  and  $z_2$ , Wieringa (1993) and Barthelmie et al. (1993) disregarded the displacement distance  $z_d$  (a reasonable assumption for very smooth and homogeneous surfaces), thus obtaining from Eq. (1),

$$z_0 = \exp[(u_2 \ln z_1 - u_1 \ln z_2)/(u_2 - u_1)] \quad (2)$$

It follows that the surface roughness length  $z_0$  can be determined from the mean wind speeds  $u_1$  and  $u_2$  corresponding to the two different heights  $z_1$  and  $z_2$  respectively. Wieringa (1993) pointed out that the Profile Method is very sensitive to the quality of measured wind data: a small wind measurement error will result in a large error in estimating the surface roughness length  $z_0$ .

## 2.2 Turbulence-Intensity (TI) Method

Introducing  $\sigma_u$  as the standard deviation of the longitudinal wind velocity component and rewriting Eq. (1) while disregarding the displacement distance  $z_d$ , we get

$$\frac{1}{\sigma_u / u_z} = \frac{u_*}{\kappa \cdot \sigma_u} \ln[z / z_0] \quad (3)$$

The longitudinal turbulence intensity is defined as  $I_u = \sigma_u / u_z$  and setting  $\sqrt{\beta} = \sigma_u / u_*$ , we get

$$\frac{\kappa \cdot \sqrt{\beta}}{TI_u} = \ln z - \ln z_0 \quad (4)$$

Rearranging Eq. (4),

$$z_0 = \exp(\ln z - \kappa \cdot \sqrt{\beta} / I_u) \quad (5)$$

Assuming that  $\beta$  is constant over the height throughout which the logarithmic law holds, and given  $\beta$  and the value of  $I_u$  at height  $z$ , the surface roughness length  $z_0$  can be directly determined by Eq. (5).

For a fully developed neutrally equilibrium flow within the surface layer, Lumley and Panofsky (1964) suggested that  $\sqrt{\beta}$  is independent of the underlying terrain roughness. After comparing a number of values of  $\sqrt{\beta}$  from different sites, Deaves (1981) suggested that  $\sqrt{\beta} \approx 2.79$  appears to describe adequately the fully developed equilibrium flows, i.e., flows not affected by terrain roughness changes.

### 2.3 Friction-Velocity (FV) Method

The logarithmic law defined as Eq. (1) can be rearranged to express the surface roughness length as a function of the friction velocity,

$$z_0 = z \cdot \exp(-\kappa u_z / u_*) \quad (6)$$

Thus, given the horizontal mean wind speed  $u_z$  at height  $z$ , the surface roughness length  $z_0$  can be estimated directly from the friction velocity  $u_*$  (Park et al., 2006).

The friction velocity was defined in Patil (2006) as

$$u_* = \left( \overline{u'w'}^2 + \overline{v'w'}^2 \right)^{1/4} \quad (7)$$

where  $u'$ ,  $v'$ , and  $w'$  are the longitudinal, lateral, and vertical wind fluctuation components, respectively.

For this paper, Eq. (7) was used to calculate the friction velocity which was further used to evaluate drag coefficients in Section 4.2 and surface roughness lengths in Section 4.3. Comparisons between different methods for evaluating the friction velocity using FCMP hurricane wind speed data are shown in Appendix A.

### 2.4 Gust-Factor (GF) Method

The gust factor ( $GF$ ), that is, the ratio of maximum wind speed  $u_{\max}$  to the mean wind speed  $u_z$  at the measurement height  $z$ , can be used to estimate of the terrain roughness length as follows (Wieringa, 1993):

$$z_0 = z \exp\left( -\frac{Af_T [1.42 + 0.3 \ln(-4 + 10^3 / L)]}{GF - 1 + A - f_T A} \right) \quad (8)$$

where,  $GF = u_{\max} / u_z$  and  $A$  is the attenuation of  $u_{\max}$  by anemometry. Wieringa (1993) and Barthelmie et al. (1993) proposed the value of  $A$  as 0.9 and 0.87 respectively.  $f_T$ , a factor depending on the averaging time for the mean speed, is unity for 10-minute averaging time and increases to 1.1 for hourly averaging time.  $L$  is the average wavelength of the maximum gusts and varies usually between 50 m to 100 m (Wieringa, 1993).

### 2.5 Hybrid Method

The Hybrid Method uses the non-zero displacement distance, multiple-level mean wind data, and height-invariant friction velocity. From the logarithmic law for two heights  $z_1$  and  $z_2$ , we get,

$$z_1 - z_d = \exp(\kappa u_1 / u_*) z_0 \quad (9)$$

$$z_2 - z_d = \exp(\kappa u_2 / u_*) z_0 \quad (10)$$

From Eqs. (9) and (10), we get

$$z_1 - z_2 = z_0 [\exp(\kappa u_1 / u_*) - \exp(\kappa u_2 / u_*)] \quad (11)$$

Rewriting Eq. (11),

$$z_0 = \frac{z_1 - z_2}{[\exp(\kappa u_1 / u_*) - \exp(\kappa u_2 / u_*)]} \quad (12)$$

### 2.6 Terrain Method

The Terrain Method consists of using accepted roughness values for various types of homogeneous terrain, and is the simplest way to estimate surface roughness lengths.

Its main disadvantage is that the roughness length values strongly depend on the perception of the individual observer. Wieringa (1993) compared several experimental roughness lengths for homogeneous terrains as proposed by several researchers and found that they varied significantly for the same type of terrain, and that most of the terrain roughness evaluations underestimated the actual terrain roughness lengths by a factor of about two.

In this paper, Terrain Method uses the typical values of  $z_0$  as provided by Table C6-8 in ASCE 7-05 Commentary corresponding to different exposures (suburban area, wooded area, flat open airport, water surface in hurricane prone regions) applicable to various upwind sectors for the selected FCMP towers.

## 2.7 Drag Coefficients and Sea Surface Roughness Lengths

The drag coefficient,  $C_D$ , is commonly used to describe the aerodynamic properties of wind-terrain interaction. It is defined as

$$C_D = (u_* / u_z)^2 \quad (13)$$

Using Eq. (1) and assuming zero displacement distance, we get

$$z_0 = z \exp\left(-\kappa / \sqrt{C_D}\right) \quad (14)$$

$C_D$  and  $z_0$  are interchangeable descriptions of surface terrain properties, that is,  $z_0$  can be estimated if  $C_D$  is known and vice-versa. For this paper, Eq. (13) was used to evaluate drag coefficients in Section 4.2.

Relationships between drag coefficient  $C_D$ , surface roughness length  $z_0$ , and mean wind speed  $u_z$  at the measurement height  $z = 10$  m over the sea surface under neutral

conditions were presented, among others, by Garratt (1977), Large and Pond (1982), Yelland and Taylor (1996).

### 2.8 Terrain Roughness Changes

If the upwind terrain changes at a fetch distance  $x$  upwind from the location of interest, the surface stress will change correspondingly and the logarithmic wind profile will be applicable with the local roughness only within an internal boundary layer (IBL) with a height of  $\delta(x)$ . An outer boundary layer (OBL) exists, where the air flow is not influenced by the local terrain roughness, but will be governed by the surface roughness upstream of the terrain roughness change (Panofsky and Townsend, 1964).

The estimates of whether the elevations at which the wind measurements were performed are within the IBL are based on the following model, where  $x$  denoted the upwind fetch distance and the IBL height is denoted by  $\delta(x)$ .

Wood (1982) presented a general IBL growth model for both smooth-to-rough (SR) and rough-to-smooth (RS) terrain changes under neutral conditions as,

$$\delta(x) = 0.28 z_{0\text{rougher}} \left( x / z_{0\text{rougher}} \right)^{0.8} \quad (15)$$

where  $z_{0\text{rougher}}$  is the surface roughness length over the rougher upwind terrain.

Based on Eq. (15), required upwind fetches for given IBL height of 10 m are shown in Fig. 1 as a function of surface roughness length.

## *2.9 Summary of Methods for Surface Roughness Length Estimation*

The various methods for estimating terrain roughness lengths as described above are listed in Table 1.

### **3. Hurricane Wind Data Measurements**

The current study uses high-resolution (10 Hz) surface wind data collected in real time during hurricane passages to evaluate the surface roughness lengths for different wind directions over inhomogeneous coastal terrains around the FCMP towers used for data collections. The data acquisition system measures the horizontal wind speed and direction, and the vertical wind speed at 5 m and 10 m levels.

The current study uses wind data collected during three hurricane passages, namely Hurricanes Jeanne (2004), Isabel (2003), and Floyd (1999). The three selected FCMP observation sites were in the coastal areas shown in Fig. 2. For Hurricane Jeanne (2004) the FCMP tower (named Jeanne T3) was located in Vero Beach, Florida (27°39'20.2"N – 80°24'49.0"W) in the Municipal Airport area; a rougher terrain was present 195 m upwind on the eastside. For Hurricane Isabel (2003) the FCMP tower (named Isabel T2) was deployed at the Atlantic Beach, North Carolina (34°41'54"N – 76°40'45"W), in a parking lot followed by dunes and open water located in the south-east direction. Cul-de-sac with sparse trees were located in the west and northwest. For Hurricane Floyd (1999) the FCMP tower (named Floyd T3) was deployed at Vero Beach, Florida (26°53'49"N – 80°03'47"W) and the nearest coastal line was about 500 m eastward of the observation site.

Jeanne T3 collected the surface wind from 2009 UTC on 25 September to 0709 UTC on 26 September in 2004. Isabel T2 captured the surface wind from 1530 UTC on 16 September to 0645 UTC on 19 September in 2003. Floyd T3 went operational over a period between 1930 UTC on 14 September and 1315 UTC on 15 September in 1999.

#### **4. Estimation of Surface Roughness Lengths and Other Parameters**

Wind data collected from Jeanne T3, Isabel T2, and Floyd T3, were pre-processed and only data sets satisfying quality-control requirements were used for this study. Data pre-processing and data quality-control requirements include: (1) from the available records, 7.5-min adjacent hourly segments were obtained, which were analyzed separately; (2) decomposing the wind records into the longitudinal, lateral, and vertical components; (3) 6 m/s at 10 m height was the minimum requirement for segment mean wind speed in order to satisfy the strong wind and neutral stability conditions (Wieringa, 1976); (4) eliminating segments with direction shifts larger than 20 °(Masters, 2004).

After pre-processing, the FCMP tower data were used to analyze wind parameters such as mean wind characteristics and drag coefficient as presented in Sections 4.1 and 4.2. Finally, the data were used to calculate the surface roughness lengths around the tower sites. Section 4.3 presents the estimated surface roughness lengths and compares the roughness lengths as estimated by different methods summarized in Table 1.

##### *4.1 Basic Mean Wind Characteristics*

The hourly mean wind speeds at 10 m height vary from 12.3 m/s to 28.6 m/s for Jeanne T3, from 6.0 m/s to 22.7 m/s for Isabel T2, and from 6.7 m /s to 14.0 m /s for

Floyd T3. The observed maximum wind speeds on site (3-sec gust) are 47.5 m/s, 34.5 m/s, and 24.6 m/s for Jeanne T3, Isabel T2, and Floyd T3, respectively. The mean wind speed increased with height for all three hurricanes. Trends of the mean wind speed time histories at the two different observation heights (5 m and 10 m) are very similar for each of the three tower observations. Mean wind direction time histories at the two different observation heights (5 m and 10 m) coincide for each of the three tower observations. In this paper, the wind direction is always measured clockwise from the north as shown in Fig. 2.

#### *4.2 Drag Coefficient Estimation*

The drag coefficient  $C_D$  and the surface roughness length  $z_0$  are interchangeable descriptions of surface terrain properties. Like the surface roughness length  $z_0$ , if the surface terrain is inhomogeneous around the location of interest and changes significantly with direction,  $C_D$  will also change with direction. For the 10 m level  $C_D$  values for Jeanne T3, Isabel T2, and Floyd T3 were estimated using Eq. (13) and plotted as functions of the mean wind direction as shown in Fig. 3.

$C_D$  values for Jeanne T3 were much lower than the values for Isabel T2 and Floyd T3. This can be attributed to the location of Jeanne T3 in a comparatively smoother terrain for the Municipal Airport area.  $C_D$  values change from 0.001 to 0.0027 for Jeanne T3, from 0.001 to 0.03 for Isabel T2, and from 0.005 to 0.032 for Floyd T3. The changes of  $C_D$  values correspond to the variation of surface terrain roughness as a function of azimuth around each tower.

To compare the drag coefficient values over sea surface and inland surface under strong wind conditions, the variations of  $C_D$  values with the mean wind speed over sea were estimated using various methods, as proposed by Garratt (1977), Large and Pond (1982), Yelland and Taylor (1996). The values of  $C_D$  and  $z_0$  as functions of the mean wind speed at 10 m level over sea under neutral conditions, as proposed by various researchers, are compared in Fig. 4.

For Isabel T2, the mean wind speed at 10 m level was approximately 16 m/s for the seaward direction between 290 ° to 330 °. The inland drag coefficient values for this direction as obtained from Fig. 3 range from 0.014 to 0.022. The drag coefficient value over sea surface as obtained from Fig. 4 is 0.002, corresponding to a wind speed of 16 m/s. As expected, the  $C_D$  values over the coastal land for Isabel T2 (Fig. 3) are much larger than the  $C_D$  values over the sea surface under the same wind conditions. Similar results were found for Floyd T3.

#### *4.3 Surface Roughness Length Estimation and Comparisons*

The logarithmic wind profile is applicable with the local roughness only within the IBL. In order to calculate the required fetch corresponding to the given observation height to check whether wind measurements are within the IBL, calculated required fetches and actual fetches were binned into sectors with 20 ° intervals, where sector 1 covered 350 ° to 10 °, sector 2 from 10 ° to 30 ° and so on. As  $z_0$  is needed as input for required fetch calculations as formulated by Wood (1982), estimates of  $z_0$  were obtained

by the Terrain Method. The required fetches corresponding to the observation height of 10 m for the selected FCMP tower sites were sorted by sectors and shown in Table 2.

Results show that wind measurements at 10 m elevation are within the IBL for the three selected FCMP towers (Jeanne T3, Isabel T2 and Floyd T3), except wind measurements within sectors 1, 2, 3, 4, and 18 for Isabel T2. For sectors 1, 2, 3, 4, 18 for Isabel T2, the maximum distance from the tower to the location of the terrain roughness change is approximately 100 m. The observation height of 10 m is within the OBL, since  $100\text{ m} < 125\text{ m} = 10\text{ m} \times 12.5$ , the approximate criterion suggested by Simiu and Scanlan (1996).

Based on the surface wind measurements from the FCMP towers (Jeanne T3, Isabel T2, and Floyd T3) under strong wind conditions, the surface roughness lengths around the tower site were estimated by using various methods summarized in Table 1. The surface roughness lengths for various wind directions were estimated and plotted in Figs. 5 through 7.

Fig. 5 presents the values of surface roughness lengths for Jeanne T3 as obtained by the Profile Method, Hybrid Method, Turbulence-Intensity Method, Friction-Velocity Method, and Terrain Method; Figs. 6 and 7 compare the surface roughness lengths as obtained by the Hybrid Method, Turbulence-Intensity Method, Friction-Velocity Method, and Terrain Method for Isabel T2 and Floyd T3, respectively.

For Jeanne T3, the values of the surface roughness lengths based on the Gust-Factor Method vary from 0.09m to 1.15m. These values are much higher than those estimated by using other methods, and were therefore not shown in Fig. 5. For Jeanne T3, most of the surroundings had airport terrain exposure within a radius of 500 m, as the

tower was located in the Municipal Airport area. This airport terrain exposure accounts for the estimated lower values of surface roughness lengths for Jeanne T3 as compared to those for Isabel T2 and Floyd T3 (Figs. 5, 6, 7). For Jeanne T3, the Turbulence-Intensity Method and the Hybrid Method yielded large values of surface roughness lengths between wind directions of 90 ° to 100 °, and the Profile Method yielded large values at about 90 ° (Fig. 5). These large values can be attributed to the rougher terrain 195 m upwind on the eastside of the tower Jeanne T3 (Fig. 2).

For Isabel T2, the Gust-Factor Method and the Profile Method yielded terrain roughness length values as high as 1.5 m and 1.8 m, respectively. In view of those overestimations, the values using the Gust-Factor Method and Profile Method were not shown in the plot (Fig. 6). For Isabel T2, the Turbulence-Intensity Method, the Friction-Velocity Method, and the Hybrid Method yielded two reasonable higher values of surface roughness lengths (Fig. 6) in the two directions, 220 ° and 310 °, which correspond to the rougher and longer fetches of surface terrains (Fig. 2). The Friction-Velocity Method yielded higher values for those two directions as compared to the values given by the Hybrid Method and the Turbulence-Intensity Method. The surface roughness length values given by the Turbulence-Intensity Method and the Hybrid Method are comparable in magnitude and trend. As mentioned earlier, for sectors 1, 2, 3, 4, 18 for Isabel T2, the observation height of 10 m is within the OBL. Thus, the sea surface roughness upwind of the terrain discontinuity governs the wind characteristics. Turbulence-Intensity Method, Hybrid Method, Friction-Velocity Method, when applied for these sectors, yielded low surface roughness length values (Fig. 6) that are in agreement with sea surface characteristics.

For Floyd T3, the Gust-Factor Method and the Profile Method overestimated the surface roughness lengths yielding maximum values of 3.2 m and 2.5 m, respectively, and thus the values were not shown in the plot (Fig. 7). For Floyd T3, the Turbulence-Intensity Method, the Friction-Velocity Method, and the Hybrid Method yielded large values of surface roughness lengths (Fig. 7) in the direction between 310° and 320° which corresponds to long fetches of rougher built-up terrains (Fig. 2). Surface roughness length values obtained by the Friction-Velocity Method are higher than the values obtained by the Turbulence-Intensity Method and the Hybrid Method for this sector. The three methods yielded very small values of surface roughness lengths (approximate 0.1 m) in the direction of 10° to 26° (Fig. 7), which corresponds to the direction of the upwind smoother inland surface terrain (Fig. 2).

## **5. Conclusions**

Based on the in-situ surface wind measurement data obtained from FCMP towers (Jeanne T3, Isabel T2, and Floyd T3) during three hurricane passages over the coastal areas, this study estimates the surface roughness lengths for the non-homogenous coastal terrains around the tower sites. Different methods were used and surface roughness length values were compared to assess the performances of these methods. The study also evaluated drag coefficients as obtained for these strong hurricane winds passing over the coastal terrains. The conclusions of this study are summarized below:

(1) Surface roughness lengths obtained for directionally non-homogeneous coastal terrains by using the Turbulence-Intensity Method and the Hybrid Method show good agreement both in magnitude and trend for all the towers. The Friction-Velocity Method

results are comparable to the results obtained from the two above mentioned methods except for some higher values resulting from its application to Isabel T2 and Floyd T3.

(2) Estimates based on the Gust-Factor Method are significantly larger than those obtained by the other methods and exhibit wide scatters for all the three towers. The cause for the overestimations and wide scatter is not completely understood and further investigation on the wind and turbulence characteristics (such as the gust factor) under strong hurricane winds is needed.

(3) For the airport terrain for Jeanne T3, the results from the Profile Method are comparable to those from other methods (Turbulence-Intensity Method, Hybrid Method, and Friction-Velocity Method). However, the Profile Method yielded unreasonably high values of roughness lengths for Isabel T2 and Floyd T3. This shows the sensitivity of the Profile Method to the quality of measured wind data and depicts how a probable small wind measurement error may have resulted in a large error in estimating the surface roughness length. These erroneous results obtained by the Profile Method reflect the drawbacks of this method and show agreement with the inference made by Wieringa (1993).

## **ACKNOWLEDGEMENT**

The authors gratefully acknowledge valuable suggestions and reviews by Dr. Emil Simiu of the Florida International University.

## Appendix A. Comparison of Two Methods for Estimating Friction Velocity

Two definitions of friction velocity  $u_*$  have been used in literature. Patil (2006) used the friction velocity defined as (see Eq. 7)

$$u_{*1} = \left( \overline{u'w'}^2 + \overline{v'w'}^2 \right)^{1/4} \quad (\text{A.1})$$

where  $u'$ ,  $v'$ , and  $w'$  are the longitudinal, lateral, and vertical wind fluctuation components, respectively.

Large and Pond (1982), and Grimmond et al. (1998) used the friction velocity as,

$$u_{*2} = \left( \overline{u'w'} \right)^{1/2} \quad (\text{A.2})$$

For the three selected FCMP towers (Jeanne T3, Isabel T2, Floyd T3), friction velocities were estimated using the hurricane wind speed data. The values of  $u_{*1}$  versus  $u_{*2}$  are plotted in Fig. A1. Although there are slight variations at scattered locations,  $u_{*1}$  and  $u_{*2}$  values are comparable for all the cases.

## **Table Captions**

Table 1: Summary of methods for estimating surface roughness lengths

Table 2. Required fetches and actual fetches for selected FCMP tower sites

## **Figure Captions**

Figure 1. Required upwind fetch for given height of IBL as a function of terrain roughness

Figure 2. FCMP tower sites during hurricane passages

Figure 3. Estimated drag coefficients of surface terrains around FCMP towers as functions of wind direction

Figure 4. Drag coefficient and roughness length over sea using three methods

Figure 5. Comparison of roughness length estimated by various methods at Jeanne T3

Figure 6. Comparison of roughness length estimated by various methods at Isabel T2

Figure 7. Comparison of roughness length estimated by various methods at Floyd T3

Figure A1. Comparison of two different definitions of friction velocity

## References

- American Society of Civil Engineers (ASCE) 7-05, 2006. Minimum Design Loads for Buildings and Other Structures, 319
- Barlow, J. B., Rae, W. H., Pope, A., 1999. Low Speed Wind Tunnel Testing 3rd John Wiley & Sons, P652-P656.
- Barthelmie, R. J., Palutikof, J. P., Davies, T. D., 1993. Estimation of sector roughness lengths and the effect on prediction of the vertical wind speed profile, *Boundary-Layer Meteorology* 66, 19-47.
- Bottema, M., 1996. Roughness parameters over regular rough surfaces: Experimental requirements and model validation, *Journal of Wind Engineering and Industrial Aerodynamics* 64, 249- 265.
- Deaves, D. M., 1981. Terrain-dependence of longitudinal RMS velocities in the neutral atmosphere, *Journal of Wind Engineering and Industrial Aerodynamics*, 8, 259-274.
- Dong, Z., Gao, S., Fryrear, D. W., 2001. Drag coefficients, roughness length and zero-plane displacement height as disturbed by artificial standing vegetation, *Journal of Arid Environments* 49, 485-505.
- Garratt, J. R., 1977. Review of drag coefficients over ocean and continents, *Monthly Weather Review*, 105, 915-929.
- Grimmond, C. S. B., King, T. S., Roth, M., Oke, T. R., 1998. Aerodynamic Roughness of Urban Areas Derived From Wind Observations, *Boundary-Layer Meteorology* 89: 1-24.
- Large, W. Pond, G., S., 1982. Sensible and latent heat flux measurements over the ocean, *Journal of Physical Oceanography* 12, 464-482.
- Lumley, J. L., Panofsky, H. A., 1964. The structure of atmospheric turbulence, Wiley, New York.
- MacDonald, R. W., Griffiths, R. F., Hall, D. J., 1998. An improved method for the estimation of surface roughness of obstacle arrays, *Atmospheric Environment*, Vol. 32, No. 11, 1857-1864.
- Masters, F. J., 2004. Measurement, modeling and simulation of ground-level tropical cyclone winds. PhD dissertation, University of Florida.
- Panofsky, H. A., Townsend, A. A., 1964. Change of terrain roughness and the wind profile, *Quart. J. R. Met. Soc.* 90, 147-155.

- Park, M. S., Park, S. U., 2006. Effects of topographical slope angle and atmospheric stratification on surface-layer turbulence, *Boundary-Layer Meteorology* 118, 613–633.
- Patil, M. N., 2006. Aerodynamic drag coefficient and roughness length for three seasons over a tropical western Indian station, *Atmospheric Research* 80, 280–293.
- Simiu, E., Scanlan, R., 1996. *Wind Effects on Structures*, 3rd Edition, Wiley, New York.
- Wieringa, J., 1976. An objective exposure correction method for average wind speeds measured at a sheltered location, *Quart. J. R. Met. Soc.*, 102, 241-253.
- Wieringa, J., 1993. Representative roughness parameters for homogeneous terrain. *Boundary Layer Meteorology* 63, 323–363.
- Wood, D. H., 1982. Internal boundary layer growth following a step change in surface roughness, *Boundary Layer Meteor.* 22, 241–244.
- Yelland, M. J., Taylor, P. K., 1996, Wind stress measurements from the open ocean, *Journal of Physical Oceanography* 26, 541-558.

Table 1: Summary of methods for estimating surface roughness lengths

No.	Methods	Equation	Parameters Used	Remarks
1	Profile	(2)	$u_1, u_2, z_1, z_2$	Using multiple levels of mean wind speed
2	Turbulence-Intensity (TI)	(5)	$z, \kappa, \beta, TI_u$	Using turbulence intensity
3	Friction-Velocity (FV)	(6), (7)	$z, \kappa, u_z, u', v', w'$	Using single-layer fluctuating wind
4	Gust-Factor (GF)	(8)	$A, f_T, L, GF$	Using gust factor
5	Hybrid	(12)	$u_1, u_2, z_1, z_2, u_*, \kappa$	Using two-layer mean and fluctuating wind speed
6	Terrain			Based on ASCE 7-05 Commentary

Table 2. Required fetches and actual fetches for selected FCMP tower sites

(a) Jeanne T3 (for IBL height of 10 m)

Sector No.	1	2	3	4	5	6	7
Wind direction	(-10, 10]	(10, 30]	(30, 50]	(50, 70]	(70, 90]	(90, 110]	(110, 130]
Crude $z_0$ (m)	0.3	0.3	0.3	0.3	0.3	0.3	0.3
Required fetch (m)	118	118	118	118	118	118	118
Actual fetch (m)	555	500	500	580	860	195	1390

(b) Isabel T2 (for IBL height of 10 m)

Sector No.	1	2	3	4	12	13	14	15	16	17	18
Wind direction	(-10, 10]	(10, 30]	(30, 50]	(50, 70]	(210,230]	(230,250]	(250,270]	(270,290]	(290,310]	(310,330]	(330,350]
Crude $z_0$ (m)	0.02	0.02	0.02	0.02	0.3	0.3	0.3	0.3	0.3	0.3	0.02
Required fetch (m)	232	232	232	232	118	118	118	118	118	118	232
Actual fetch (m)	100	95	90	85	430	810	1755	270	270	200	100

(c) Floyd T3 (for IBL height of 10 m)

Sector No.	1	2	16	17	18
Wind direction	(-10,10]	(10,30]	(290,310]	(310,330]	(330,350]
Crude $z_0$ (m)	0.3	0.3	0.3	0.3	0.3
Required fetch (m)	118	118	118	118	118
Actual fetch (m)	250	405	1215	1620	350

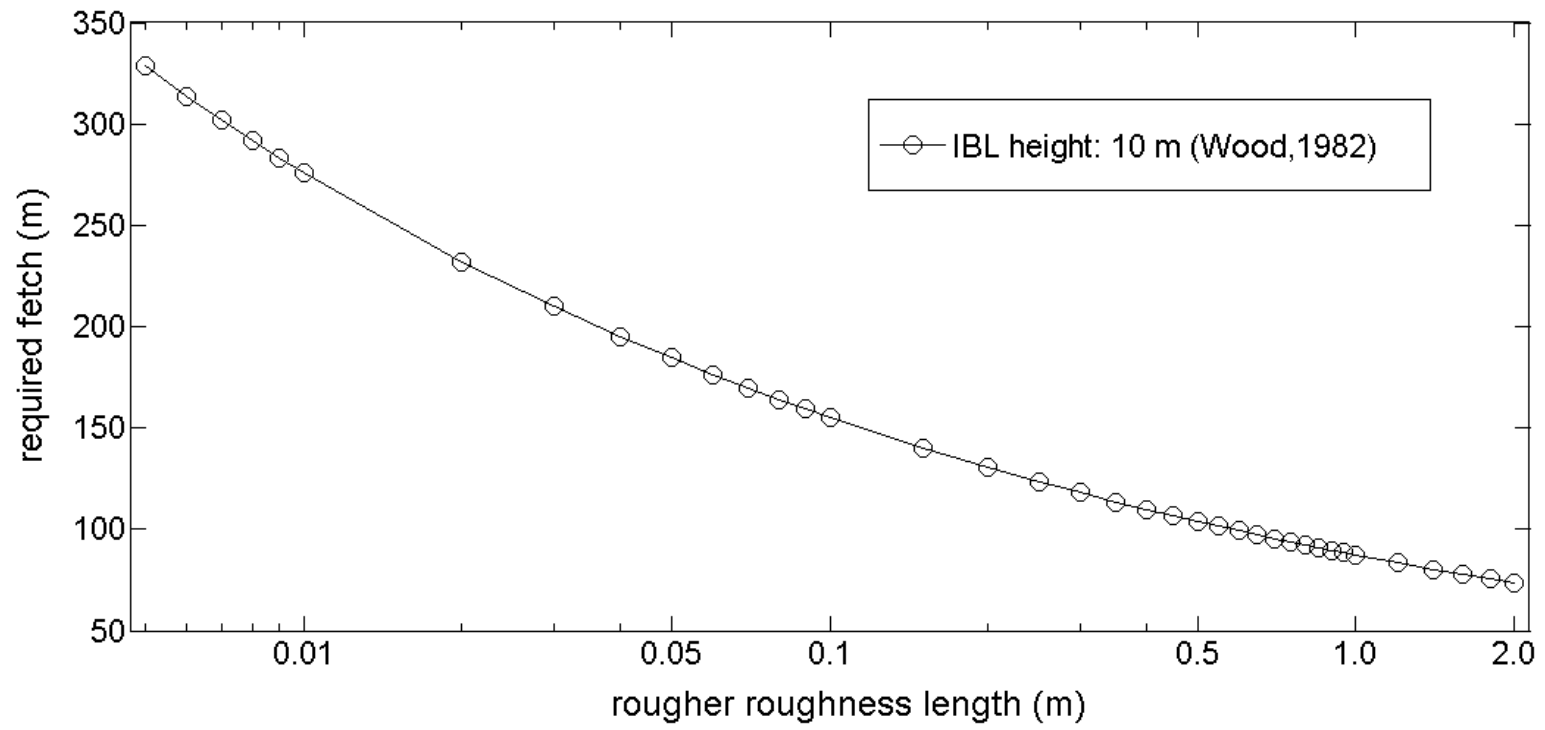


Figure 1. Required upwind fetch for given height of IBL as a function of terrain roughness

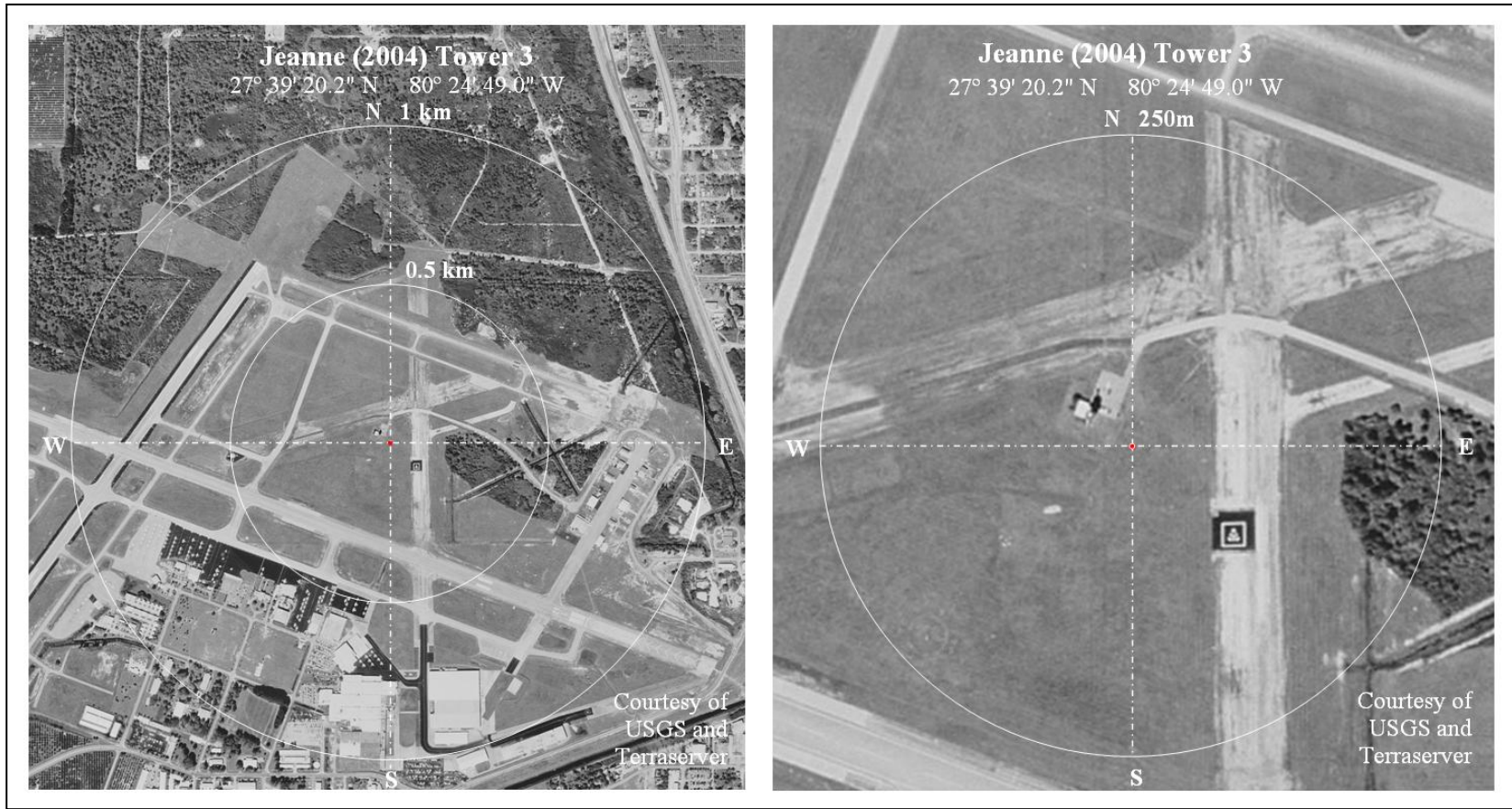


Figure 2. FCMP tower sites during hurricane passages

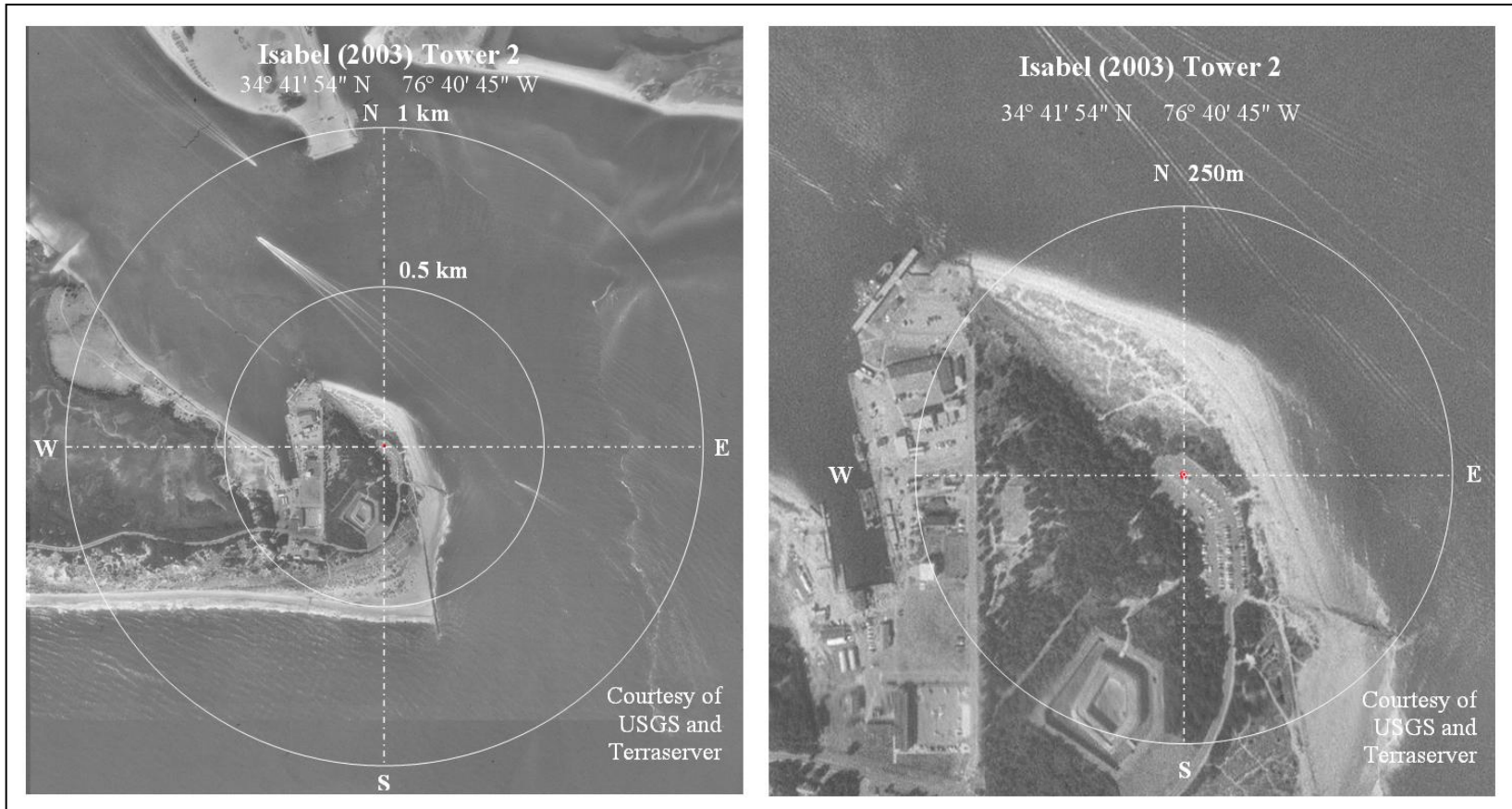


Figure 2. (Continued)



Figure 2. (Continued)

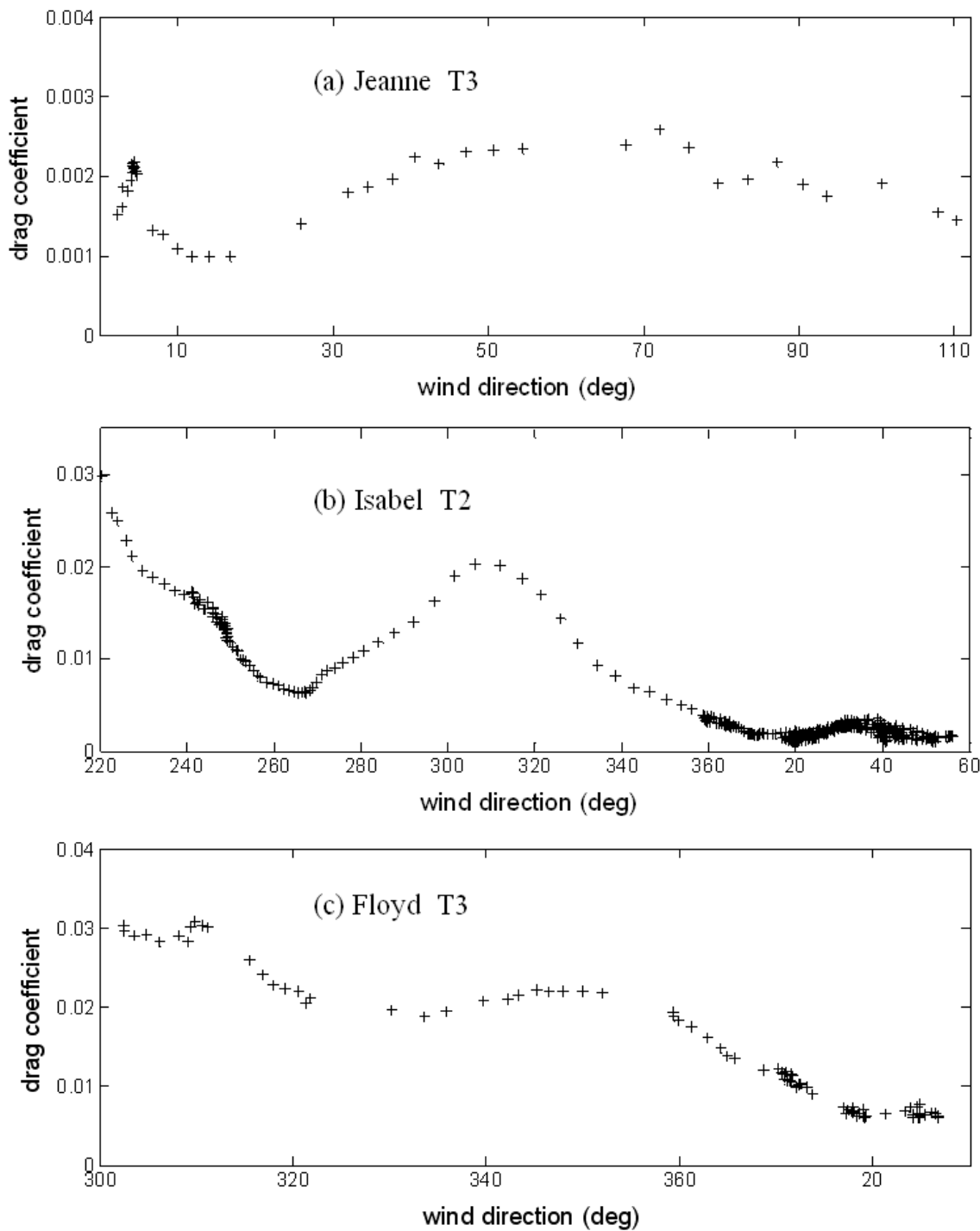


Figure 3. Estimated drag coefficients of surface terrains around FCMP towers as functions of wind direction

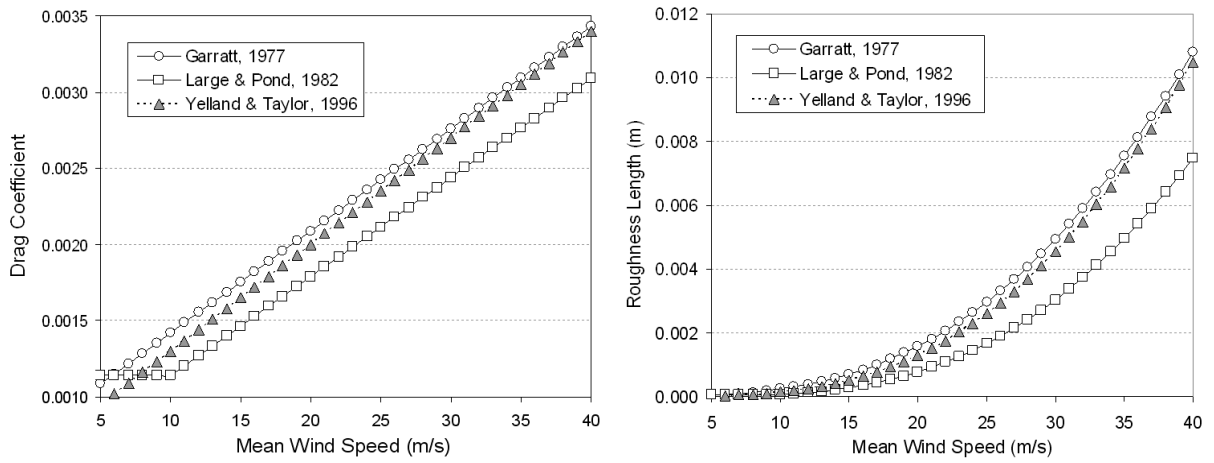


Figure 4. Drag coefficient and roughness length over sea using three methods

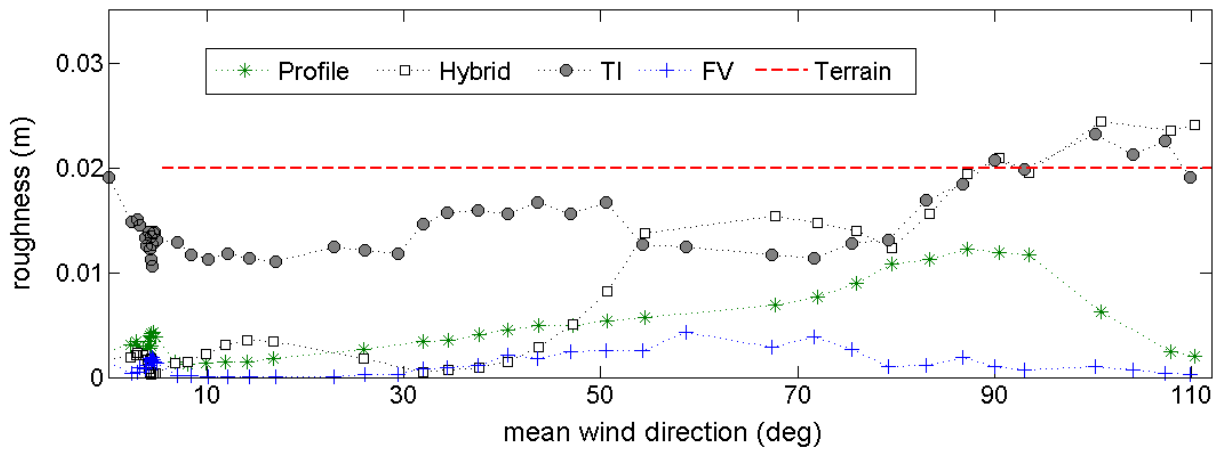


Figure 5. Comparison of roughness length estimated by various methods at Jeanne T3

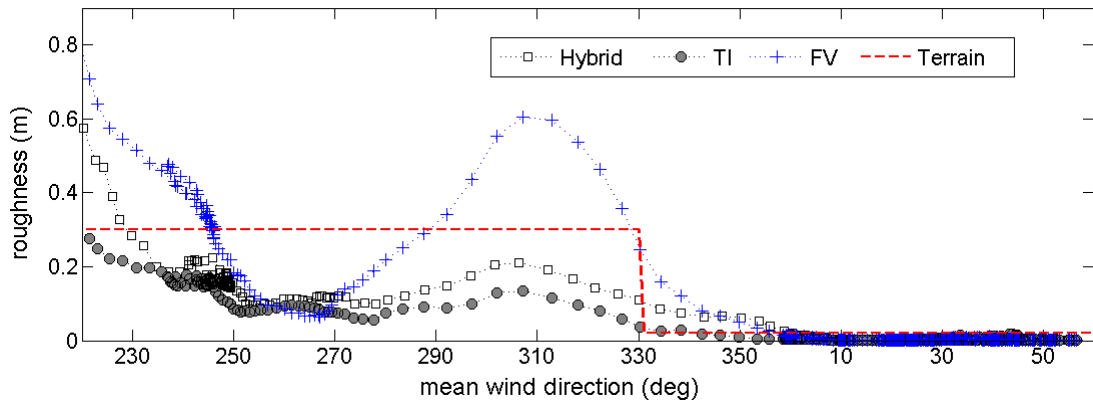


Figure 6. Comparison of roughness length estimated by various methods at Isabel T2

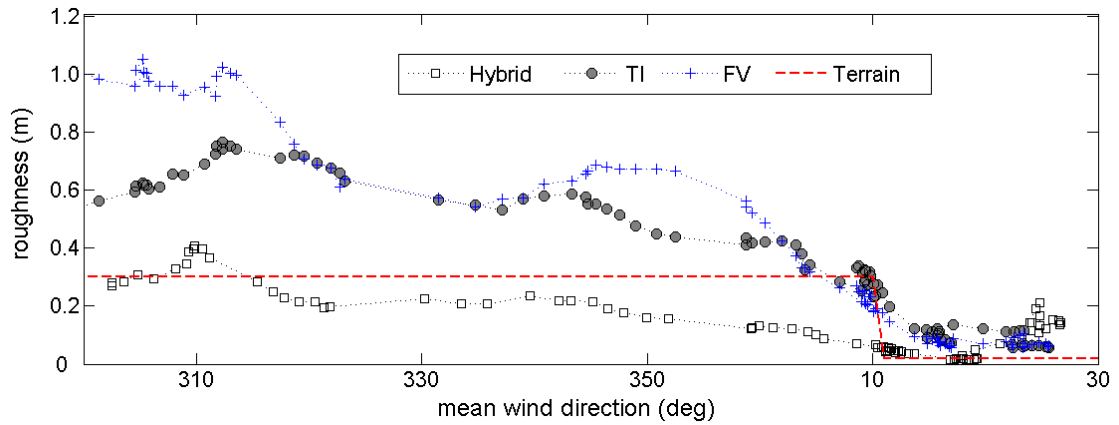


Figure 7. Comparison of roughness length estimated by various methods at Floyd T3

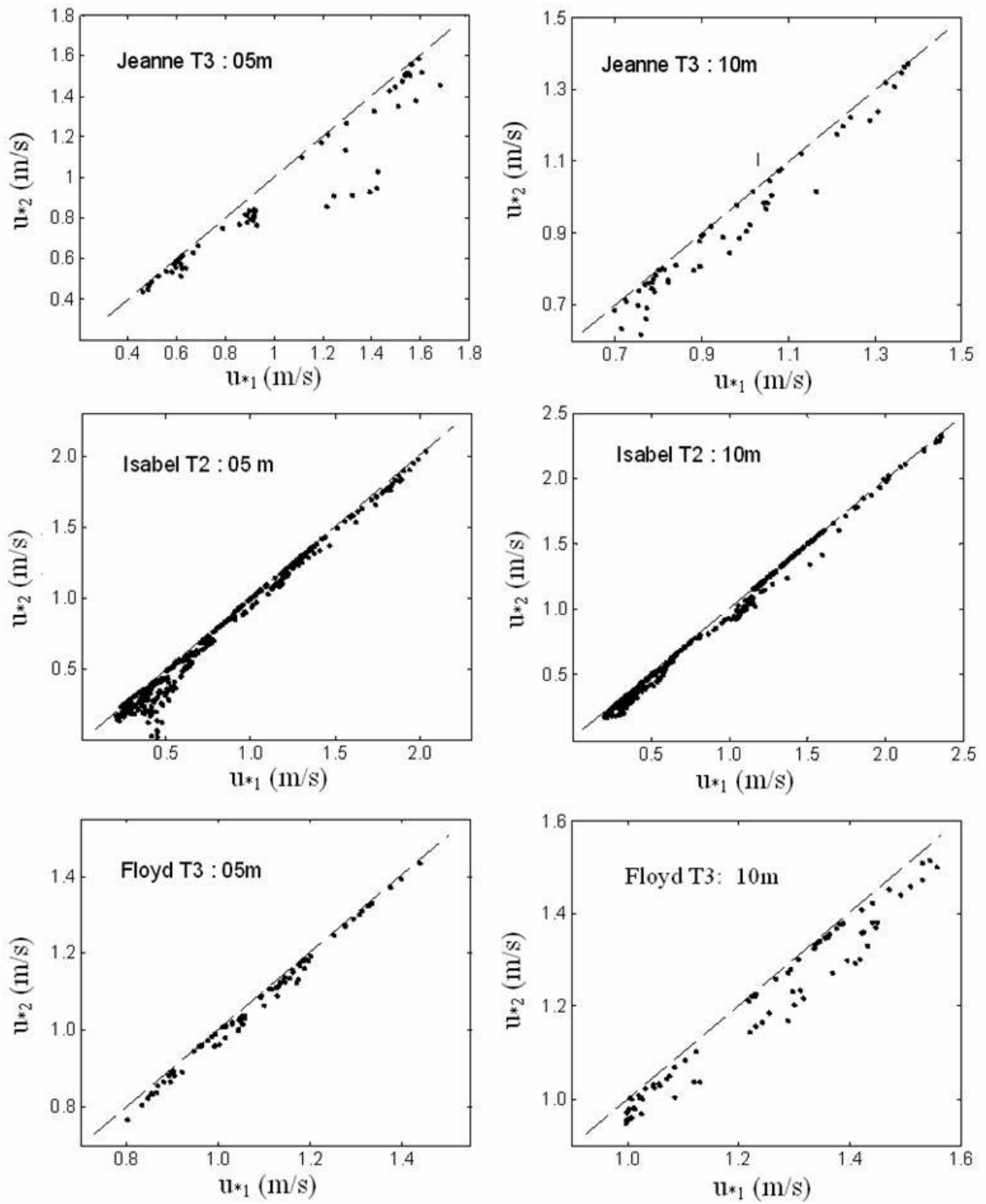


Figure A1. Comparison of two different definitions of friction velocity

### **III. GUST FACTORS AND TURBULENCE INTENSITIES FOR HURRICANE WINDS**

#### **Abstract**

In wind engineering applications the gust factor is used to convert the mean wind speed averaged over a relatively long reference period (e.g., one hour) to the peak wind speed averaged over a short period (e.g., 3 s). In this Chapter, hurricane wind gust factors are estimated from Florida Coastal Monitoring Program (FCMP) measurements of surface hurricane wind speeds over sea surface and open flat terrain in coastal areas. Comparisons are made with wind gust factors for open flat terrain, for which estimates are available in the literature. Comparisons show that the Durst model, currently used in US design standards and codes, underestimates gust factors of hurricane winds for gust durations of less than 20 s. Consideration should be given to this finding when updating the information provided in the current ASCE 7 Standard Commentary on the 3-s gust factor for hurricane winds over open terrain. The study also compares hurricane wind gust factors obtained from FCMP data with non-hurricane wind gust factors obtained from surface wind data collected at eight Automated Surface Observing Systems (ASOS) stations. In addition, hurricane wind turbulence intensities and their variability are estimated.

#### **1. Introduction**

The gust factor (GF) is defined as the ratio of the peak wind speed averaged over a short period (e.g., 3 s) to the mean wind speed averaged over a relatively long reference period (e.g., one hour). The GF is used primarily to convert mean speeds used in

laboratory measurements to peak gust speeds used in design provisions or in wind speed climatological measurements.

A number of studies on gust factors have been reported in the literature. Based on wind measurements at Cardington, England, Durst (1960) derived a statistical relationship between maximum wind speeds averaged over various periods to the corresponding hourly mean wind speeds, for sites with open terrain exposure and flat topography. Based on the Digital Anemograph Logging Equipment (DALE) wind data from the United Kingdom Meteorological Office, Ashcroft (1994) found values of gust factors in fair agreement with those obtained by Durst (1960).

Using the statistical method described by Durst (1960), Krayner and Marshall (1992) compared gust factors derived from hurricane wind records with those derived by Durst from non-hurricane wind records. They found that in hurricane winds the ratio of the 2-s gust factor (i.e., the gust factor for peak wind speeds averaged over 2 s) to the 10-min mean speed is about 1.55, as compared to the corresponding Durst value of 1.40, and that more than 80 % of the observed gust factors were higher for hurricane winds than for extratropical winds. Using wind data collected from both landfalling tropical cyclones and extratropical systems, Paulsen and Schroeder (2005) found that for terrains with the same roughness, mean gust factors for tropical cyclone winds were higher than those for extratropical winds. Similar results had been presented by Schroeder and Smith (2003).

However, according to Vickery and Sherlj (2005), gust factors associated with hurricane winds did not differ appreciably from those associated with extratropical winds, i.e., the results obtained by Krayner and Marshall (1992) are not valid. Similarly, according to Sparks and Huang (2001), who used Automated Surface Observing System

(ASOS) and Coastal Marine Automated Network (C-MAN) data, gust factors for inland stations in hurricane conditions were essentially the same as those in extratropical cyclones.

The literature review indicates that to date no definitive conclusion has been reached regarding the relative magnitude of gust factors for hurricane and non-hurricane winds. Additional research is therefore needed in support of future design provisions in codes and standards. This Chapter presents results of such research.

The Florida Coastal Monitoring Program (FCMP), focused on investigating surface level hurricane wind behavior and resulting wind loads on low-rise structures, has acquired surface wind measurements during hurricane passages. This study uses selected FCMP data to estimate gust factors, and to compare them with those obtained by Durst (1960) and by Krayer and Marshall (1992). The estimates are affected by errors due to the anemometer response characteristics, which are such that high-frequency components of the turbulence are filtered out. These errors are estimated in the Appendix to this Chapter. In addition, the study presents results on the effect of observational height, wind speed, and surface roughness length on the magnitude of the gust factor. Finally, the study presents FCMP-based estimates of turbulence intensities and their variability.

The Chapter is organized as follows. Section 2 describes methods for gust factor and turbulence intensity estimation. The estimation of the gust factor requires the estimation of the normalized standard deviation and of a peak factor, while the estimation of the turbulence intensity is based on the normalized standard deviation estimate for very small time averaging periods. Sections 3, 4, and 5 describe the hurricane wind speed measurements, basic mean wind speed characteristics, and the estimation of surface

roughness lengths, respectively. Sections 6 and 7 describe the estimation of normalized standard deviations and peak factors, and comparisons with results available in the literature. Section 8 is devoted to the estimation of the gust factors and their variability, and to comparisons with available results. Section 9 presents the conclusions of this work.

## 2. Methods for Gust Factor and Turbulence Intensity Estimation

Consider a record of length  $T$  and, within that record, all the successive intervals of length  $t$  such that  $t < T$ . Denote by  $u_{\max}$  the maximum value, within a period  $T$ , of the wind speeds averaged over the intervals of length  $t$ , and by  $U$  the mean wind speed averaged over the time period  $T$ . The gust factor for the record of length  $T$  is defined as

$$GF(T, t) = u_{\max}(T, t) / U(T) \quad (1)$$

Wind engineers commonly use 2 or 3 seconds for  $t$ , and 10 minutes to 1 hour for  $T$ . The ASCE 7 Standard wind speed map uses wind speeds expressed in terms of the 3 second gust at 10 m height in open country terrain.

A commonly used expression for the gust factor is (Durst 1960, Wieringa 1973),

$$GF(T, t) = 1 + g(T, t) \cdot SD_u(T, t) \quad (2)$$

where  $g$  is the peak factor and  $SD_u$  is the normalized standard deviation, defined as:

$$SD_u(T, t) = \frac{\sqrt{\sum_{i=1}^N u_i^2 / (N - 1)}}{U(T)} \quad (3)$$

where  $u'_i$  ( $i=1,2,\dots,N$ ) are departures from the mean wind speed  $U(T)$  over a given observation period  $T$ , and  $N=T/t$ .  $SD_u(T,t)$  is approximately equal to the turbulence intensity  $TI_u$  for short gust durations  $t$ , that is:

$$TI_u = \sigma_u / U \quad (4)$$

where  $\sigma_u$  is the standard deviation of the longitudinal wind velocity component.

Equation (3) with  $t = 0.2$  s and  $T = 5$  min was used for estimating  $TI_u$  by Schroeder and Smith (2003). Furthermore, replacing  $u'$  with  $v'$  and  $w'$  (the lateral and vertical wind fluctuation components) in  $SD_u(T,t)$ , Eq. (4) can be used to evaluate the lateral turbulence intensity ( $TI_v$ ) and vertical turbulence intensity ( $TI_w$ ), respectively.

Equation (2) yields

$$g(T,t) = [GF(T,t) - 1] / SD_u(T,t). \quad (5)$$

Thus, given the gust factor  $GF$  and the normalized standard deviation  $SD_u$ , the peak factor  $g$  can be directly estimated from Eq. (5).

The gust factor based on a *set* of records, each of which has length  $T$ , is defined as the mean of the respective gust factors  $GF(T, t)$ . For that set of records a standard deviation (s.d.) may be calculated that reflects the variability of the gust factors based on the individual records.

### 3. Hurricane Wind Data Measurements

This study uses surface wind data with 10 Hz resolution collected in real time during hurricane passages to evaluate gust factors and turbulence statistics of hurricane winds.

The Young anemometry system measures the horizontal wind speed and direction, and the vertical wind speed at 5 m and 10 m levels (Masters, 2004).

This study uses wind data collected during five hurricane passages, namely Hurricanes Irene (1999), Gordon (2000), Isidore (2002), Lili (2002), and Ivan (2004). Six selected FCMP observation sites were in the coastal areas, as shown in Fig. 1.

For *Hurricane Irene* (1999) the FCMP tower (named *Irene T1*) was located in Melbourne Beach, Florida (28 04'07.0"N – 80 33'25.0"W), west of the sea coastline.

For *Hurricane Gordon* (2000) the FCMP tower (named *Gordon T3*) was deployed at the Honeymoon Island, Florida (28 03'41"N – 82 49'44"W), northeast of the sea shoreline.

For *Hurricane Isidore* (2002) the FCMP tower (named *Isidore T2*) was deployed at the Gulf Breeze, Florida (30 21'08"N – 87 10'25.0"W), north of the sea coastline.

For *Hurricane Lili* (2002) the FCMP tower (named *Lili T3*) was deployed at Lydia, Louisiana (29 54'50"N – 91 45'35"W). Around the tower was flat open land with hardly any obstacles.

For *Hurricane Ivan* (2004) one FCMP tower (named *Ivan T1*) was located in Pensacola Regional Airport, Florida (30 28'45.4"N – 87 11'12.8"W), and another FCMP tower (named *Ivan T2*) was located in Fairhope, Alabama (30 28'21.0"N – 87 52'30.0"W), north of the Fairhope Municipal Airport.

Irene T1 captured the surface wind from 0507 UTC to 1639 UTC on 16 October in 1999. Gordon T3 collected the surface wind from 1730 UTC on 17 September to 1250 UTC on 18 September in 2000. Isidore T2 collected the surface wind from 2044 UTC on

26 September to 1136 UTC on 28 September in 2002. Lili T3 went operational between 0415 UTC on 3 October and 1802 UTC on 4 October in 2002. Ivan T1 and Ivan T2 collected the surface wind from 2026 UTC on 14 September to 2000 UTC on 16 September and from 0053 UTC to 1453 UTC on 16 September in 2004, respectively.

Wind data collected from the six selected FCMP towers (Irene T1, Isidore T2, Gordon T3, Ivan T1, Ivan T2 and Lili T3) were pre-processed and only data sets satisfying quality-control requirements were used for this study. Data pre-processing and data quality-control requirements include: (1) separate analysis of hourly record segments with overlapping 15-min segments; (2) decomposition of the records into longitudinal, lateral, and vertical components; (3) 10 m/s at 10 m height was the minimum requirement for segment mean wind speed, to satisfy the strong wind and neutral stability conditions; (4) segments with direction shifts larger than 20 ° were not considered, to avoid records in which wind speeds may correspond to more than one terrain exposure (Masters, 2004).

#### **4. Basic Mean Wind Characteristics**

In this Chapter, the wind direction is measured clockwise from the north as shown in Fig. 1. For Irene T1, Isidore T2 and Gordon T3, the wind characteristics are governed by the sea surface roughness upwind of the location of interest; for Ivan T1, Ivan T2 and Lili T3, the wind characteristics are governed by flat open land terrain roughness. The hourly mean wind speeds at 10 m height vary from 18.8 m/s to 25.5 m/s for Irene T1, from 12.1 m/s to 18.4 m/s for Isidore T2, from 14.7 m/s to 18.5 m/s for Gordon T3, from 11.1 m/s to 29.9 m/s for Ivan T1, from 15.8 m/s to 24.3 m/s for Ivan T2, and from 11.5 m/s to 22.5 m/s for Lili T3, as shown in Table 1.

The observed 3-s peak gusts are 35.5 m/s, 27.1 m/s, 29.8 m/s, 47.5 m/s, 39.9 m/s and 35.8 m/s for Irene T1, Isidore T2, Gordon T3, Ivan T1, Ivan T2 and Lili T3, respectively. The mean wind speed increased with height for all five hurricanes. Mean wind direction time histories are similar at the two different observation heights (5 m and 10 m) for each of the six tower observations.

## 5. Estimation of Surface Roughness Lengths

If the upwind terrain changes at a fetch distance  $x$  upwind from the location of interest, the logarithmic wind profile will be applicable with the local roughness only within an internal boundary layer (IBL) with a height of  $\delta(x)$ . Within the outer boundary layer (OBL), where the air flow is governed by the surface roughness upstream of the terrain roughness change, the mean wind profile will be described by the logarithmic law in which that surface roughness is used (Bradley, 1968).

For Irene T1, Isidore T2 and Gordon T3, wind passed from the smooth sea to rough land. The maximum distance from the tower to the location of the terrain roughness change is approximately 100 m (Fig. 1). According to Simiu and Scanlan (1996), elevations larger than approximately 1/12.5 times the fetch are within the OBL. For Irene T1, Isidore T2 and Gordon T3 the 10 m observation height can be considered as being within the OBL, since  $10 \text{ m} > 100 \text{ m}/12.5$ .

For Ivan T1, the observation with wind direction varying clockwise from  $135^\circ$  to  $240^\circ$  is within the IBL since the distance downwind of the roughness change is longer than 1000 m, as shown in Fig. 1. For Ivan T2 and Lili T3, the homogeneous terrain has fetch larger than 5 km upwind of the location of interest. This suggests that the wind

speeds at 10 m height are within the IBL, where the logarithmic wind profile will be applicable with the local surface roughness.

The flow features are influenced by the terrain roughness. Given the values of the longitudinal turbulence intensity ( $TI_u$ ) at measurement height  $z$ , the logarithmic law in neutral conditions can be used to estimate the surface roughness length  $z_0$  as follows (Wieringa, 1993),

$$z_0 = \exp\left(\ln z - \sqrt{\beta} \cdot \kappa / TI_u\right) \quad (6)$$

where  $\sqrt{\beta} = \sigma_u / u_*$  is the ratio of the standard deviation ( $\sigma_u$ ) of longitudinal wind component to the friction velocity ( $u_*$ );  $\kappa = 0.4$  is the von Karman constant.

For a fully developed neutrally stratified flow within the surface layer, according to Lumley and Panofsky (1964),  $\sqrt{\beta}$  is a constant and is independent of the underlying terrain roughness. According to Deaves (1981),  $\sqrt{\beta} \approx 2.79$  appears to describe adequately fully developed non-hurricane equilibrium flows over open terrain. Values of  $\sqrt{\beta}$  obtained by the FCMP wind measurements can be higher than those provided by Deaves (1981). The mean values of  $\sqrt{\beta}$  are: 4.08, 3.32, 3.10 over water for Irene T1, Isidore T2, and Gordon T3, respectively, and 3.38, 2.85 and 2.72 over open terrain for Ivan T1, Ivan T2 and Lili T3, respectively. In one of the three open terrain records,  $\sqrt{\beta}$  exceeds by about 20 % the typical value proposed by Deaves (1981).

Based on surface wind measurements from the FCMP towers (Irene T1, Isidore T2, Gordon T3, Ivan T1, Ivan T2 and Lili T3) under strong wind conditions, the surface

roughness lengths around the tower site were estimated by using Eq. (6). For sea surface (Irene T1, Isidore T2 and Gordon T3), the surface roughness lengths vary from 0.0002 m to 0.006 m; for open terrain (Ivan T1, Ivan T2 and Lili T3), the surface roughness lengths vary from 0.0080 m to 0.0589 m. Estimated mean surface roughness lengths around the tower sites are shown in Table 2. The estimates of surface roughness lengths are used in Sections 6 through 8.

## 6. Estimation and Comparison of Normalized Standard Deviation

Normalized standard deviations  $SD_u$  (Eq. 3) are affected by surface roughness elements. Estimates of surface roughness lengths in Section 5 were used to stratify the estimates of  $SD_u$  at 10 m height into four roughness regimes (RR),  $0.0002 \text{ m} \leq z_0 \leq 0.001 \text{ m}$  (named RR1),  $0.001 \text{ m} \leq z_0 \leq 0.006 \text{ m}$  (named RR2),  $0.008 \text{ m} \leq z_0 \leq 0.03 \text{ m}$  (named RR3),  $0.03 \text{ m} \leq z_0 \leq 0.06 \text{ m}$  (named RR4), which were also used for comparisons of peak factors in Section 7 and gust factors in Section 8. Figure 2 presents estimated values of  $SD_u$  at 10 m elevation for terrains with various surface roughness lengths. Results show that higher values of  $SD_u$  correspond to rougher terrains.

Estimated values of  $SD_u$  become fairly stable for gust duration  $t$  less than approximately 1 s for each roughness regime, as shown in Fig. 2. In addition, as expected, the estimates of  $SD_u$  were found to decrease as the observational height increases.

To compare observed values of  $SD_u$  based on hourly mean wind speeds at 10 m elevation with those obtained by Durst (1960) and Krayner and Marshall (1992), the

estimates of  $SD_u$  over surface roughness regimes of 0.008 m – 0.03 m (RR3) and 0.03 m – 0.06 m (RR4) are plotted in Fig. 3. For RR3, estimated values of  $SD_u$  are larger than those proposed by Durst for gust durations less than 3 s and are lower for gust durations larger than 3 s, as shown in Fig. 3. Values of  $SD_u$  obtained by Krayner and Marshall are larger than those obtained by the FCMP wind measurements.

As mentioned earlier,  $SD_u(T, t)$  can be used to estimate the turbulence intensity for short gust durations  $t$  and mean wind speeds over the observation period  $T$ . Equation (3) with  $T = 60$  min and  $t = 0.1$  s (corresponding to the sampling frequency of 10 Hz) was used for estimating the longitudinal, lateral and vertical turbulence intensities ( $TI_u, TI_v$ , and  $TI_w$ ). The turbulence intensity based on a set of hourly records is defined as the mean of the respective turbulence intensities. The estimates of the turbulence intensity and the turbulence intensity ratio at 10 m elevation are summarized in Table 3.

Both  $TI_u$  and  $TI_w$  increase as the surface roughness increases. Estimates of  $TI_u$  over sea (11.8 % and 13.3 %) are lower than those over flat open land (17.7 % and 20.4 %). The vertical turbulence intensity  $TI_w$  has a similar pattern, and varies from 4.0 % and 4.6 % for sea surface to 7.0 % and 8.5 % for flat open land exposure.

The results show that  $TI_u > TI_v > TI_w$  for each roughness regime. The mean ratios between the lateral and longitudinal turbulence intensities ( $TI_v/TI_u$ ) vary from 0.73 to 0.89; the mean ratios between the vertical and longitudinal turbulence intensities ( $TI_w/TI_u$ ) vary from 0.34 to 0.42, as shown in Table 3.

## 7. Peak Factor Estimation and Comparisons

Peak factors  $g$  based on hourly mean wind speeds at 10 m height were estimated using Eq. (5) and plotted as function of the gust duration for various surface roughness regimes, as shown in Fig. 4. Estimates of  $g$  exhibit wider scatter for hurricane winds over sea (Irene T1, Isidore T2 and Gordon T3) compared with those over flat land (Ivan T1, Ivan T2 and Lili T3), particularly for gust durations less than 10-s. No relation is apparent between  $g$  values and the underlying surface terrain roughness, except that  $g$  is smaller for  $t < 100$  s over sea surface, as shown in Fig. 4.

For 10 m elevation, a comparison of observed values of  $g$  ( $T = 3600$  s) over surface roughness regimes of 0.008 m – 0.03 m (RR3) and 0.03 m – 0.06 m (RR4) with those obtained by other researchers is shown in Fig. 5. The results show that the observed  $g$  values are larger than those obtained by Durst (1960) and Krayner and Marshall (1992). The differences increase as the gust duration increases.

## 8. Gust Factor Estimation, Comparisons, and Variability

In this section, estimated gust factors of hurricane wind velocity fluctuations in the surface layer are evaluated for terrains with various roughness lengths, and for two observational heights (5 m and 10 m). The section also compares these results with results obtained by other investigators.

### *8.1 Gust factor dependence on surface roughness length and observational height*

For each record, the gust factor was estimated using Eq. (1). The gust factor based on a *set* of records, each of which has length  $T$ , is defined as the mean of the respective gust factors  $GF(T, t)$ . The estimated gust factors based on hourly mean wind speeds ( $T = 1$  hr.) at 10 m elevation are plotted in Fig. 6 for both sea surface and open land. Gust factors are heavily dependent on terrain conditions, higher values of the gust factor corresponding to the rougher surface terrains, as shown in Fig. 6.

Gust factors increase with the upstream surface roughness. Estimated values of gust factors over land ( $0.008 \text{ m} \leq z_0 \leq 0.06 \text{ m}$ ) are significantly higher than those over sea surface ( $0.0002 \text{ m} \leq z_0 \leq 0.006 \text{ m}$ ). For example, values of 3-s gust factors are 1.32, 1.41, 1.59 and 1.69 for roughness regime RR1, RR2, RR3 and RR4, respectively. The dependence of the estimates of gust factors on surface roughness conditions is in agreement with the results of Ashcroft (1994) for non-hurricane winds and Schroeder and Smith (2003) for hurricane winds.

For the observational heights of 5 m and 10 m, hurricane wind gust factors were estimated and plotted in Fig. 7. Results show that the values of gust factor decrease with increasing observation height. For example, for roughness regime  $0.008 \text{ m} \leq z_0 \leq 0.03 \text{ m}$ , the 3-s gust factors are 1.64 and 1.59 for 5 m and 10 m levels, respectively.

### *8.2 Gust factors for various hurricanes and mean wind speed regimes*

Gust factors were estimated for each of the six FCMP tower sites. Figure 8 presents the resulting gust factor curves at 10 m elevation for different hurricanes.

Estimated values of gust factors obtained from Ivan T1, Ivan T2 and Lili T3 (i.e., over open terrain) are significantly higher than those obtained from Irene T1, Isidore T2 and Gordon T3 (i.e., over sea surface). This is consistent with the observation that gust factors increase with upstream surface roughness.

For hurricane winds over open land the estimated gust factors for Ivan T1, Ivan T2 and Lili T3 are comparable, except for some slightly lower values resulting from Lili T3, as shown in Fig. 8.

For hurricane winds over sea surface (Irene T1, Isidore T2 and Gordon T3), the estimated values of gust factor for Isidore T2 are higher than those from Irene T1 and Gordon T3. This can be attributed to a comparatively rougher surface for Isidore T2, since the estimated mean surface roughness length of 0.0032 m for Isidore T2 is larger than the values 0.0015 m and 0.0007 m for Irene T1 and Gordon T3 (Table 2), respectively.

To investigate the effects of wind speed on the variation of gust factors of hurricane winds at 10 m elevation, the estimated gust factors were separated into two mean hourly wind speed regimes,  $10 \text{ m/s} \leq U \leq 20 \text{ m/s}$  and  $20 \text{ m/s} \leq U \leq 30 \text{ m/s}$ . Figure 9 presents estimated values of gust factors at 10 m elevation for the two mean hourly wind speed regimes for both sea surface and open terrain. The estimated gust factors of hurricane wind velocity fluctuations are comparable over the two different mean wind speed regimes, except that values of gust factors for  $10 \text{ m/s} \leq U \leq 20 \text{ m/s}$  are slightly higher than those obtained from  $20 \text{ m/s} \leq U \leq 30 \text{ m/s}$  for open terrain, as shown in Fig. 9 (b).

### 8.3 Comparison of gust factors for hurricane and non-hurricane winds

To compare the gust factors associated with hurricane winds and those associated with non-hurricane winds, this study estimated the non-hurricane wind gust factors by using surface wind data collected by eight Automated Surface Observing Systems (ASOS) stations in 2004, as shown in Table 4. The section also compares these results with results obtained from FCMP observations.

Estimated 5-s gust factors based on hourly non-hurricane winds vary from 1.40 to 1.50, as shown in Table 5. The 5-s gust factors obtained from FCMP hurricane winds are 1.54 and 1.64 for roughness regimes of  $0.008 \text{ m} \leq z_0 \leq 0.03 \text{ m}$  and  $0.03 \text{ m} \leq z_0 \leq 0.06 \text{ m}$  (Table 6), respectively. Thus, for the 5-s gust factors, the estimated values associated with hurricane winds are higher than those associated with non-hurricane winds. For example, the hurricane wind gust factor can be more than 10 % higher than the gust factor associated with non-hurricane for the roughness regime of  $0.008 \text{ m} \leq z_0 \leq 0.03 \text{ m}$ , and more than 17 % higher for the roughness regime of  $0.03 \text{ m} \leq z_0 \leq 0.06 \text{ m}$ .

Figure 10 shows the histograms of gust factors for non-hurricane winds from two ASOS stations and for FCMP hurricane winds over the roughness regimes of  $0.008 \text{ m} \leq z_0 \leq 0.03 \text{ m}$  and  $0.03 \text{ m} \leq z_0 \leq 0.06 \text{ m}$ . The distribution of gust factors of non-hurricane winds from KCPR and KBIL are roughly similar, as shown in Fig. 10.

#### 8.4 Comparison of estimated gust factors with results obtained by other investigators

*Open terrain with roughness  $0.008 \text{ m} \leq z_0 \leq 0.03 \text{ m}$  (regime RR3), 10 m elevation:*

The estimated gust factor curve based on the in-situ hurricane wind measurement data obtained from FCMP closely matches the Durst curve, which is used by current US design codes and standards (ASCE 7-05), for gust durations larger than 20 s, but its ordinates are higher than those of the Durst curve for gust durations of less than 20 s, as shown in Fig. 11 and Table 7. The estimated values of the gust factor from the FCMP wind measurements are lower than those obtained by Krayner and Marshall (1992), as shown in Fig. 11. The 3-s gust factors based on hourly mean wind speed are 1.52, 1.59 and 1.66 for Durst (1960), FCMP hurricane winds, and Krayner and Marshall (1992), respectively (Table 7).

*Open terrain with roughness  $0.03 \text{ m} \leq z_0 \leq 0.06 \text{ m}$  (regime RR4), 10 m elevation:*

The ordinates of the estimated gust factor curve based on the in-situ hurricane wind measurement data obtained from FCMP are higher than those of the Durst curve, as shown in Fig. 11 and Table 7. The estimated values of the gust factor from the FCMP wind measurements are higher than those obtained by Krayner and Marshall (1992) for gust durations of less than 4 s, as shown in Fig. 11. The 3-s gust factors based on hourly mean wind speed are 1.52, 1.69 and 1.66 for Durst (1960), FCMP hurricane winds, and Krayner and Marshall (1992), respectively.

The above results suggest that that an upward adjustment of the Durst curve may be needed for evaluating the gust factors associated with hurricane winds over coastal areas. For open terrain and  $0.008 \text{ m} \leq z_0 \leq 0.03 \text{ m}$ , the degree of upward adjustment is not as

high as proposed by Krayner and Marshall (1992) (Fig. 11 and Table 7); for peak 3-s gusts the upward adjustment would be about 5 %. However, for open terrain and  $0.03 \text{ m} \leq z_0 \leq 0.06 \text{ m}$  the upward adjustment would be about 11 %.

The measurement system mechanically filters the amplitudes of short wavelength gusts due to the response characteristics of the wind anemometry (Schroeder and Smith, 2003). For this reason, the actual gust factor ordinates are slightly higher than those estimated from FCMP measurements. As shown in Appendix A, for very short averaging times (e.g.,  $t < 0.2 \text{ s}$ ), the gust factors estimated from FCMP records are lower than the actual gust factors by about 2 % for flow over water and 4 % for flow over open terrain. For longer averaging times these percentages decrease. These results reinforce the conclusion that the FCMP-based gust factor estimates presented in this Chapter for periods of about 3 s or so are larger than their counterparts for non-hurricane winds as estimated by Durst.

## **9. Conclusions**

Using the surface wind measurements collected by FCMP towers (Irene T1, Isidore T2, Gordon T3, Ivan T1, Ivan T2 and Lili T3) during hurricane passages, this study presents estimates of gust factors, and of turbulence statistics, for hurricane winds over coastal areas under neutral conditions. The conclusions are listed below:

(1) For 10 m elevation over open exposure terrain the Durst model yields lower gust factors than those based on the FCMP data for gust durations less than 20 s, and closely matches the estimated gust factor curve for gust durations larger than 20 s. For open

terrain and  $0.008 \text{ m} \leq z_0 \leq 0.03 \text{ m}$ , the Kraye-Marshall (1992) model yields higher gust factors than those based on the FCMP data, particularly for gust durations less than 100 seconds. However, for open terrain and  $0.008 \text{ m} \leq z_0 \leq 0.03 \text{ m}$ , FCMP data yields higher gust factors than those obtained by Kraye-Marshall (1992), particularly for gust durations less than 10 s.

(2) Estimated values of 5-s gust factor associated with hurricane winds based on FCMP data are higher than those associated with non-hurricane winds obtained from eight ASOS stations; for winds over roughness regimes of  $0.008 \text{ m} \leq z_0 \leq 0.03 \text{ m}$  and  $0.03 \text{ m} \leq z_0 \leq 0.06 \text{ m}$ , hurricane wind gust factors can be more than 10 % and 17 % higher, respectively, than the non-hurricane gust factors.

(3) The dependence of the estimates of gust factors on upstream surface roughness conditions is in agreement with the results of Ashcroft (1994), and Schroeder and Smith (2003). Values of gust factors of hurricane winds at 5 m elevation were larger than those at 10 m elevation.

(4) Estimated values of turbulence intensities of longitudinal and vertical wind components increase as the terrain roughness increases. Results showed that  $TI_u > TI_v > TI_w$  for each roughness regime. In addition, estimated peak factors were larger than those based on Durst (1960) and Kraye and Marshall (1992).

(5) For short averaging time (e.g.,  $t < 0.2 \text{ s}$ ), the FCMP-based gust factors are underestimated by about 2 % for flow over water and 4 % for flow over open terrain. As the averaging times increase (e.g.,  $t = 3 \text{ s}$ ), the underestimates are smaller than these values.

(6) Current US codes standards and codes require the use of 3-s gust factors based on hourly mean wind speeds, over open terrain. According to Durst (1960), the value of this gust factor is 1.52, while according to Krayner and Marshall (1992) it is 1.66. The estimates based on the FCMP yielded, to within an underestimation of less than 4 %, values of about 1.59 for hurricane winds over terrain with  $0.008 \text{ m} \leq z_0 \leq 0.03 \text{ m}$ , and 1.69 for hurricane winds over terrain with  $0.03 \text{ m} \leq z_0 \leq 0.06 \text{ m}$ . This suggests that 3-s gust factors in the ASCE Standard 7-10 should be augmented accordingly with respect to current values based on Durst (1960).

## Appendix A. Corrections to Gust Factor Estimates

Owing to their response characteristics the Young anemometers filter out short wavelength gusts (Schroeder and Smith, 2003). Ordinates of spectra  $S_u^F$  estimated from FCMP records are therefore lower at reduced frequencies  $f = nz/U > 0.2$  or so than their Kaimal spectra  $S_u^K$  counterparts, which represent approximately spectra based on Kolmogorov theory validated by careful measurements. For this reason, the actual turbulence intensity and gust factors are higher than their FMCP-based counterparts by amounts estimated in this Appendix.

The ratio of the corrected estimate of the longitudinal turbulence intensity to the estimated turbulence intensity based on FCMP records is

$$\gamma_{TI} = \left[ \left( \int_0^\infty \frac{S_u^F}{u_*^2} dn + \int_{n_1}^\infty \frac{S_u^K}{u_*^2} dn - \int_{n_1}^\infty \frac{S_u^F}{u_*^2} dn \right) / \int_0^\infty \frac{S_u^F}{u_*^2} dn \right]^{1/2} \quad (\text{A.1})$$

where  $n$  is the frequency in Hz,  $U$  is the mean wind speed in m/s and  $z$  is the height above ground in meter (m), and where it is assumed that  $n_1 = 0.2U/z$ . The friction velocity  $u_*$  is defined as

$$u_* = \left( \overline{u'w'^2} + \overline{v'w'^2} \right)^{1/4} \quad (\text{A.2})$$

where  $u'$ ,  $v'$ , and  $w'$  are the longitudinal, lateral, and vertical wind fluctuation components, respectively. The expression for  $S_u^K$  is (Kaimal et al., 1972)

$$\frac{nS_u^K(n)}{u_*^2} = \frac{105f}{(1+33f)^{5/3}} \quad (\text{A.3})$$

Given the values of turbulence intensity  $TI^F$  estimated from the FCMP records, the corrected turbulence intensity  $TI^A$  is

$$TI^A = TI^F \cdot \gamma_{TI} \quad (\text{A.4})$$

The peak factors  $\bar{K}^A$  can be estimated by the expression

$$\bar{K}^A = \left[ 2 \ln(\nu^A T) \right]^{1/2} + 0.577 / \left[ 2 \ln(\nu^A T) \right]^{1/2} \quad (\text{A.5})$$

(see, e.g., Simiu and Scanlan, 1996, p.639-640). The mean upcrossing rate  $\nu^A$  has the expression

$$\nu^A = \left\{ \frac{\left[ \int_0^\infty n^2 S_u^A dn \right]}{\left[ \int_0^\infty S_u^A dn \right]} \right\}^{1/2} \quad (\text{A.6a})$$

$$\nu^A = \left\{ \frac{\left[ \int_0^\infty n^2 S_u^F dn + \int_{n_1}^\infty n^2 (S_u^K - S_u^F) dn \right]}{\left[ \int_0^\infty S_u^F dn + \int_{n_1}^\infty (S_u^K - S_u^F) dn \right]} \right\}^{1/2} \quad (\text{A.6b})$$

where  $T$  is the observation period in seconds (in this case 3600 s).

Peak factors  $\bar{K}^F$  based on FCMP records can be estimated by

$$\bar{K}^F = \left[ 2 \ln(v^F T) \right]^{1/2} + 0.577 / \left[ 2 \ln(v^F T) \right]^{1/2} \quad (\text{A.7})$$

$$v^F = \left( \int_0^\infty n^2 S_u^F dn / \int_0^\infty S_u^F dn \right)^{1/2} \quad (\text{A.8})$$

We can now write the ratio, for short averaging times (0.2 s, say), of the corrected estimate of the gust factor to the estimated value based on FCMP records:

$$\gamma_{GF} = GF^A / GF^F = \left( 1 + \bar{K}^A \cdot TI^A \right) / \left( 1 + \bar{K}^F \cdot TI^F \right) \quad (\text{A.9})$$

Estimates of surface roughness lengths in Section 5 were used to stratify the computational results into four roughness regimes (RR),  $0.0002 \text{ m} \leq z_0 \leq 0.001 \text{ m}$  (named RR1),  $0.001 \text{ m} \leq z_0 \leq 0.006 \text{ m}$  (named RR2),  $0.008 \text{ m} \leq z_0 \leq 0.03 \text{ m}$  (named RR3),  $0.03 \text{ m} \leq z_0 \leq 0.06 \text{ m}$  (named RR4).

The peak factor and turbulence intensity are shown in Table A.1 for both the FCMP and the corrected case. Also shown in Table A.1 are the respective gust factors. It is seen that the corrected gust factors are about 2 % and 4 % higher than those obtained from the FCMP wind measurements for sea surface and open land, respectively. Since the contribution of the high-frequency fluctuations to the gust factor decreases as the averaging time for the gust factor increases, it is concluded that the gust factors estimated from FCMP data in the body of the Chapter are lower than the actual gust factors by less than about 2 % for flow over water and 4 % for flow over open terrain.

## **Table Captions**

Table 1: Hourly mean wind speed statistics at 10 m elevation

Table 2: Surface roughness lengths

Table 3: Hurricane wind turbulence intensities at 10 m elevation

Table 4. ASOS stations selected for analysis

Table 5. 5 s gust factors (GF) of non-hurricane winds from ASOS at 10 m elevation

Table 6. Gust factors of hurricane winds from FCMP at 10 m elevation

Table 7. Comparison of gust factors based on Durst, Krayner and Marshall, and FCMP hurricane winds at 10 m elevation

Table A.1 Actual gust factor and turbulence intensity ordinates at 10 m elevation

## **Figure Captions**

Figure 1. FCMP tower sites selected for analysis

Figure 2. Estimated normalized standard deviation at 10 m elevation for various surface roughness length

Figure 3. Comparison of normalized standard deviations at 10 m elevation over open terrain

Figure 4. Estimated peak factors at 10 m elevation for terrains with various surface roughness lengths

Figure 5. Comparison of peak factors at 10 m elevation over open terrain

Figure 6. Gust factors at 10 m elevation for terrains with various surface roughness lengths

Figure 7. Estimated gust factors for various observation heights (5 m and 10 m) and surface roughness regimes

Figure 8. Gust factors at 10 m elevation for six hurricane records

Figure 9. Variation of gust factors with wind speed at 10 m elevation

Figure 10. Histogram of gust factors based on hourly wind speeds at 10 m elevation

Figure 11. Comparison of gust factor curves of wind speed at 10 m elevation

## References

- ASCE/SEI 7-05, 2006: Minimum Design Loads for Buildings and Other Structures.
- Ashcroft, J., 1994: The relationship between the gust ratio, terrain roughness, gust duration and the hourly mean wind speed, *Journal of Wind Engineering and Industrial Aerodynamics*, 53, 331-355.
- Bradley, E. F., 1968: A Micrometeorological Study of Velocity Profiles and Surface Drag in the Region Modified by a Change in Surface Roughness, *Quart. J. Roy. Meteorol. Soc.*, 94, 361-379.
- Deaves, D. M., 1981: Terrain-dependence of longitudinal RMS velocities in the neutral atmosphere, *Journal of Wind Engineering and Industrial Aerodynamics*, 8, 259-274.
- Durst, C. S., 1960: Wind speeds over short periods of time, *The Meteorological Magazine*, 89, 181-186.
- Kaimal, J. C., J. C. Wyngaard, Y. Izumi and O. R. Coté 1972: Spectral Characteristics of Surface-Layer Turbulence, *Quart. J. Roy. Meteorol. Soc.*, 98, 563–598.
- Krayer W. R., and R. D. Marshall, 1992: Gust factors applied to hurricane winds, *Bulletin American Meteorological Society*, 73, 613-617.
- Lumley, J. L., and H. A. Panofsky, 1964: *The structure of atmospheric turbulence*, Wiley, New York.
- Masters, F. J., 2004: Measurement, modeling and simulation of ground-level tropical cyclone winds. Ph.D. dissertation, University of Florida.
- Paulsen, B. M., and J. L. Schroeder, 2005: An Examination of Tropical and Extratropical Gust Factors and the Associated Wind Speed Histograms, *Journal of Applied Meteorology*, 44, 270-280.
- Schroeder, J. L., and D. A. Smith, 2003: Hurricane Bonnie wind flow characteristics as determined from WEMITE, *Journal of Wind Engineering and Industrial Aerodynamics* 91, 767–789.
- Simiu, E., and R. Scanlan, 1996: *Wind Effects on Structures*, 3rd Edition, Wiley, New York.
- Sparks, P. R., and Z. Huang, 2001: Gust factors and surface-to-gradient wind-speed ratios in tropical cyclones, *Journal of Wind Engineering and Industrial Aerodynamics*, 89, 1047–1058.
- Vickery, P. J., and P. F. Skerlj, 2005: Hurricane Gust Factors Revisited, *Journal of Structural Engineering*, 825-832.

Wieringa, J., 1973: Gust factors over open water and build-up country, *Boundary-Layer Meteorology*, 3, 424-441.

Wieringa, J., 1993: Representative roughness parameters for homogeneous terrain. *Boundary-Layer Meteorology*, 63, 323-363.

Table 1: Hourly mean wind speed statistics at 10 m elevation

FCMP Tower		Sea surface			Open terrain		
		Irene T1	Isidore T2	Gordon T3	Ivan T1	Ivan T2	Lili T3
Wind direction		(70 ;10 ) CCW*	(110 ;200 ) CW*	(180 ;290 ) CW*	(135 ;240 ) CW*	(50 ;300 ) CW*	(145 ;230 ) CW*
Wind speed (m/s)	min	18.8	12.1	14.7	11.1	15.8	11.5
	max	25.5	18.4	18.5	29.9	24.3	22.5
	mean	22.7	15.5	17.2	19.6	18.8	15.0
	s.d.	2.3	2.2	0.7	5.3	2.5	3.4
Number of segments		30	50	18	37	41	27

\* CW: clockwise; CCW: counter-clockwise (e.g., wind direction during Irene T1 varies counter-clockwise from 70 °to 10 °).

Table 2: Surface roughness lengths (in meters)

FCMP Tower		Sea surface			Flat open land		
		Irene T1	Isidore T2	Gordon T3	Ivan T1	Ivan T2	Lili T3
Min		0.0006	0.0011	0.0002	0.0080	0.0116	0.0082
Max		0.0040	0.0060	0.0014	0.0551	0.0497	0.0589
Mean		0.0015	0.0032	0.0007	0.0222	0.0257	0.0248
s.d.		0.0009	0.0015	0.0004	0.0121	0.0091	0.0147

Table 3: Hurricane wind turbulence intensities at 10 m elevation

FCMP Tower	Sea surface (Irene T1, Isidore T2 and Gordon T3)		Flat open land (Ivan T1, Ivan T2 and Lili T3)	
	RR1*	RR2*	RR3*	RR4*
$TI_u$ (%)	11.83	13.34	17.75	20.43
$TI_v$ (%)	10.55	10.01	13.34	14.84
$TI_w$ (%)	4.05	4.58	7.05	8.52
$TI_v/TI_u$ (%)	89.13	75.25	75.31	72.69
$TI_w/TI_u$ (%)	34.21	34.36	39.70	41.62

\* RR: roughness regime; RR1, RR2, RR3 and RR4 are defined in Section 6.

Table 4. ASOS stations selected for analysis

No.	Station Name	Location Indicator	Station Position	State
1	Natrona County International Airport	K CPR	42 53'51"N 106 28'23"W	WY
2	Sheridan County Airport	K SHR	44 46'10"N 106 58'08"W	WY
3	Billings Logan International Airport	K BIL	45 48'25"N 108 32'32"W	MT
4	Great Falls International Airport	K GTF	47 28'24"N 111 22'56"W	MT
5	Austin Straubel International Airport	K GRB	44 28'46"N 088 08'12"W	WI
6	La Crosse Municipal Airport	K LSE	43 52'46"N 091 15'24"W	WI
7	Bishop Airport	K BIH	37 22'16"N 118 21'29"W	CA
8	Ely Airport	K ELY	39 17'42"N 114 50'43"W	NV

\* Location indicator, assigned by the International Civil Aviation Organization (ICAO)

Table 5. 5-s gust factors (GF) of non-hurricane winds from ASOS at 10 m elevation

ASOS Stations	Location Indicator							
	KCPR	KSHR	KBIL	KGTF	KGRB	KLSE	KBIH	KELY
GF *	1.40	1.48	1.42	1.41	1.49	1.50	1.48	1.50
s.d. *	0.10	0.16	0.12	0.11	0.10	0.11	0.11	0.12
Number of segments	4969	1119	2008	3247	393	504	734	794

\* GF based on a set of records is defined as the mean of the respective gust factors. The standard deviation (s.d.) reflects the variability of the gust factors based on the individual records.

Table 6. Gust factors of hurricane winds from FCMP at 10 m elevation

Roughness Regime **	3 s gust factor				5 s gust factors			
	RR1	RR2	RR3	RR4	RR1	RR2	RR3	RR4
GF *	1.32	1.41	1.59	1.69	1.30	1.37	1.54	1.64
s.d. *	0.03	0.05	0.06	0.13	0.03	0.04	0.06	0.11
Number of segments	24	74	82	23	24	74	82	23

\* GF based on a set of records is defined as the mean of the respective gust factors. The standard deviation (s.d.) reflects the variability of the gust factors based on the individual records.

\*\* RR: roughness regime. RR1, RR2, RR3 and RR4 are defined in Section 6.

Table 7. Comparison of gust factors based on Durst, Kraye and Marshall, and FCMP hurricane winds at 10 m elevation

$t$ (sec)		1	2	3	5	10	20	30	60
$GF(1hr,t)$	Durst (1960)	1.56	1.54	1.52	1.48	1.43	1.37	1.32	1.25
	K&M (1992)*	1.73	1.69	1.66	1.62	1.55	1.47	1.42	1.32
	FCMP: RR3**	1.66	1.62	1.59	1.54	1.47	1.38	1.33	1.26
	FCMP: RR4**	1.79	1.73	1.69	1.64	1.57	1.47	1.43	1.35

\* Kraye and Marshall (1992)

\*\* RR: roughness regime. RR3: [0.008 m – 0.03 m); RR4: [0.03 m – 0.06 m)

Table A.1 Actual gust factor and turbulence intensity ordinates at 10 m elevation

Variables		Sea surface		Over land	
		RR1	RR2	RR3	RR4
Anemometer Height $z$ (m)		10	10	10	10
Mean Wind Speed $U$ ( $ms^{-1}$ )		18.01	17.79	18.31	16.95
Turbulence Intensity	$\gamma_{TI}$	1.03	1.02	1.05	1.05
	$TI^F$ (%)	11.83	13.34	17.75	20.43
	$TI^A$ (%)	12.18	13.61	18.64	21.45
Gust Factor	$v^F$	0.22	0.24	0.27	0.24
	$\overline{K}^F$	3.81	3.83	3.86	3.83
	$GF^F$	1.45	1.51	1.69	1.78
	$v^A$	0.43	0.40	0.48	0.47
	$\overline{K}^A$	3.98	3.97	4.01	4.01
	$GF^A$	1.48	1.54	1.75	1.86
	$\gamma_{GF}$	1.02	1.02	1.04	1.04

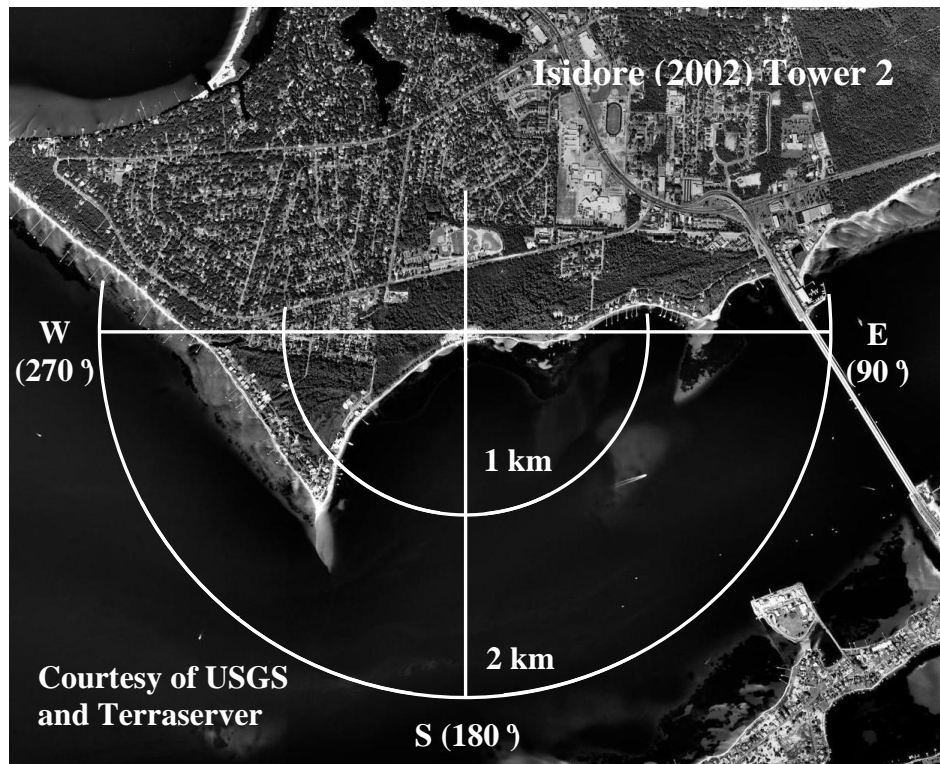
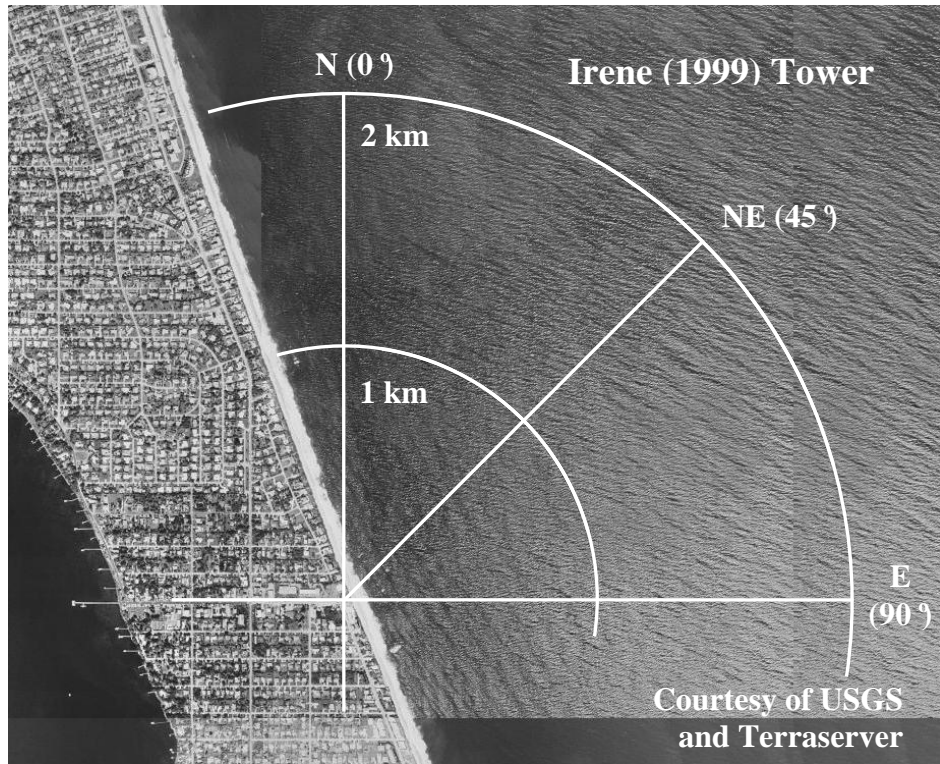


Figure 1. FCMP tower sites selected for analysis

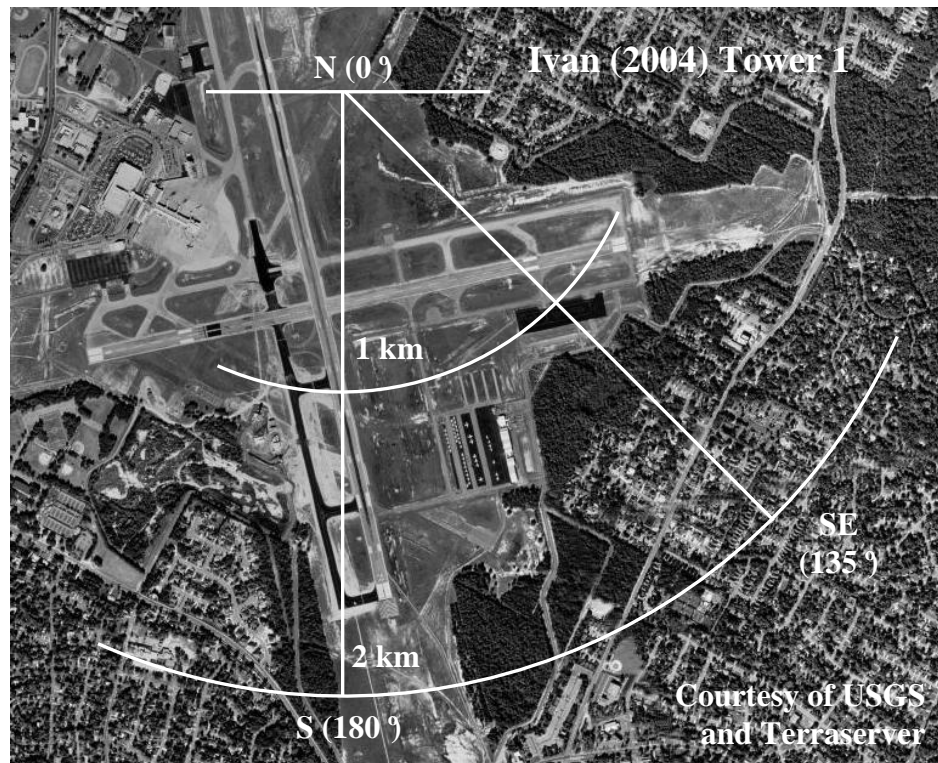
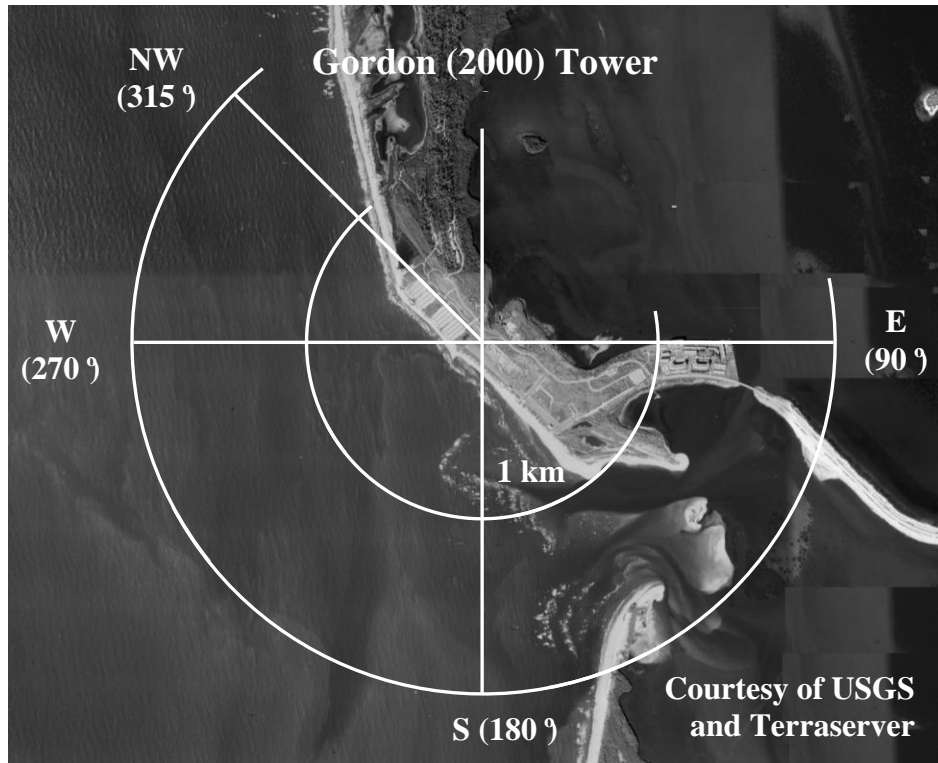


Figure 1. (Continued)

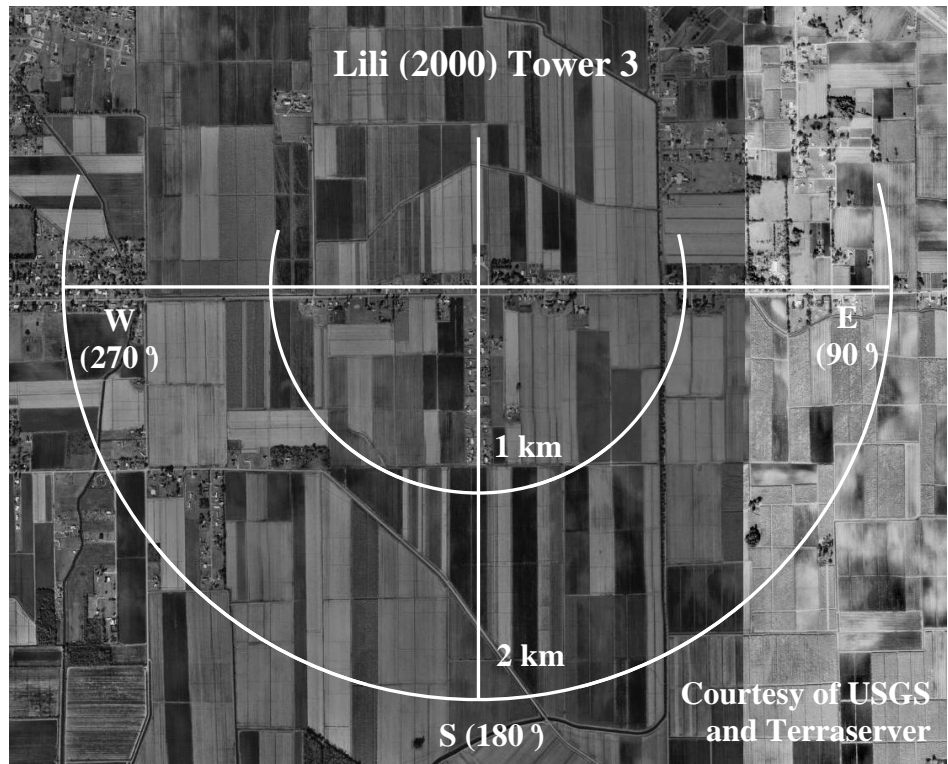
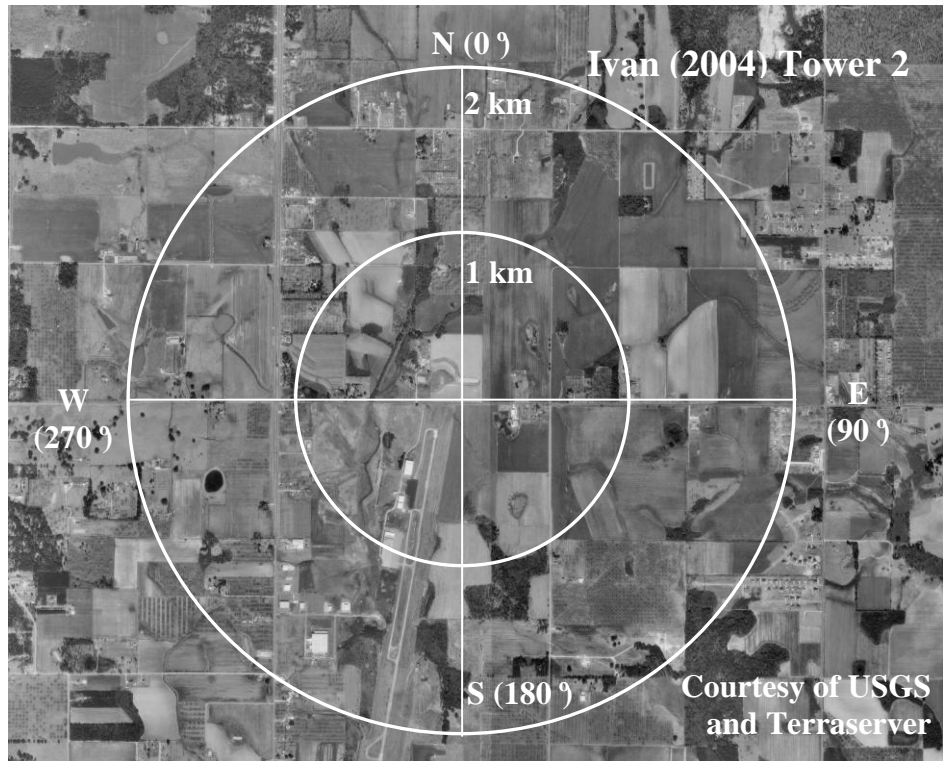


Figure 1. (Continued)

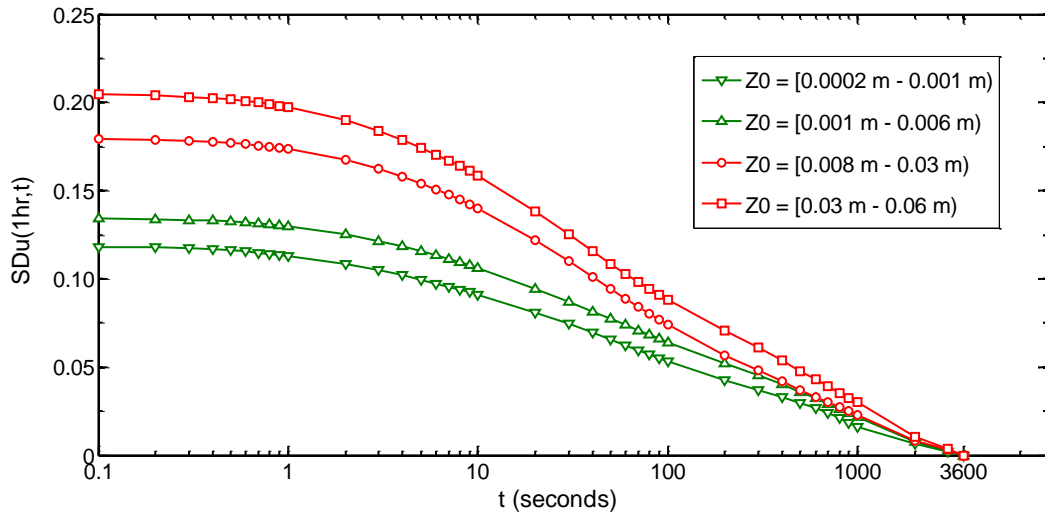


Figure 2. Estimated normalized standard deviation at 10 m elevation for various surface roughness length

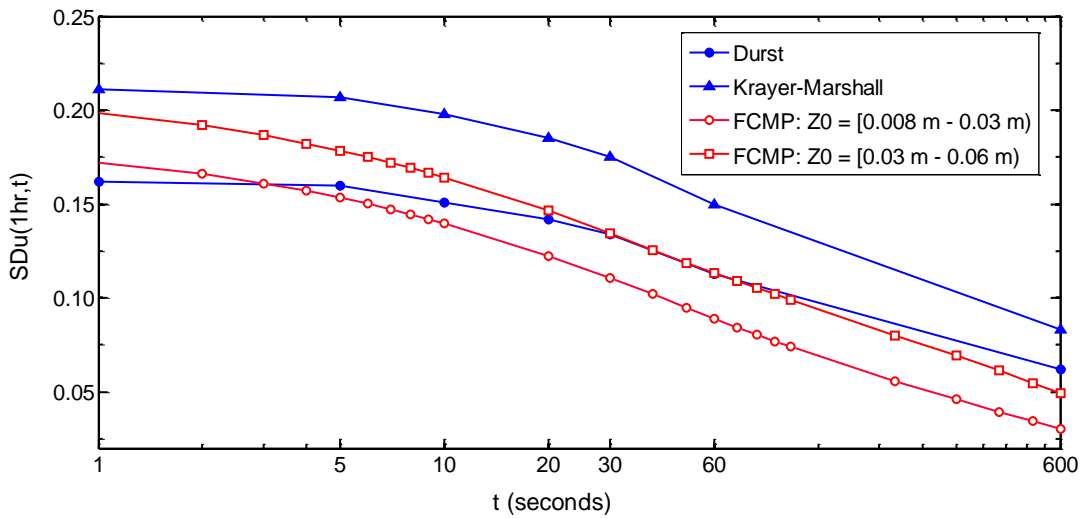


Figure 3. Comparison of normalized standard deviations at 10 m elevation over open terrain

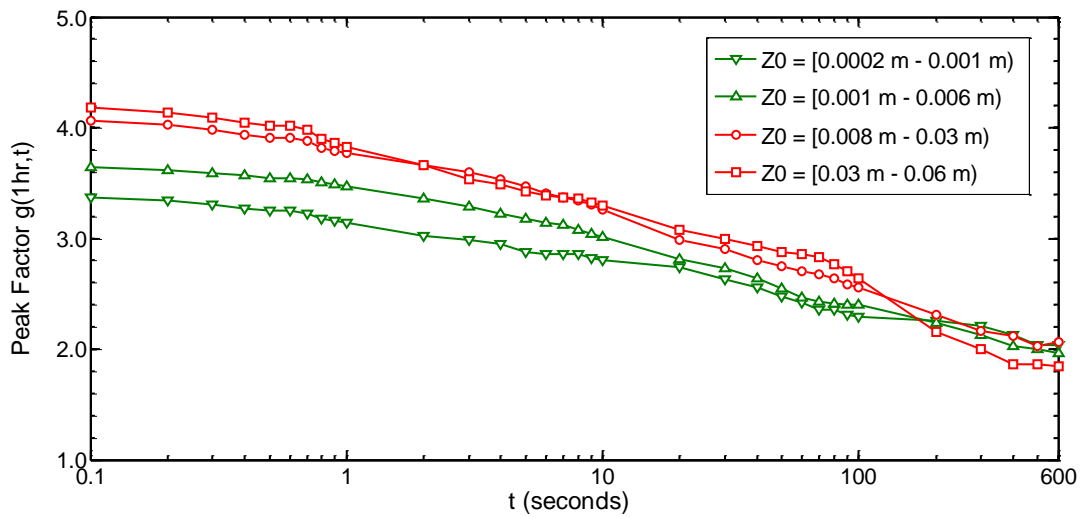


Figure 4. Estimated peak factors at 10 m elevation for terrains with various surface roughness lengths

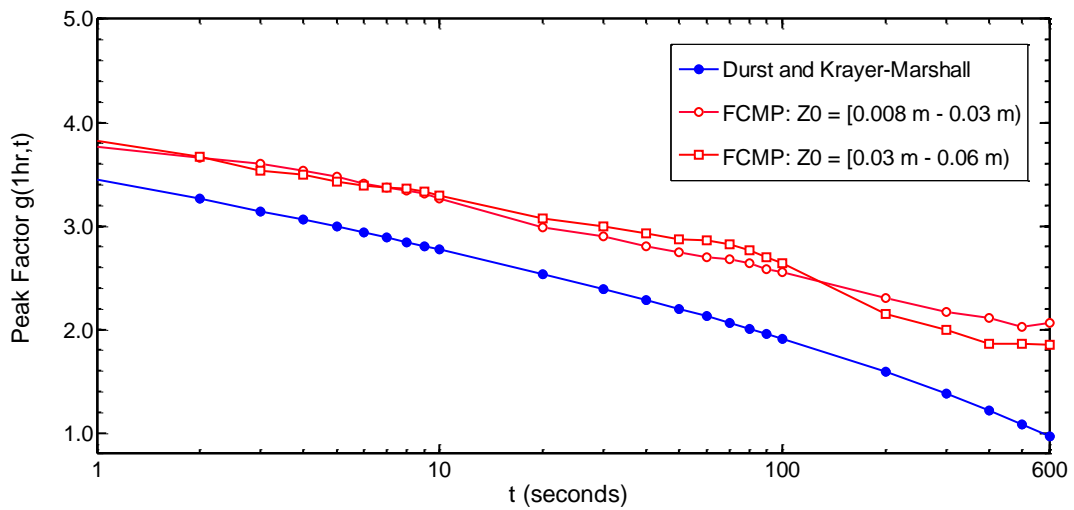


Figure 5. Comparison of peak factors at 10 m elevation over open terrain

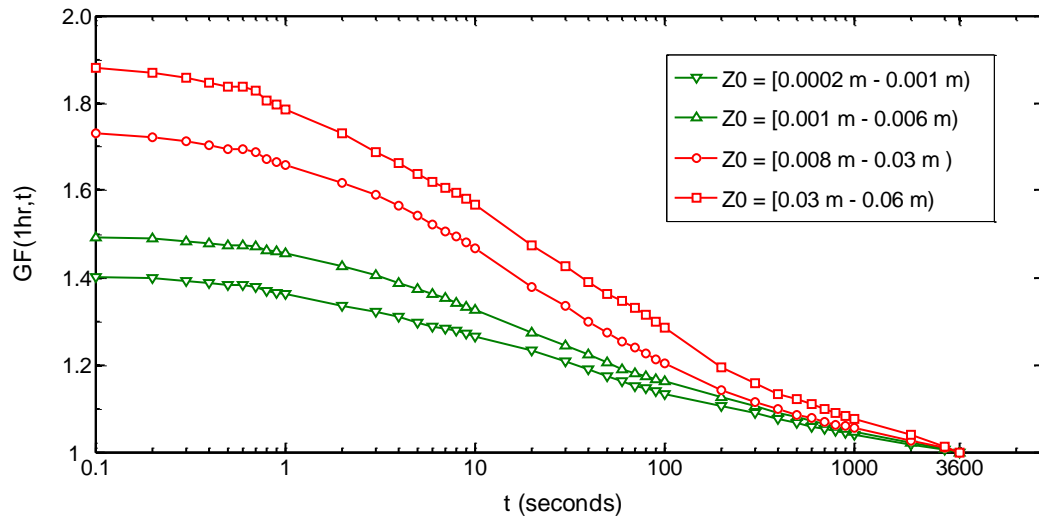


Figure 6. Gust factors at 10 m elevation for terrains with various surface roughness lengths

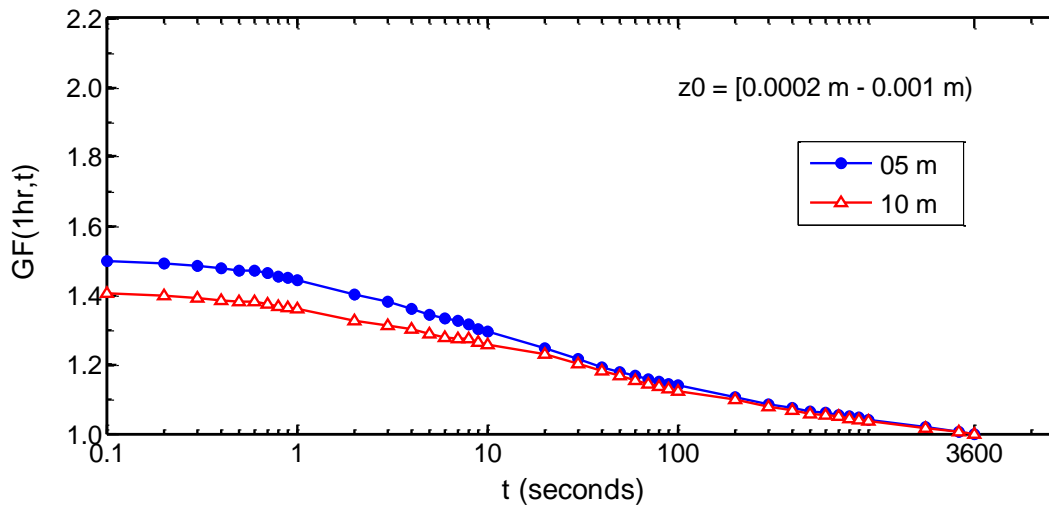


Figure 7. Estimated gust factors for various observation heights (5 m and 10 m) and surface roughness regimes

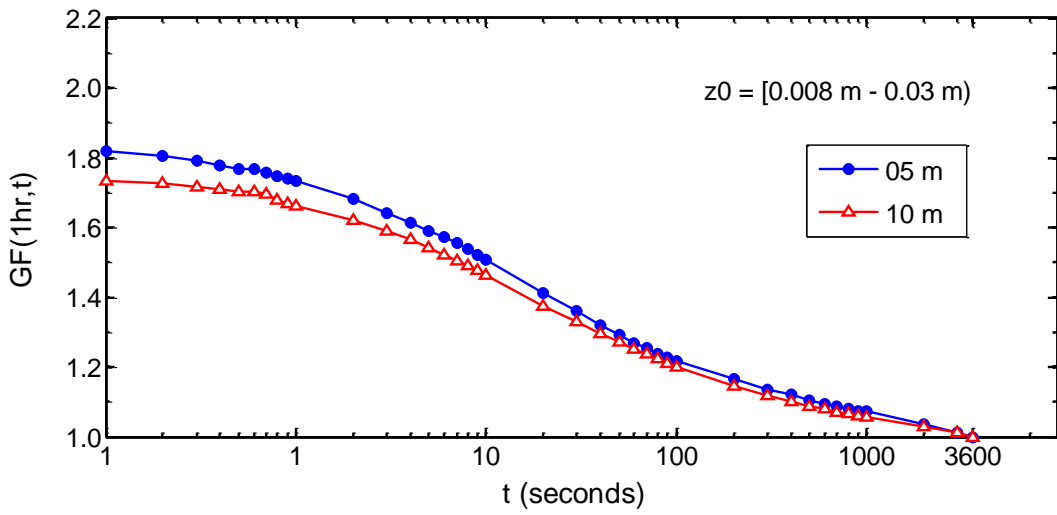
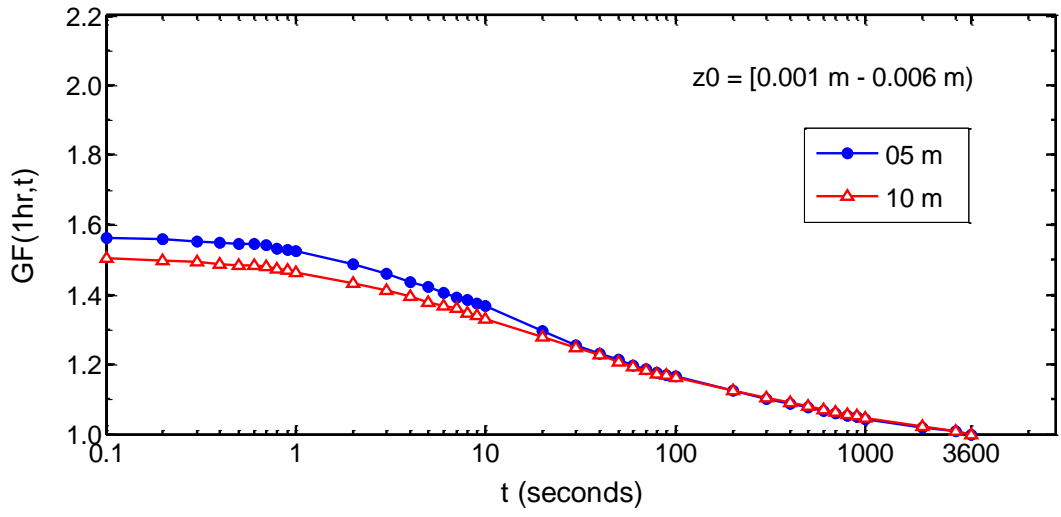


Figure 7. (Continued)

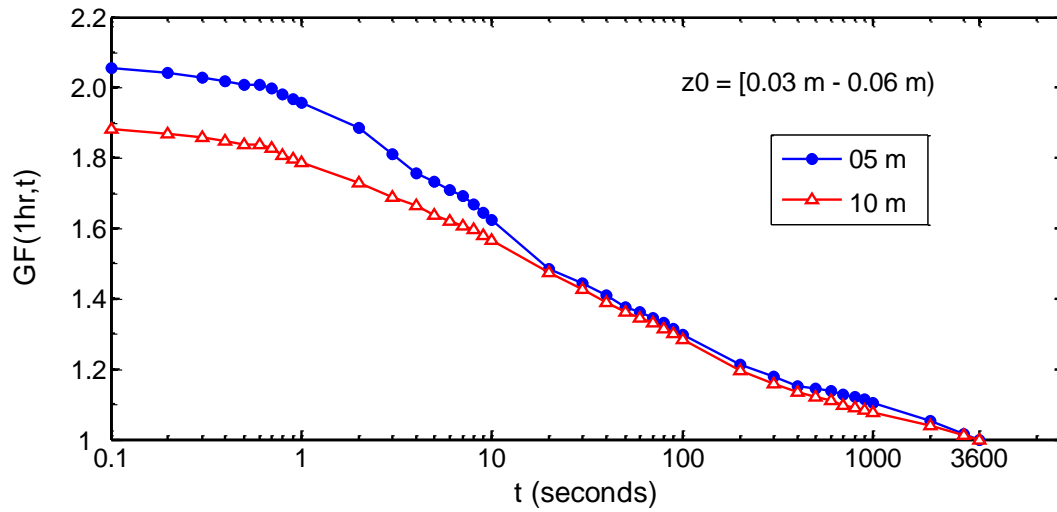


Figure 7. (Continued)

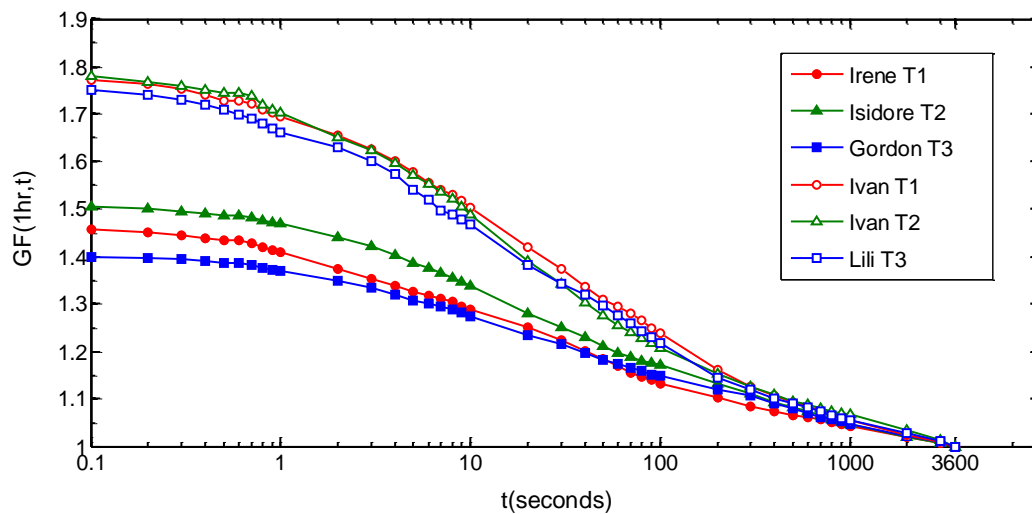


Figure 8. Gust factors at 10 m elevation for six hurricane records

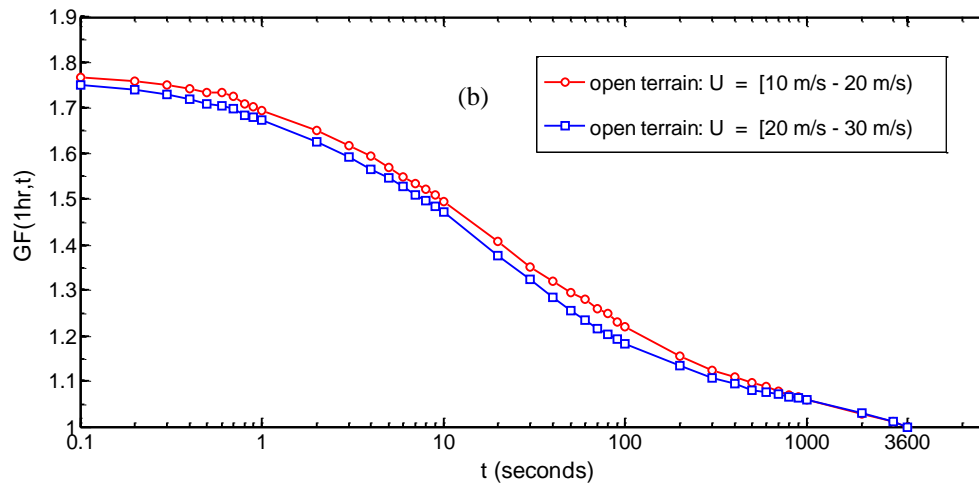
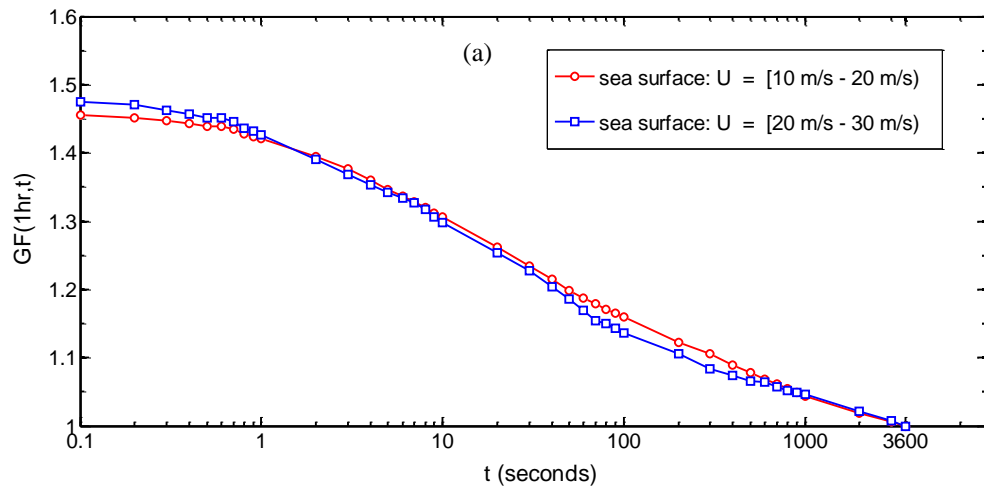


Figure 9. Variation of gust factors with wind speed at 10 m elevation

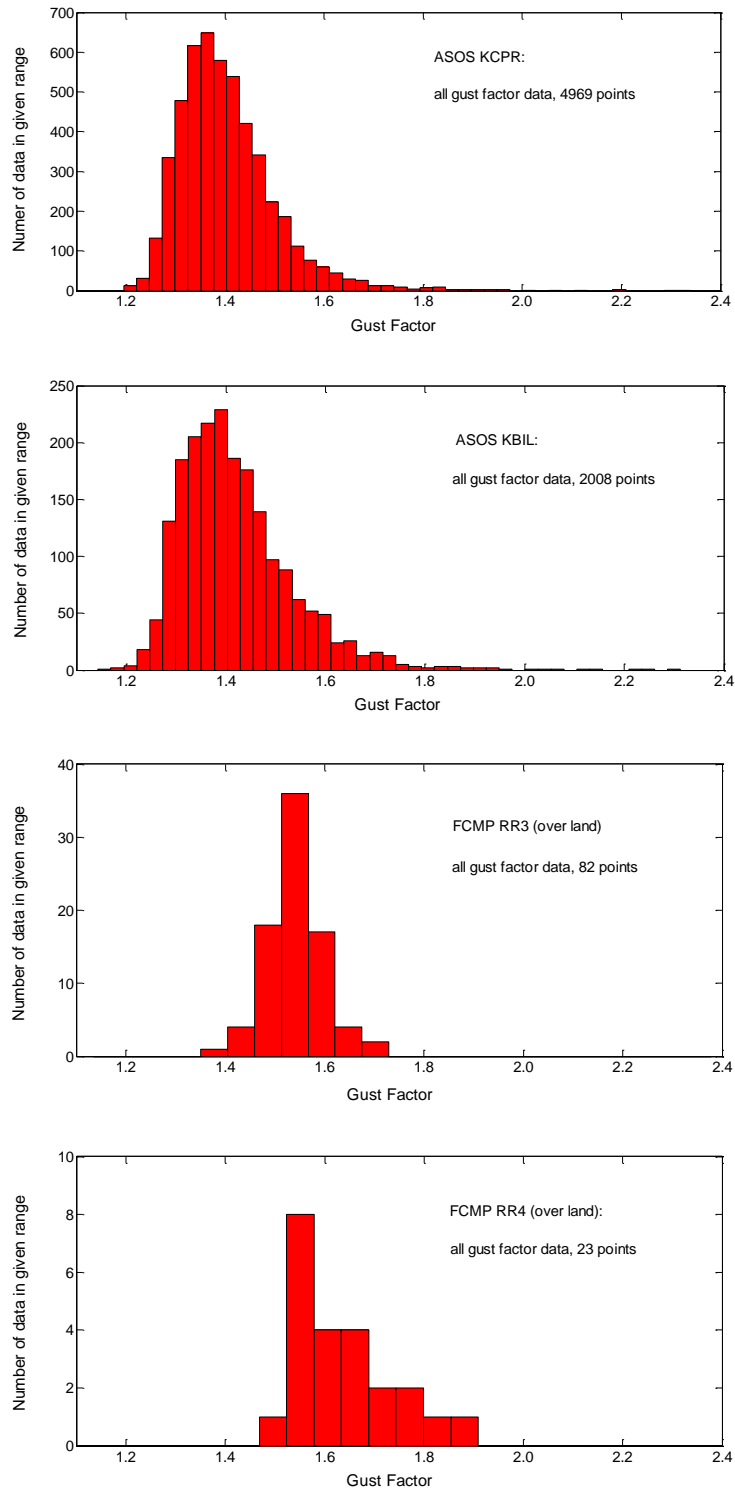


Figure 10. Histogram of gust factors based on hourly wind speeds at 10 m elevation

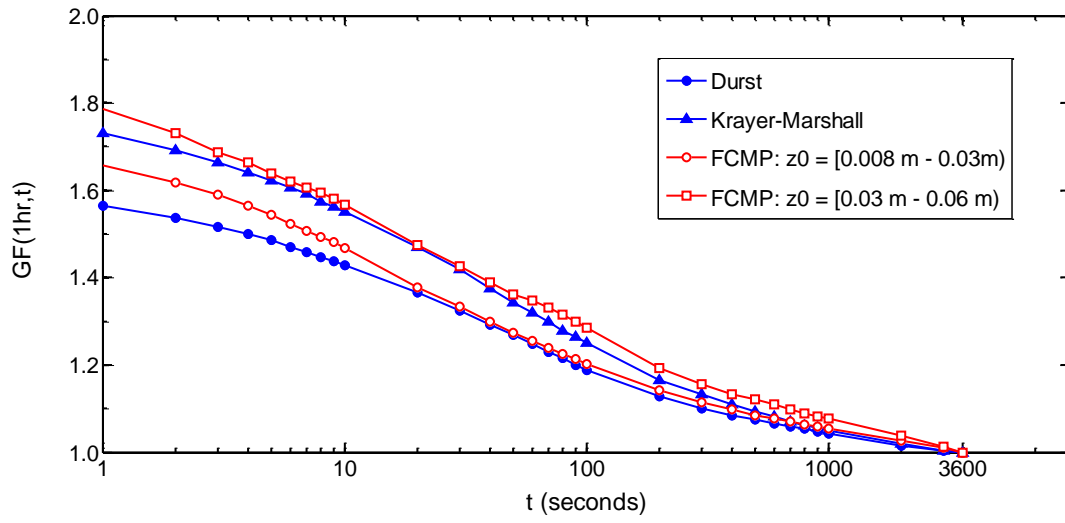


Figure 11. Comparison of gust factor curves of wind speed at 10 m elevation

## **IV. HURRICANE WIND POWER SPECTRA, CO-SPECTRA, AND INTEGRAL LENGTH SCALES**

### **Abstract**

Atmospheric turbulence is an important factor in the modeling of wind forces on structures and the losses they produce in extreme wind events. However, while turbulence in non-hurricane winds has been thoroughly researched, turbulence in hurricanes that affect the Gulf and Atlantic coasts has only recently been the object of systematic study. In this Chapter, Florida Coastal Monitoring Program surface wind measurements over sea surface and open flat terrain are used to estimate hurricane wind spectra and co-spectra as well as integral length scales. From the analyses of wind speeds obtained from six towers in five hurricanes it can be concluded with high confidence that the turbulent energy at lower frequencies is considerably higher in hurricane than in non-hurricane winds. Estimates of turbulence spectra, co-spectra, and integral turbulence scales presented in the Chapter can be used for the development in experimental facilities of hurricane wind flows and the forces they induce on structures. Information on the variability of turbulence features, needed for structural reliability studies, is also presented.

### **1. Introduction**

Turbulent fluctuations in the surface layer of the atmosphere have a significant effect on wind loads and the losses they produce in high winds (Cramer, 1960; Garg et al., 1997). While much research has been performed on turbulence structure, it has largely

been concerned with non-hurricane winds; investigations into wind turbulence features in strong hurricane winds, particularly those affecting the Gulf and Atlantic coasts, have been much less active. The purpose of this Chapter is to present results of hurricane wind speed analyses with a view to improving current knowledge on their turbulence spectra, co-spectra, and integral turbulence scales.

Turbulence spectra provide information on the frequency distribution of the turbulent kinetic energy (TKE) of the various fluctuating velocity components. Of great interest from a structural engineering point of view are turbulence fluctuations in the surface layer of the atmospheric flow. The basic features of a typical surface wind velocity spectrum were modeled by Van der Hoven (1957). Two major spectral peaks are identified in the spectrum, one at a period corresponding to the passage of large scale weather systems and one at a period corresponding to micrometeorological scale turbulence generated by surface roughness. The spectral gap with an approximate time scale of one hour appears as a large valley separating the synoptic scale peak from the micrometeorological scale peak (Stull, 1988). This Chapter is concerned with turbulence on the micrometeorological scale.

The Florida Coastal Monitoring Program (FCMP) provides an opportunity for investigating turbulence characteristics of hurricane winds. FCMP is focusing on investigating surface level hurricane wind behavior and the resultant wind loads on low-rise structures. In this Chapter spectra and co-spectra of the wind velocity turbulence and integral length scales in the surface layer are described using hurricane wind data obtained from the FCMP. The Chapter compares estimates of spectra, co-spectra and

integral length scales obtained in this study for flow over open terrain and over water with estimates obtained by other investigators. In addition, the Chapter examines the variability of the turbulent flow features from hurricane to hurricane or, within the same hurricane, from record to record.

The Chapter is organized as follows. Section 2 presents fundamentals pertaining to turbulence on the micrometeorological scale. Sections 3 and 4 describe the hurricane wind speed data being analyzed in this Chapter, and their mean wind speed characteristics, respectively. Sections 5 and 6 present estimates of the surface roughness lengths around the six selected FCMP tower sites and the integral length scales of the hurricane winds, respectively. Section 7 presents the power spectra and co-spectra estimates and comparisons with results obtained by other investigators. Section 8 presents the conclusions of this work.

## **2. Turbulence on the Micrometeorological Scale: Fundamentals**

That spectrum of turbulence on the micrometeorological scale consists of three different regions: the energy-input or energy-containing sub-range, the inertial sub-range, and the dissipation sub-range (Panchev, 1971; Pasquill, 1974). TKE is produced in the energy-containing sub-range and is transferred into the inertial sub-range. TKE is then transferred from the inertial sub-range to the dissipation range, where it is dissipated through viscous effects (Hinze, 1975; Arya, 2001).

Spectral analysis based on field experiments and statistical theories of turbulence is useful in the study of turbulent characteristics and the energy distribution. According to

Kolmogorov's similarity hypothesis, in a flow with sufficiently large Reynolds number  $R_e$  the turbulence in the inertial sub-range can be considered locally homogeneous and isotropic. The velocity spectral density  $E(k)$  in the inertial sub-range depends for any given wave number  $k$  only on the TKE dissipation rate:

$$E(k) = \alpha \varepsilon^{2/3} k^{-5/3} \quad (1)$$

where  $\alpha$  is the Kolmogorov constant,  $\varepsilon$  is energy dissipation rate,  $k$  is the wave number defined as  $k = 2\pi/\lambda$ , and  $\lambda$  is the wave length.

For the low-frequency turbulent sub-range in neutrally stratified flows, the component spectral densities vary in proportion to the square of the friction velocity  $u_*$  (Højstrup et al., 1990):

$$S_{aa}(n \rightarrow 0) \propto u_*^2 \quad (2)$$

where  $n$  is the frequency in Hz.

The general form of the one-dimensional full-scale velocity spectrum in the neutral atmospheric surface layer can be written as (Kaimal et al., 1972; Teunissen, 1980; Olesen et al., 1984; Tieleman, 1995):

$$\frac{n S_{aa}(n)}{u_*^2} = \frac{A \hat{f}}{(1 + B \hat{f}^\alpha)^\beta}, \quad aa = (uu, vv, ww) \quad (3)$$

where  $\hat{f} = n\Lambda/U(z)$ ;  $\Lambda$  is a length scale, e.g., the height above ground ( $\Lambda = z$ ), or the longitudinal integral length scale at height  $z$  above the surface ( $\Lambda = L_u^x$ );  $U(z)$  is the longitudinal mean wind speed measured at  $z$ ;  $u, v, w$  are the longitudinal, lateral, and

vertical components, respectively. The coefficients  $A$  and  $B$  affect the position of the spectral density function. The exponents  $\alpha$  and  $\beta$  determine the spectrum shape. Estimated values of the coefficients  $A$  and  $B$  and the exponents  $\alpha$  and  $\beta$  are presented in Section 7.3.

### 3. Hurricane Wind Data Measurements

This study uses surface wind data with 10 Hz resolution collected in real time during hurricane passages to evaluate the wind spectra, co-spectra and integral length scales of hurricane winds. The Young anemometry system measures the horizontal wind speed and direction, and the vertical wind speed at 5 m and 10 m levels (Masters, 2004). The measurement system mechanically filters the amplitudes of short wavelength gusts due to the response characteristics of the wind anemometry (Schroeder and Smith, 2003). For this reason, the measurements are accurate only for low-frequency part of the spectrum (i.e., for reduced frequencies  $f = nz/U(z) < 0.2$ , say). For higher frequencies Kolmogorov's similarity hypothesis may be assumed to hold, so the actual spectral ordinates would not differ from those measured in non-hurricane winds.

This study uses wind data collected during five hurricane passages, namely Hurricanes Irene (1999), Gordon (2000), Isidore (2002), Lili (2002), and Ivan (2004). Six selected FCMP observation sites were in coastal areas.

For *Hurricane Irene* (1999) the FCMP tower (named *Irene T1*) was located in Melbourne Beach, Florida (28 04'07.0"N – 80 33'25.0"W); west of the sea shoreline.

For *Hurricane Gordon* (2000) the FCMP tower (named *Gordon T3*) was deployed at the Honeymoon Island, Florida (28°03'41"N – 82°49'44"W), northeast of the sea shoreline.

For *Hurricane Isidore* (2002) the FCMP tower (named *Isidore T2*) was deployed at the Gulf Breeze, Florida (30°21'08"N – 87°10'25.0"W); north of the sea shoreline.

For *Hurricane Lili* (2002) the FCMP tower (named *Lili T3*) was deployed at Lydia, Louisiana (29°54'50"N – 91°45'35"W). Around the tower was flat open land with hardly any obstacles.

For *Hurricane Ivan* (2004) one FCMP tower (named *Ivan T1*) was located in Pensacola Regional Airport, Florida (30°28'45.4"N – 87°11'12.8"W), and another FCMP tower (named *Ivan T2*) was located in Fairhope, Alabama (30°28'21.0"N – 87°52'30.0"W), north of the Fairhope Municipal Airport.

Irene T1 captured the surface wind from 0507 UTC to 1639 UTC on 16 October in 1999. Gordon T3 collected the surface wind from 1730 UTC on 17 September to 1250 UTC on 18 September in 2000. Isidore T2 collected the surface wind from 2044 UTC on 26 September to 1136 UTC on 28 September in 2002. Lili T3 went operational between 0415 UTC on 3 October and 1802 UTC on 4 October in 2002. Ivan T1 and Ivan T2 collected the surface wind from 2026 UTC on 14 September to 2000 UTC on 16 September and from 0053 UTC to 1453 UTC on 16 September in 2004, respectively. Wind data collected from the six selected FCMP towers (Irene T1, Isidore T2, Gordon T3, Ivan T1, Ivan T2 and Lili T3) were pre-processed and only data sets satisfying quality-control requirements were used for this study. Data pre-processing and data quality-

control requirements include: (1) separate analysis of hourly record segments with overlapping 15-min segments; (2) decomposition of the records into longitudinal, lateral, and vertical components; (3) 10 m/s at 10 m height was the minimum requirement for segment mean wind speed, to satisfy the strong wind and neutral stability conditions; (4) segments with direction shifts larger than 20 ° were not considered, to avoid records in which wind speeds may correspond to more than one terrain exposure (Masters, 2004).

#### **4. Basic Mean Wind Speeds**

In this Chapter, the wind direction is measured clockwise from the north. For Irene T1, Isidore T2 and Gordon T3, the wind characteristics are governed by the sea surface roughness upwind of the location of interest; for Ivan T1, Ivan T2 and Lili T3, the wind characteristics are governed by flat open land terrain roughness. The hourly mean wind speeds at 10 m height vary from 18.8 m/s to 25.5 m/s for Irene T1, from 12.1 m/s to 18.4 m/s for Isidore T2, from 14.7 m/s to 18.5 m/s for Gordon T3, from 11.1 m/s to 29.9 m/s for Ivan T1, from 15.8 m/s to 24.3 m/s for Ivan T2, and from 11.5 m/s to 22.5 m/s for Lili T3, as shown in Table 1.

The observed 3-sec peak gusts on site are 35.5 m/s, 27.1 m/s, 29.8 m/s, 47.5 m/s, 39.9 m/s and 35.8 m/s for Irene T1, Isidore T2, Gordon T3, Ivan T1, Ivan T2 and Lili T3, respectively. The mean wind speed increased with height for all five hurricanes. Mean wind direction time histories are similar at the two different observation heights (5 m and 10 m) for each of the six tower observations.

## 5. Estimation of Surface Roughness Lengths

The flow features are influenced by the underlying terrain roughness. Given the values of the longitudinal turbulence intensity ( $TI_u$ ) at measurement height  $z$ , the logarithmic law in neutral conditions can be used to estimate the surface roughness length  $z_0$  as follows (Wieringa, 1993):

$$z_0 = \exp(\ln z - \sqrt{\beta} \cdot \kappa / TI_u) \quad (4)$$

where  $\sqrt{\beta} = \sigma_u / u_*$  is the ratio of the standard deviation ( $\sigma_u$ ) of longitudinal wind component to the friction velocity ( $u_*$ );  $\kappa = 0.4$  is the von Karman constant.

The friction velocity  $u_*$  is defined as

$$u_* = \left( \overline{u'w'^2} + \overline{v'w'^2} \right)^{1/4} \quad (5)$$

where  $u'$ ,  $v'$ , and  $w'$  are the longitudinal, lateral, and vertical wind fluctuation components, respectively.

According to Lumley and Panofsky (1964), for a fully developed neutrally stratified flow within the surface layer,  $\sqrt{\beta}$  is a constant and is independent of the underlying terrain roughness. According to Deaves (1981),  $\sqrt{\beta} \approx 2.79$  appears to describe adequately fully developed non-hurricane equilibrium flows over open terrain. Values of  $\sqrt{\beta}$  obtained from the FCMP wind measurements are typically higher. The mean values of  $\sqrt{\beta}$  are: 4.08, 3.32, 3.10 over water for Irene T1, Isidore T2, and Gordon T3, respectively, and 3.38, 2.85 and 2.72 over open terrain for Ivan T1, Ivan T2 and Lili T3,

respectively. The ratio between the largest to the smallest  $\sqrt{\beta}$  is  $4.08/3.10 \approx 1.32$  for flow over sea surface and  $3.38/2.72 \approx 1.24$  for flow over open terrain. In one of the three open terrain records,  $\sqrt{\beta}$  exceeds by about 20 % the typical value proposed by Deaves (1981).

Based on surface wind measurements from the FCMP towers under strong wind conditions, the surface roughness lengths around the tower sites were estimated by using Eq. (4) and wind speeds at 10 m elevation. For sea surface (Irene T1, Isidore T2 and Gordon T3), the surface roughness lengths vary from 0.0002 m to 0.006 m; for open terrain (Ivan T1, Ivan T2 and Lili T3), the surface roughness lengths vary from 0.0080 m to 0.0589 m. Estimated mean surface roughness lengths around the tower sites are shown in Table 2. The estimates of surface roughness lengths are used in Section 7.

## 6. Estimation of Integral Length Scales

Atmospheric turbulence affects the aerodynamic response of structures in general and the dynamic response of flexible structures in particular (see, e.g., Simiu and Scanlan, 1996). Integral scales of turbulence are measures of the average size of the turbulent eddies of the flow. The longitudinal integral length scale ( $L_u^x$ ) in meters is defined as:

$$L_u^x = U \int_0^{\infty} \rho_{uu}(\tau) d\tau, \quad (6)$$

where  $U$  is the mean wind speed in m/s,  $\tau$  is the time lag value in seconds and  $\rho_{uu}$  is the autocorrelation coefficient function of the longitudinal wind component, defined as:

$$\rho_{uu}(\tau) = \frac{E[\{u(t) - U\}\{u(t + \tau) - U\}]}{\sigma_u^2} \quad (7)$$

where  $E[\phi(t)]$  is the expected value of the stationary random process  $\{\phi(t)\}$ .

Estimates of both  $\rho_{uu}$  and  $L_u^x$  values depend upon the length of the record being analyzed. For Irene T1, the variations of  $\rho_{uu}$  from longitudinal wind velocities at 10 m height with different segment lengths (10, 30, and 60 minutes) as a function of the lag time  $\tau$  (in seconds) are shown in Fig. 1 (a). Analyses of Isidore T2, Gordon T3, Ivan T1, Ivan T2 and Lili T3 indicate similar results. Figure 1 (b) shows the variations of  $\rho_{uu}$  at 10 m height with lag time  $\tau$ , based on one-hour segment lengths for Irene T1, Isidore T2, Ivan T2 and Lili T3. Similar results were obtained for Gordon T3 and Ivan T1.

In theory, the definition of the integral length scale pertains to an infinitely long record. In practice, since the record lengths are limited, the largest wind speed record over which the wind is stationary (in this case 60 min) provides the physically most relevant estimate of the length scale.

For the six selected FCMP observation sites, estimates of  $L_u^x$  values for various segment lengths are shown in Table 3. As expected, the longitudinal length scale increases with segment length. At 10m observation height, the 10-minute longitudinal integral length scales are 160 m, 131 m, 176 m, 154 m, 123 m and 94 m and hourly mean values are 594 m, 446 m, 365 m, 240 m, 336 m and 226 m for Irene T1, Isidore T2, Gordon T3, Ivan T1, Ivan T2 and Lili T3, respectively. It is noted that length scales are typically larger over sea surface (Irene T1, Isidore T2 and Gordon T3) than over open

terrain (Ivan T1, Ivan T2 and Lili T3). It is also noted that the length scales vary significantly from hurricane to hurricane, the ratio between the largest to the smallest length scale for 10 m elevation and a 60 min time interval being  $594/365 \approx 1.6$  for flow over sea surface, and  $366/226 \approx 1.6$  for flow over open terrain.

A linear regression was applied to fit the variations of  $L_u^x$  values with different average segment lengths, as shown in Fig. 2. The resulting fitted curve is:

$$L_u^x(T)/L_u^x(3600) = 0.272 + 0.728 \cdot T/3600 \quad (8)$$

where  $T$  is the average segment length in seconds.

The longitudinal length scale increases with the observational height as shown in Table 3 and Fig. 3. The ratios of the integral length scale at 5 m observational height to integral scale at 10 m are 0.68 and 0.83 for winds over sea surface and open terrain, respectively.

## 7. Power Spectra and Co-Spectra: Estimation and Variability

For real-valued stationary signals, power spectra and co-spectra functions describe the power distributions of signal or time series in the frequency domain and were computed by using the Welch method based on the direct Fast Fourier Transforms (FFT) of the original stationary signals. The Hanning window was used to suppress the side-lobe leakage. The computational procedure for the Welch method is described in detail by Bendat and Piersol (2000). The power spectra and co-spectra are estimated by averaging the respective power spectra and co-spectra based on the individual one-hour wind speed segments.

In this section, power spectra and co-spectra of wind velocity fluctuations in the surface layer are estimated and modeled, and are compared with results and models available in the literature.

### *7.1 Wind spectra and co-spectra over surfaces with various roughness lengths*

Wind spectra and co-spectra are affected by the upstream roughness length. Estimates of surface roughness lengths in Section 5 were used to stratify the observed wind spectra and co-spectra into two roughness regimes,  $0.0002 \text{ m} \leq z_0 \leq 0.006 \text{ m}$  corresponding to sea surface, and  $0.008 \text{ m} \leq z_0 \leq 0.06 \text{ m}$  corresponding to open terrain.

Figures 4 and 5 present the estimated power spectra at 10 m elevation for sea surface ( $0.0002 \text{ m} \leq z_0 \leq 0.006 \text{ m}$ , for Irene T1, Isidore T2 and Gordon T3) and open terrain ( $0.008 \text{ m} \leq z_0 \leq 0.06 \text{ m}$ , for Ivan T1, Ivan T2 and Lili T3), respectively. The resulting fitted curves, as well as mean curves, for power spectra of longitudinal ( $u$ ), lateral ( $v$ ) and vertical ( $w$ ) wind components at 10 m height over sea surface and open terrain are plotted in Figs. 6 and 7.

The square of friction velocity  $u_*$  (Eq. 5) and the frequency  $n$  were used to normalize the power spectral densities. The observational height  $z$  and mean wind speed  $U$  at height  $z$  were used to normalize the frequency  $n$ , that is, the reduced frequency is  $f = nz/U$ . It was found that the estimated power spectra fall faster at the high-frequency inertial subrange than the spectra yielded by Kolmogorov theory. The lack of high-frequency energy is due to the response characteristics of the wind anemometry, which

mechanically filters the amplitudes of short wavelength gusts. For this reason, as was noted earlier, the FCMP data are useful only for the lower frequency part of the spectrum, which is plotted in Figs. 6 and 7.

For sea surface, Figs. 4 and 6 show that the normalized power spectral values for longitudinal, lateral and vertical wind components from Irene T1 are higher than those from Isidore T2 and Gordon T3. For example, for  $f = 0.01$  the ratio of the largest to the smallest power spectrum ordinates is  $3.00/1.78 \approx 1.69$  for the longitudinal component and  $1.00/0.57 \approx 1.75$  for the lateral component, as shown in Fig. 6. The differences between the spectra do not appear to be related to the respective surface roughness lengths (see Table 2).

For open terrain, Figs. 5 and 7 show that the normalized power spectral values for longitudinal and lateral wind components from Ivan T1 are higher than those from Ivan T2 and Lili T3 for  $f < 0.02$ . For example, for  $f = 0.01$  the ratio of the largest to the smallest power spectrum ordinates is  $2.20/1.60 \approx 1.38$  for the longitudinal component and  $0.81/0.50 \approx 1.62$  for the lateral component, as shown in Fig. 7.

Wind spectra and co-spectra for flow over water and over open terrain are shown in Fig. 8. Spectral values for longitudinal and lateral wind components for winds over sea surface are higher than for winds over open flat terrain. For example, for the longitudinal power spectra  $S_{uu}$ , the normalized spectral peaks over sea surface and over open terrain were 2.20 and 1.80, respectively, that is, the ratio of the peaks was  $2.20/1.80 \approx 1.22$ . Similar results were found for lateral power spectra  $S_{vv}$ . The spectra of the vertical wind

component and the  $u-w$  co-spectral values over the sea surface are comparable to the values over the open terrain, as shown in Fig. 8.

### *7.2 Wind spectra and co-spectra for various observational heights and wind speeds*

The estimated power spectra and co-spectra based on one-hour wind speed segments at 10 m and 5 m elevation are plotted in Fig. 9 for open exposure with roughness lengths  $0.008 \text{ m} \leq z_0 \leq 0.06 \text{ m}$  (see Table 2). Estimates of the normalized power spectra at 5 m height are larger than those at 10 m height for longitudinal and lateral wind components. However, differences are smaller for vertical wind spectra and  $u-w$  co-spectra.

To investigate the effects of wind speed on the variation of the normalized power spectra and co-spectra of hurricane winds, the estimated power spectra and co-spectra at 10 m elevation for open exposure were separated for two mean wind speed  $U$  ranges,  $10 \text{ m/s} \leq U \leq 20 \text{ m/s}$  and  $20 \text{ m/s} \leq U \leq 30 \text{ m/s}$ . Figure 10 shows that the estimated power spectra and co-spectra of hurricane wind velocity fluctuations are comparable for different mean wind speed regimes, as expected.

### *7.3 Comparison of estimated power spectra and co-spectra with estimates reported by other investigators*

In this section, the estimated power spectra and co-spectra based on one-hour wind speed segments at 10 m height over open exposure ( $0.008 \text{ m} \leq z_0 \leq 0.06 \text{ m}$ ) are compared to the wind spectra and co-spectra curves obtained for non-hurricane winds by Lumley and Panofsky (1964), Kaimal et al. (1972) and Tieleman (1995). As mentioned earlier,

most of the spectral models for the neutral atmospheric surface layer are of the general form of Eq. (3) and are shown in Table 4. Equations and coefficients of spectra and co-spectra based on the analyses presented in this Chapter are given in Appendix A and Table A1, respectively.

For power spectra of longitudinal velocity  $S_{uu}$ , Fig. 11 (a) shows the normalized longitudinal velocity spectra  $nS_{uu}(n)/u_*^2$  as a function of reduced frequency  $f$ . Compared with the Tieleman and revised Kaimal curves, the estimated mean spectrum for hurricane wind has significantly more energy at lower frequencies ( $f < 0.02$ , say). The estimated normalized spectral peak is about 1.78, higher than the value of 1.30 from the revised Kaimal model and the Tieleman's blunt model.

For power spectra of lateral velocity  $S_{vv}$  and power spectra of vertical velocity  $S_{ww}$ , the normalized spectra are plotted in Figs. 11 (b) and (c). Similar to the longitudinal velocity spectrum, the estimated spectra of  $S_{vv}$  and  $S_{ww}$  for hurricane winds have more energy at lower frequencies than the referenced models for non-hurricane winds.

It follows that, according to the estimates presented in this study, the low-frequency energy content is significantly higher for hurricane than for non-hurricane winds. This result is consistent with results obtained for one hurricane record (Hurricane Bonnie) by Schroeder and Smith (2003).

Based on Kansas experiments, Kaimal et al. (1972) proposed a model for the power co-spectrum  $C_{uw}$  of the longitudinal and the vertical components for non-hurricane winds given by Eq. 9:

$$\frac{-nC_{uw}(n)}{u_*^2} = \frac{14f}{(1+9.6f)^{2.4}} \quad (9)$$

The estimated  $u-w$  co-spectrum  $C_{uw}$  based on the FCMP records is compared with the Kaimal model (Eq. 9) in Fig. 12. The observed normalized peak of 0.3 is lower than the value of 0.45 from the Kaimal model. The reduced frequency of 0.04 corresponding to the observed co-spectrum peak is also lower than the values of 0.15 in the Kaimal model. As indicated earlier, estimates of higher-frequency spectral components for the FCMP records are not accurate owing to the properties of the Young anemometers used in the measurements.

## 8. Conclusions

Using the surface wind measurements collected by FCMP towers (Irene T1, Isidore T2, Gordon T3, Ivan T1, Ivan T2 and Lili T3) during hurricane passages, this study presents estimates of power spectra and co-spectra, and of turbulence integral length scales, of hurricane winds over coastal areas under neutral conditions. The conclusions of this study are:

(1) Compared with power spectral models proposed by other investigators for non-hurricane winds, the observed normalized power spectra of longitudinal, lateral and vertical hurricane wind components have significantly more energy at the lower frequencies. This is in agreement with results obtained for only one hurricane record by Schroeder and Smith (2003). For  $u-w$  co-spectra, the observed co-spectral peaks and the corresponding reduced frequency are lower than the values obtained by Kaimal et al. (1972).

(2) Values of power spectra of longitudinal and lateral wind components over sea surface were higher than those over open terrain, while the spectra of the vertical wind component and the  $u-w$  co-spectral values over the two surface regimes were comparable.

(3) Values of power spectra and co-spectra of hurricane winds at 5 m elevation were larger than those at 10 m elevation, while value of power spectra and co-spectra are comparable for different wind regimes.

(4) Results showed that the longitudinal length scales increase with segment length and elevation. Typically, the longitudinal length scales are lower over open terrain than over sea surface. The ratios between largest and smallest integral turbulence scales at 10 m elevation were about 1.6 for sea surface and open terrain.

(5) For the two three-record sets, the largest ratio of the r.m.s. of the longitudinal velocity fluctuations to the friction velocity  $u_*$  was approximately 1.32 for water surface and 1.24 for open terrain; the variabilities of power spectra were approximately commensurate with the squares of these ratios for all turbulent fluctuations.

## **Appendix A. Coefficients of Power Spectra and Cospectra of Hurricane Winds Based on FCMP Dataset**

The spectra and co-spectra estimated from the FCMP dataset were used to develop a series of power spectral curves for hurricane winds. The results showed that second power numerator and third power denominator polynomials fit the observed spectra and co-spectra best, that is,

$$\frac{nS_{aa}}{u_*^2} = \frac{p_1 f^2 + p_2 f + p_3}{f^3 + q_1 f^2 + q_2 f + q_3}, \quad a = u, v, w \quad (\text{A.1})$$

$$\frac{nC_{uw}}{u_*^2} = \frac{p_1 f^2 + p_2 f + p_3}{f^3 + q_1 f^2 + q_2 f + q_3} \quad (\text{A.2})$$

where  $f$  is the reduced frequency defined earlier, and  $n$  is the frequency in Hz. It is again noted that these curves do not predict correctly the actual variation of the non-dimensionalized spectra with frequency  $f$  for higher frequencies.

Table A1 presents the coefficients  $p_i$  and  $q_i$  ( $i=1,2,3$ ) for power spectra and co-spectra of hurricane wind components at two observational heights and for sea surface and open terrain under near-neutral conditions.

## Table Captions

Table 1: Hourly mean wind speed statistics at 10 m elevation

Table 2: Surface roughness lengths (in meters)

Table 3: Longitudinal integral length scales at 5 m and 10 m elevations

Table 4: Spectral models for the neutral non-hurricane atmospheric surface layer

Table A1. Coefficients of power spectra and co-spectra of hurricane winds at 5 m and 10 m elevations

## Figure Captions

Figure 1. (a) Variation of autocorrelation coefficient with segment length at 10 m elevation for Irene T1;

(b) Autocorrelation coefficient based on one-hour wind speed segments at 10 m elevation at four selected FCMP sites

Figure 2. Integral length scale ratios based on different average segment lengths

Figure 3. Ratios of the integral length scales at 5 m elevation to those at 10 m elevation

Figure 4. Wind spectra at 10 m elevation over sea surface

Figure 5. Wind spectra over at 10 m elevation open terrain

Figure 6. Fitted curves of wind spectra at 10 m elevation over sea surface

Figure 7. Fitted curves of wind spectra at 10 m elevation over open terrain

Figure 8. Wind spectra and co-spectra at 10 m elevation for terrains with various surface roughness lengths

Figure 9. Variation of wind spectra and co-spectra with observational height

Figure 10. Variation of wind spectra and co-spectra with wind speed

Figure 11. (a) Longitudinal wind spectra estimation and comparison at 10 m elevation; (b) Lateral wind spectra estimation and comparison at 10 m elevation; (c) Vertical wind spectra estimation and comparison at 10 m elevation.

Figure 12.  $u-w$  co-spectra comparison at 10 m elevation

## Reference

- Arya, S. P., 2001: Introduction to micrometeorology, 2nd Edition, Academic Press.
- Bendat J. S., and Piersol A. G., 2000: Random data analysis and measurement procedures (3rd Edition). John Wiley & Sons.
- Cramer H. E., 1960: Use of power spectra and scales of turbulence in estimating wind loads, *Meteorological Monographs*, 4 (22), 12-18.
- Deaves D. M., 1981: Terrain-dependence of longitudinal RMS velocities in the neutral atmosphere, *Journal of Wind Engineering and Industrial Aerodynamics*, 8, 259-274.
- Garg R. K., Lou J. X., Kasperski M., 1997: Some features of modeling spectral characteristics of flow in boundary layer wind tunnels, *Journal of Wind Engineering and Industrial Aerodynamics*, 72, 1-12.
- Hinze J. O., 1975: Turbulence, 2nd Edition, McGraw-Hill, New York.
- Højstrup J., Larsen S. E., Madsen P. H., 1990: Power Spectra of Horizontal Wind Components in the Neutral Atmospheric Surface Boundary Layer, Ninth Symposium on Turbulence and Diffusion, AMS, 305-308.
- Kaimal J. C., Wyngaard J. C., Izumi Y., Coté O. R., 1972: Spectral Characteristics of Surface-Layer Turbulence, *Quart. J. Roy. Meteorol. Soc.*, 98, 563-598.
- Lumley J. L., Panofsky H. A., 1964: The structure of atmospheric turbulence, Wiley, New York.
- Masters F. J., 2004: Measurement, modeling and simulation of ground-level tropical cyclone winds. Ph.D. dissertation, University of Florida.
- Olesen H. R., Larsen S. R., Hestrup J., 1984: Modeling velocity spectra in the lower part of the planetary boundary layer. *Bound.-Layer Meteorology*, 29, 285-312.
- Panchev S., 1971: Random Functions and Turbulence. Pergamon Press., Oxford.
- Pasquill F., 1974: Atmospheric diffusion, 2nd Edition, John Wiley and Sons, New York.
- Schroeder J. L., Smith D. A., 2003: Hurricane Bonnie wind flow characteristics as determined from WEMITE, *Journal of Wind Engineering and Industrial Aerodynamics*, 91, 767-789.
- Simiu E., Scanlan R., 1996: Wind Effects on Structures, 3rd Edition, Wiley, New York.
- Stull R. B., 1988: An introduction to boundary layer meteorology, Kluwer Academic Publishers.

- Teunissen H. W., 1980: Structure of mean winds and turbulence in the planetary boundary layer over rural terrain, *Bound.-Layer Meteorology*, 19, 187-221.
- Tieleman H. W., 1995: Universality of velocity spectra, *Journal of Wind Engineering and Industrial Aerodynamics*, 56, 55-69.
- Van Der Hoven, 1957: Power spectrum of horizontal wind speed in the frequency range from 0.0007 to 900 cycles per hour, *Journal of Meteorology*, Vol. 14, 160-164.
- Wieringa J., 1993: Representative roughness parameters for homogeneous terrain. *Boundary Layer Meteorology*, 63, 323–363.

Table 1: Hourly mean wind speed statistics at 10 m elevation

FCMP Tower		Sea surface			Flat open land		
		Irene T1	Isidore T2	Gordon T3	Ivan T1	Ivan T2	Lili T3
Wind direction		(70 ;10 °) CCW*	(110 ;200 °) CW*	(180 ;290 °) CW*	(135 ;240 °) CW*	(50 ;300 °) CW*	(145 ;230 °) CW*
Wind speed (m/s)	min	18.8	12.1	14.7	11.1	15.8	11.5
	max	25.5	18.4	18.5	29.9	24.3	22.5
	mean	22.7	15.5	17.2	19.6	18.8	15.0
	s.d.	2.3	2.2	0.7	5.3	2.5	3.4
Number of segments		30	50	18	37	41	27

\* CW: clockwise; CCW: counter-clockwise (e.g., wind direction at Irene T1 varies counter-clockwise from 70 °to 10 °).

Table 2: Surface roughness lengths (in meters)

FCMP Tower	Sea surface			Flat open land		
	Irene T1	Isidore T2	Gordon T3	Ivan T1	Ivan T2	Lili T3
Min	0.0006	0.0011	0.0002	0.0080	0.0116	0.0082
Max	0.0040	0.0060	0.0014	0.0551	0.0497	0.0589
Mean	0.0015	0.0032	0.0007	0.0222	0.0257	0.0248
s.d.	0.0009	0.0015	0.0004	0.0121	0.0091	0.0147

Table 3: Longitudinal integral length scales at 5 m and 10 m elevations

unit: m

Tower Site	Anemometer height	5min	10min	20min	30min	40min	50min	60min
Irene T1 (sea surface)	5 m	91	123	183	231	297	357	456
	10 m	123	160	229	331	399	484	594
Isidore T2 (sea surface)	5 m	70	93	132	203	240	255	293
	10 m	94	131	199	295	354	383	446
Gordon T3 (sea surface)	5 m	71	116	135	146	170	195	222
	10 m	108	176	223	266	281	330	365
Ivan T1 (open land)	5 m	95	126	145	165	170	182	197
	10 m	115	154	180	205	209	224	240
Ivan T2 (open land)	5 m	88	105	134	134	161	213	314
	10 m	102	123	154	162	186	282	366
Lili T3 (open land)	5 m	67	82	95	107	122	147	189
	10 m	79	94	116	134	151	182	226

Table 4: Spectral models for the neutral non-hurricane atmospheric surface layer

Formula	Author(s)	Notes
$\frac{nS_{uu}(n)}{u_*^2} = \frac{200f}{(1+50f)^{5/3}}$	Kaimal et al., 1972, corrected for low frequency *	$u$ -component
$\frac{nS_{uu}(n)}{u_*^2} = \frac{252.6f}{(1+60.62f)^{5/3}}$	Tieleman, 1995	$u$ -component, blunt model for perturbed terrain
$\frac{nS_{uu}(n)}{u_*^2} = \frac{128.28f}{1+475.09f^{5/3}}$	Tieleman, 1995	$u$ -component, point model for FSU **
$\frac{nS_{vv}(n)}{u_*^2} = \frac{15f}{(1+9.5f)^{5/3}}$	Kaimal et al., 1972	$v$ -component
$\frac{nS_{vv}(n)}{u_*^2} = \frac{53.76f}{(1+20.16f)^{5/3}}$	Tieleman, 1995	$v$ -component, blunt model for perturbed terrain
$\frac{nS_{vv}(n)}{u_*^2} = \frac{27.3f}{1+75.84f^{5/3}}$	Tieleman, 1995	$v$ -component, point model for FSU
$\frac{nS_{ww}(n)}{u_*^2} = \frac{3.36f}{1+10f^{5/3}}$	Lumley and Panofsky, 1964	$w$ -component
$\frac{nS_{ww}(n)}{u_*^2} = \frac{2f}{1+5.3f^{5/3}}$	Kaimal et al., 1972	$w$ -component
$\frac{nS_{ww}(n)}{u_*^2} = \frac{5.13f}{(1+4.92f)^{5/3}}$	Tieleman, 1995	$w$ -component, blunt model for perturbed terrain
$\frac{nS_{ww}(n)}{u_*^2} = \frac{2.604f}{1+7.232f^{5/3}}$	Tieleman, 1995	$w$ -component, point model for FSU

\* Simiu and Scanlan (1996), p. 59. The correction augmented the lower frequency spectral components so that the r.m.s.( $u$ )=2.45  $u_*$ .

\*\* FSU: flat, smooth and uniform terrain.

Table A1. Coefficients of power spectra and co-spectra of hurricane winds at 5 m and 10 m elevations

Spectra/Co-spectra	$p_1$	$p_2$	$p_3$	$q_1$	$q_2$	$q_3$
$S_{uu}$ , 10 m, over land	0.1628	0.001173	6.714E-8	0.08184	4.553E-4	1.674E-6
$S_{vv}$ , 10 m, over land	-0.1262	0.1982	2.392E-5	1.336	0.1577	0.001378
$S_{ww}$ , 10 m, over land	0.0482	0.03648	-1.427E-5	-0.06981	0.08011	0.002837
$C_{uw}$ , 10 m, over land	-0.3493	0.2655	-3.63E-5	4.253	0.6107	0.007725
$S_{uu}$ , 10 m, sea	-24140	18540	1.478	31360	7333	7.328
$S_{vv}$ , 10 m, sea	-0.9672	0.6902	0.002884	0.06322	0.6324	0.006139
$S_{ww}$ , 10 m, sea	0.04932	0.02918	-2.596E-6	-0.2149	0.07535	0.002403
$C_{uw}$ , 10 m, sea	-6064	2918	-4.165	3454	8964	40.44
$S_{uu}$ , 5 m, over land	-4986	4669	0.07119	32850	1602	2.573
$S_{vv}$ , 5 m, over land	-0.513	0.544	6.366E-5	4.388	0.2381	0.001236
$S_{ww}$ , 5 m, over land	0.02433	0.02475	-8.78E-6	-0.01359	0.0348	0.001277
$C_{uw}$ , 5 m, over land	-0.02076	0.01877	-2.838E-5	0.2847	0.02471	6.058E-4
$S_{uu}$ , 5 m, sea	-1.455	0.7739	8.842E-5	1.872	0.2373	4.377E-4
$S_{vv}$ , 5 m, sea	-0.03654	0.0379	5.961E-5	-0.02487	0.03728	1.253E-4
$S_{ww}$ , 5 m, sea	-4257	2652	-1.648	8607	2591	241.2
$C_{uw}$ , 5 m, sea	-0.03534	0.01639	-1.351E-5	0.1077	0.03069	4.39E-4

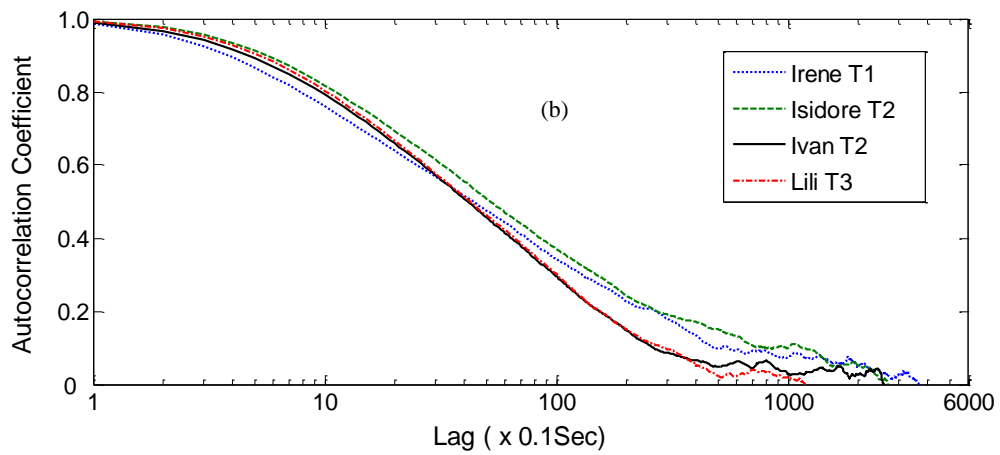
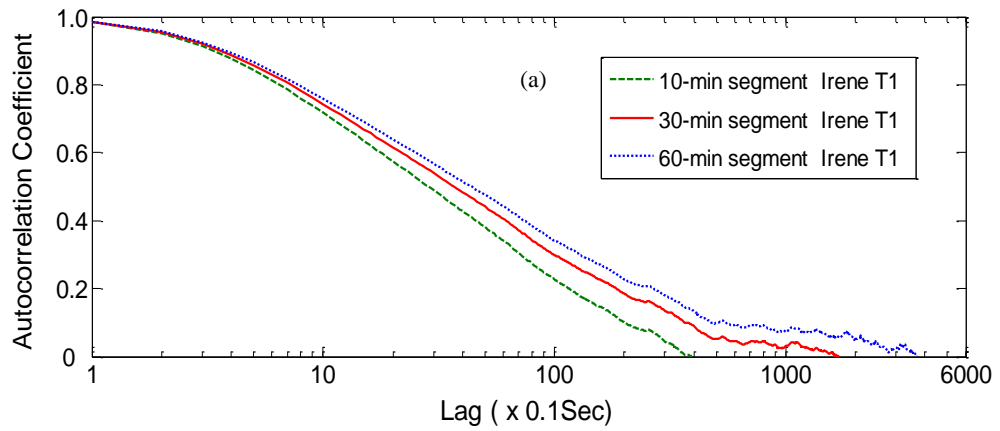


Figure 1. (a) Variation of autocorrelation coefficient with segment length at 10 m elevation for Irene T1; (b) Autocorrelation coefficient based on one-hour wind speed segments at 10 m elevation at four selected FCMP sites

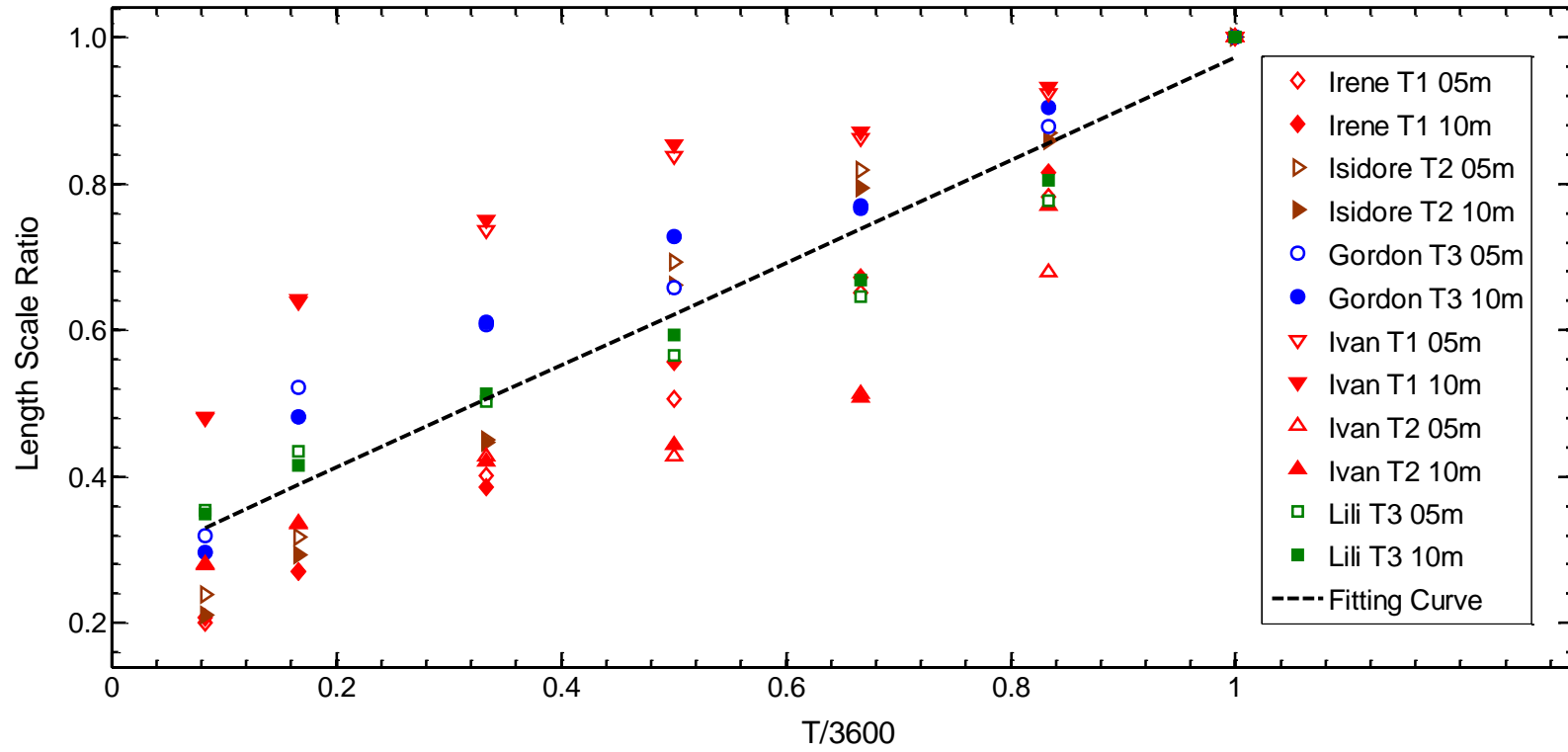
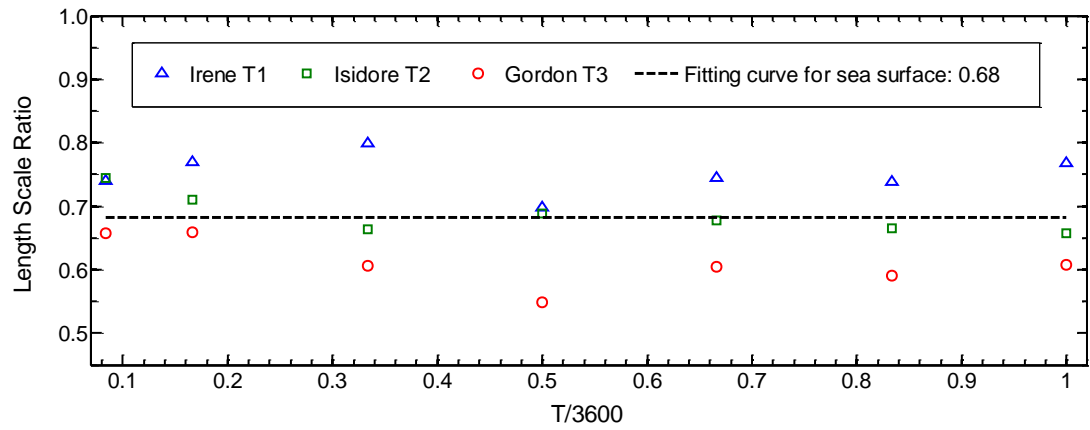
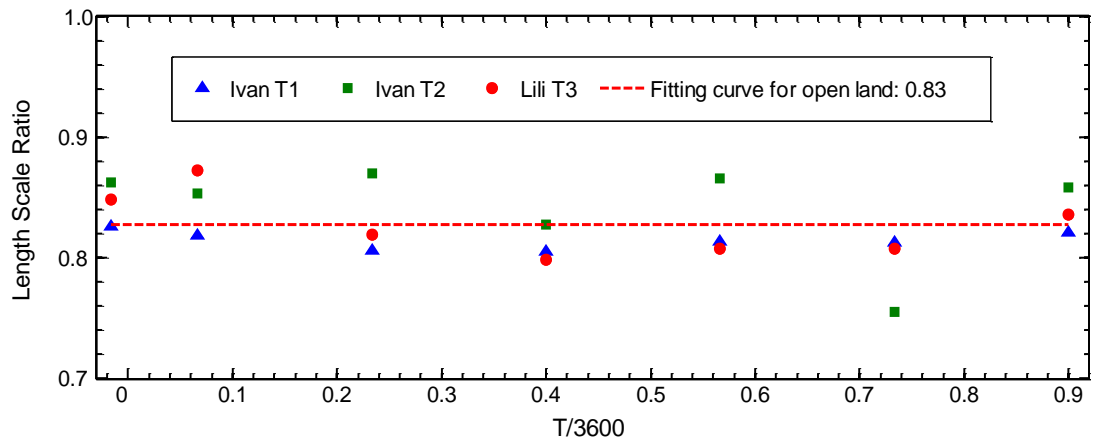


Figure 2. Integral length scale ratios based on different average segment lengths



(a)



(b)

Figure 3. Ratios of the integral length scales at 5 m elevation to those at 10 m elevation

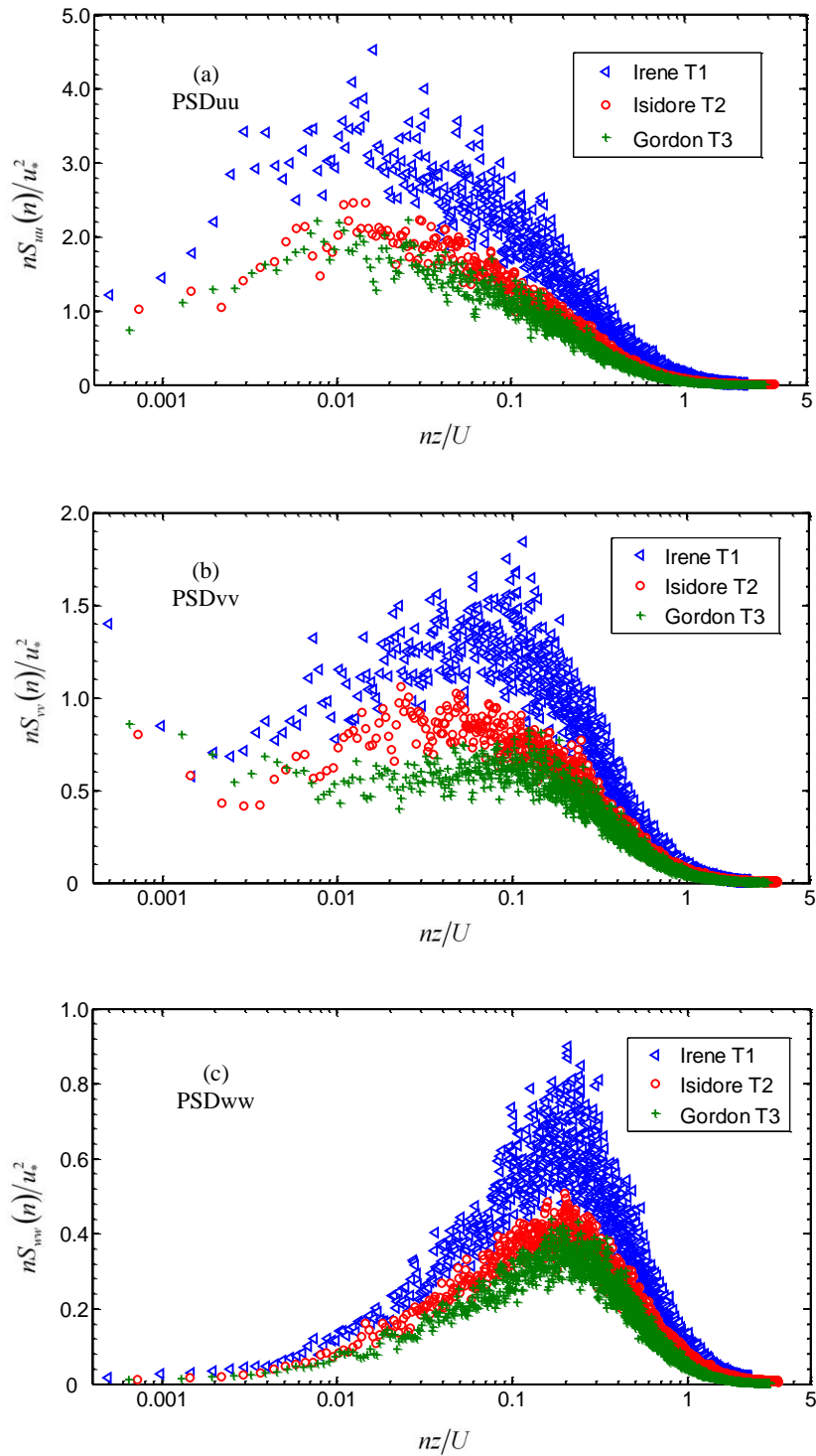


Figure 4. Wind spectra at 10 m elevation over sea surface

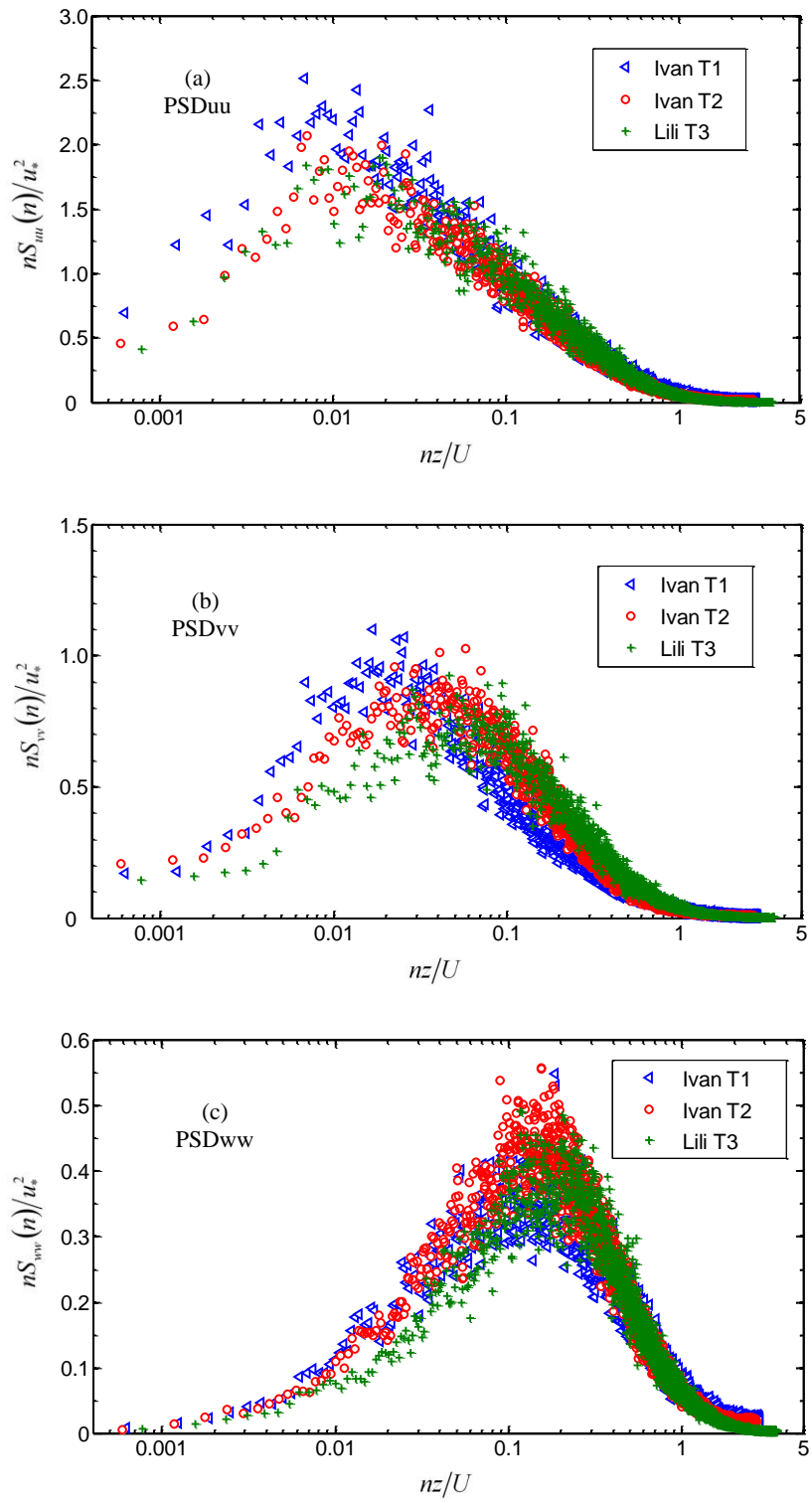


Figure 5. Wind spectra at 10 m elevation over open terrain

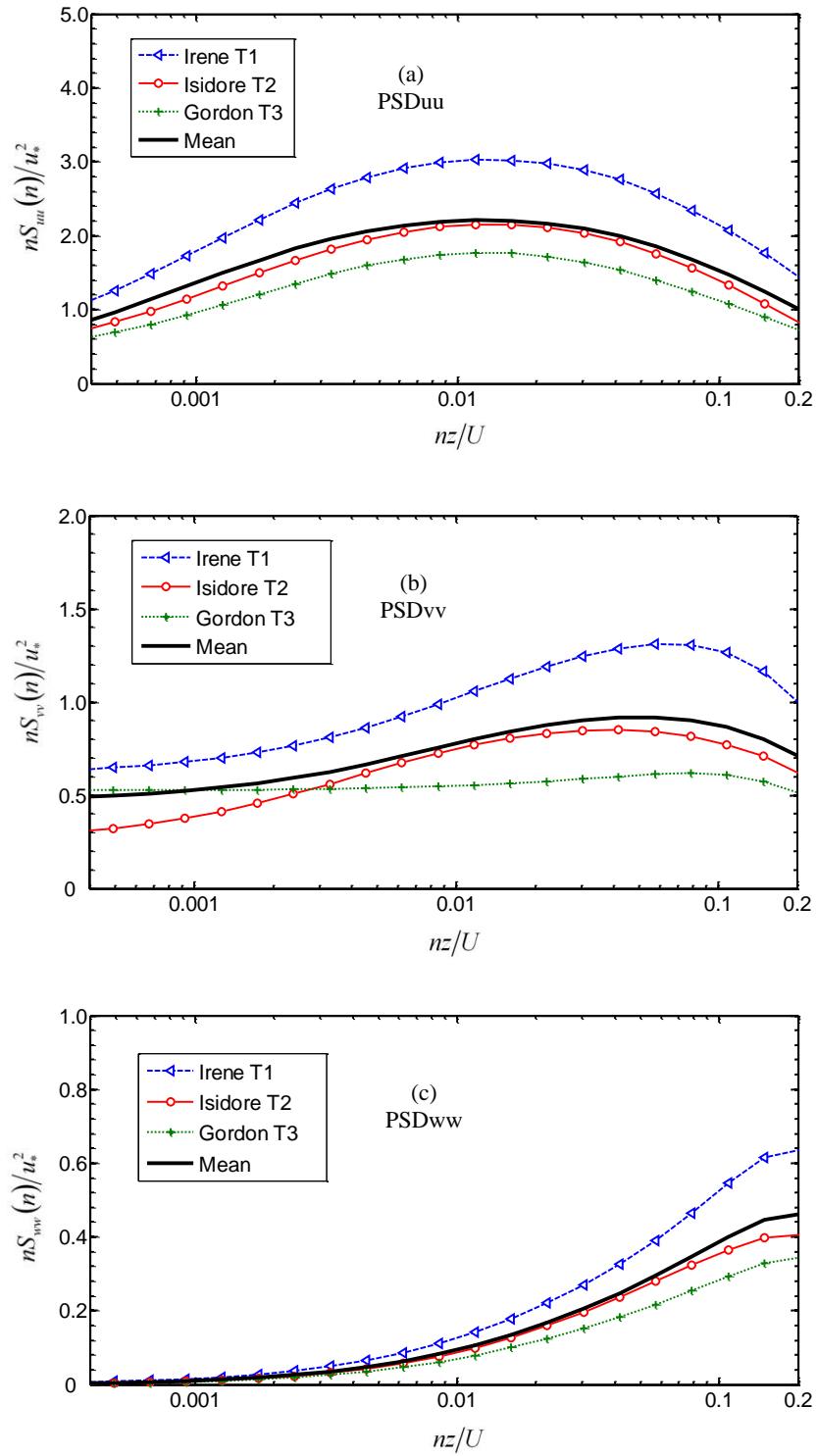


Figure 6. Fitted curves of wind spectra at 10 m elevation over sea surface

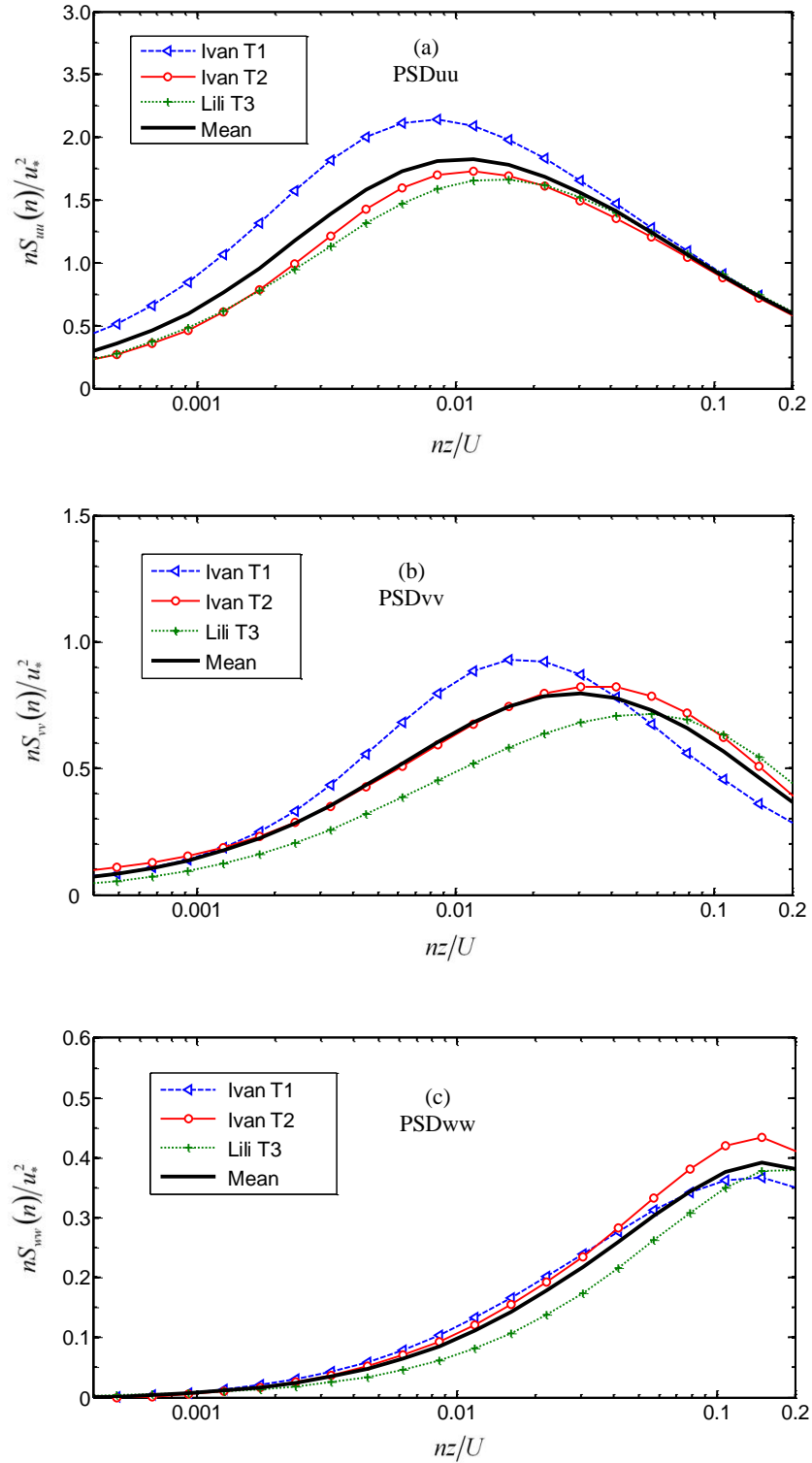


Figure 7. Fitted curves of wind spectra at 10 m elevation over open terrain

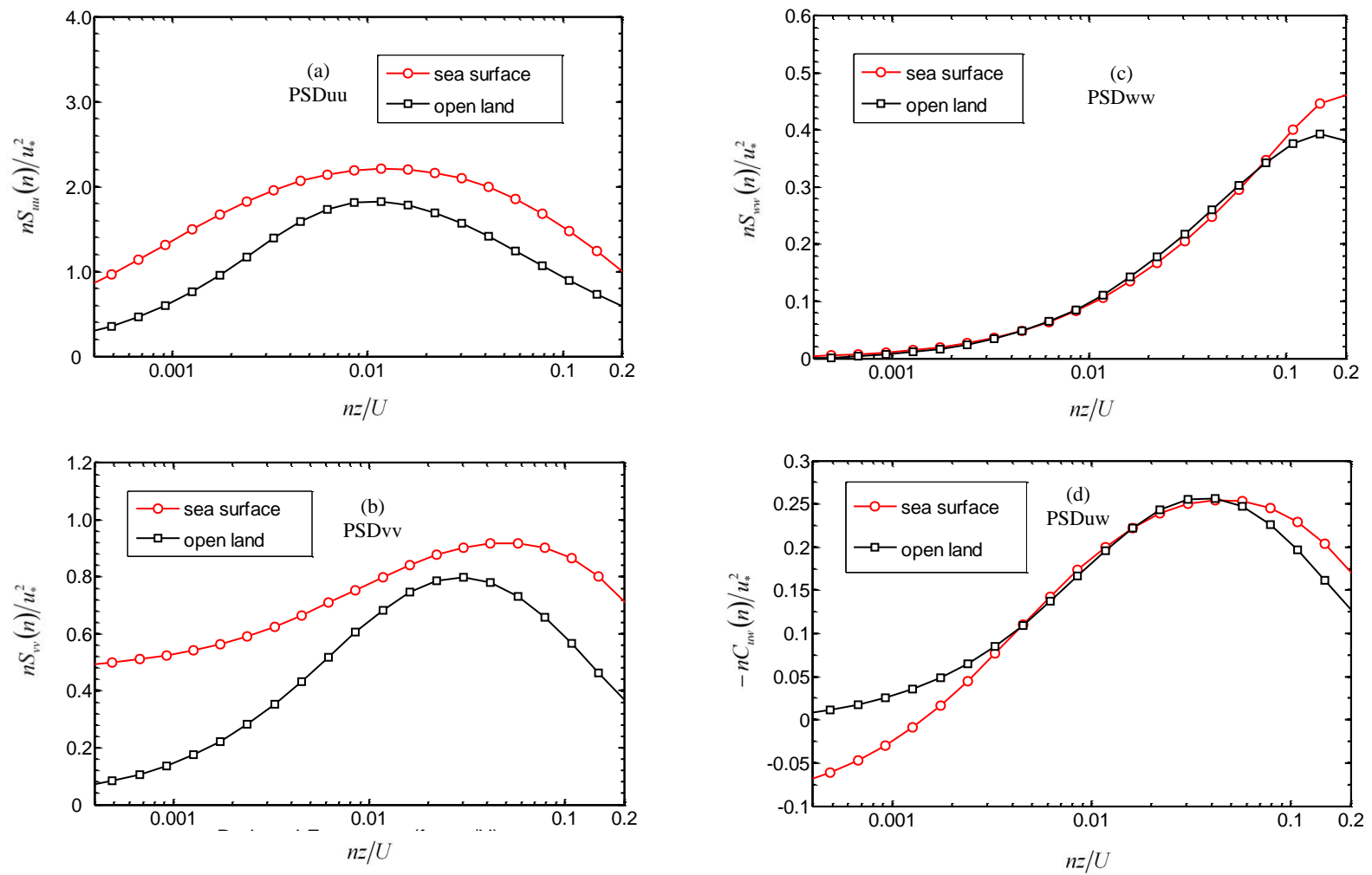


Figure 8. Wind spectra and co-spectra at 10 m elevation for terrains with various surface roughness lengths

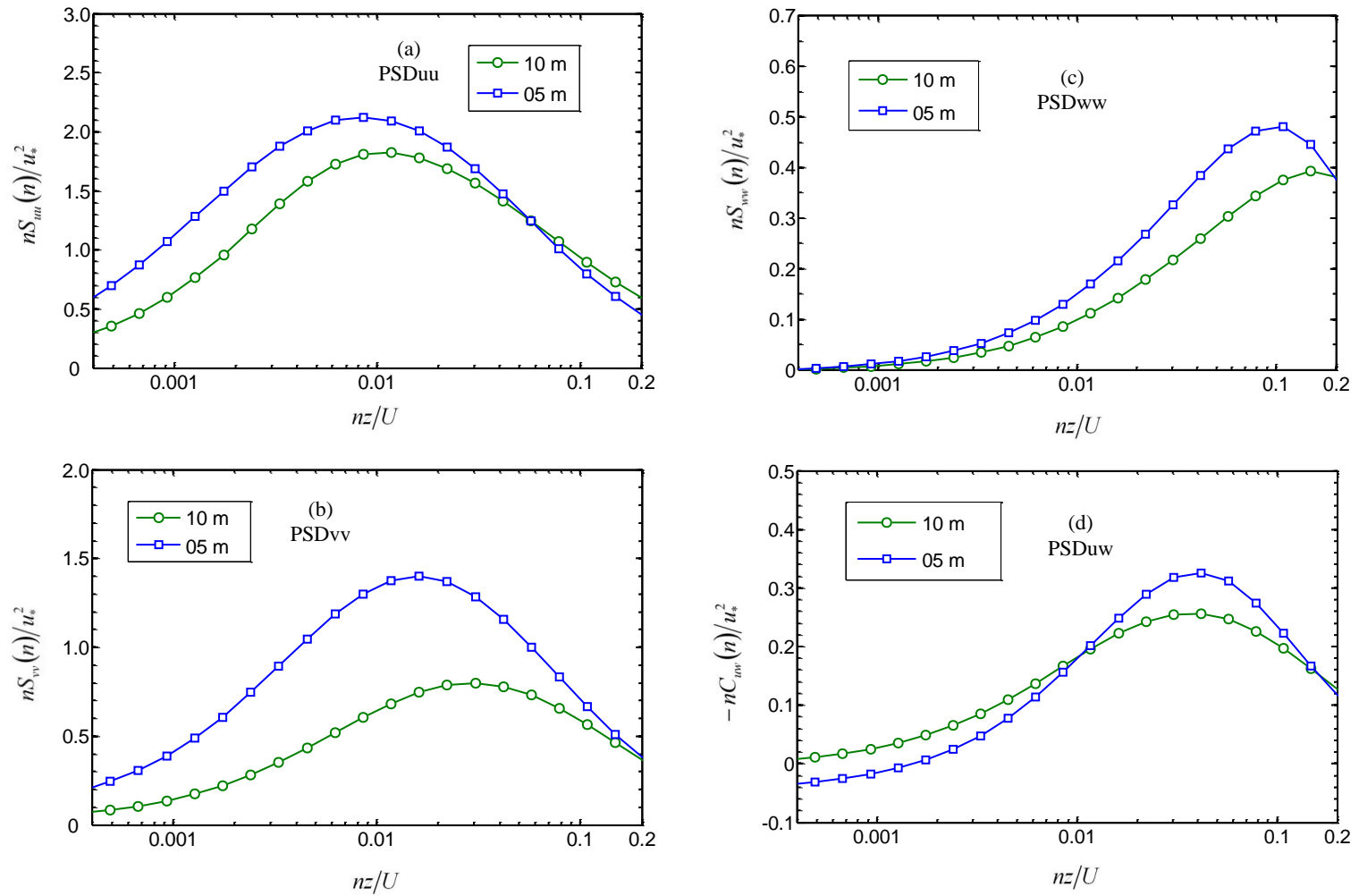


Figure 9. Variation of wind spectra and co-spectra with observational height

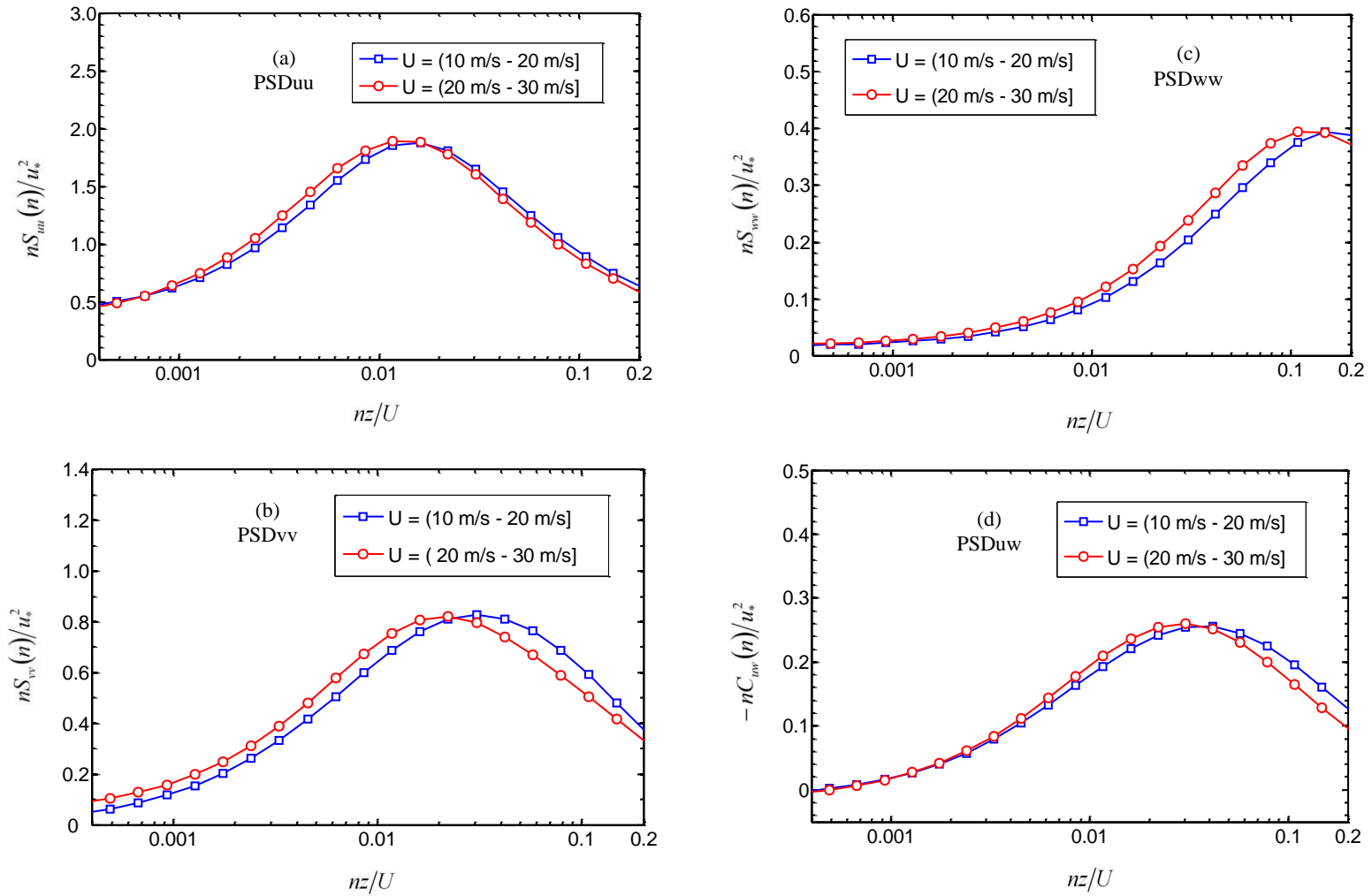


Figure 10. Variation of wind spectra and co-spectra with wind speed at 10 m elevation

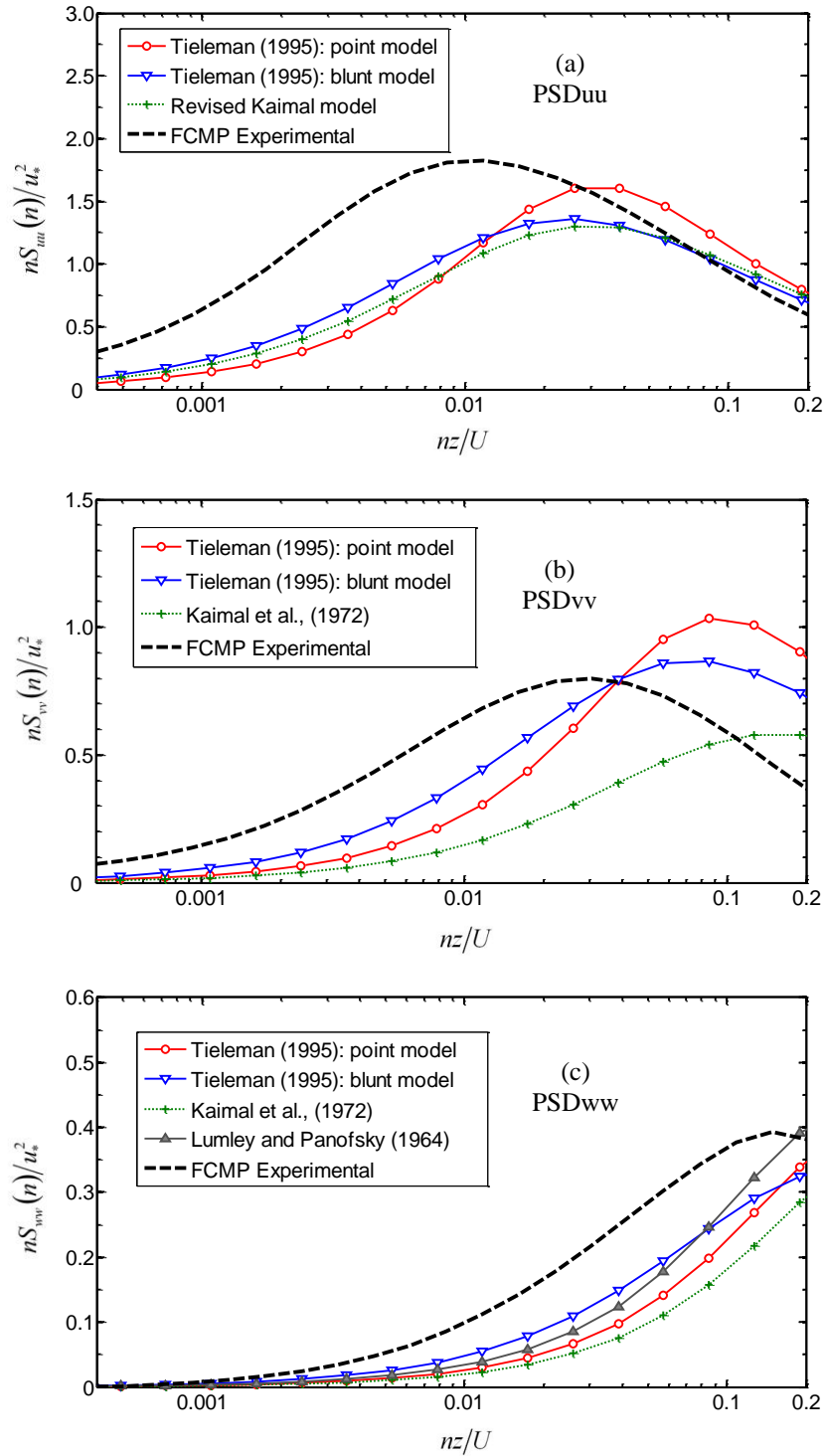
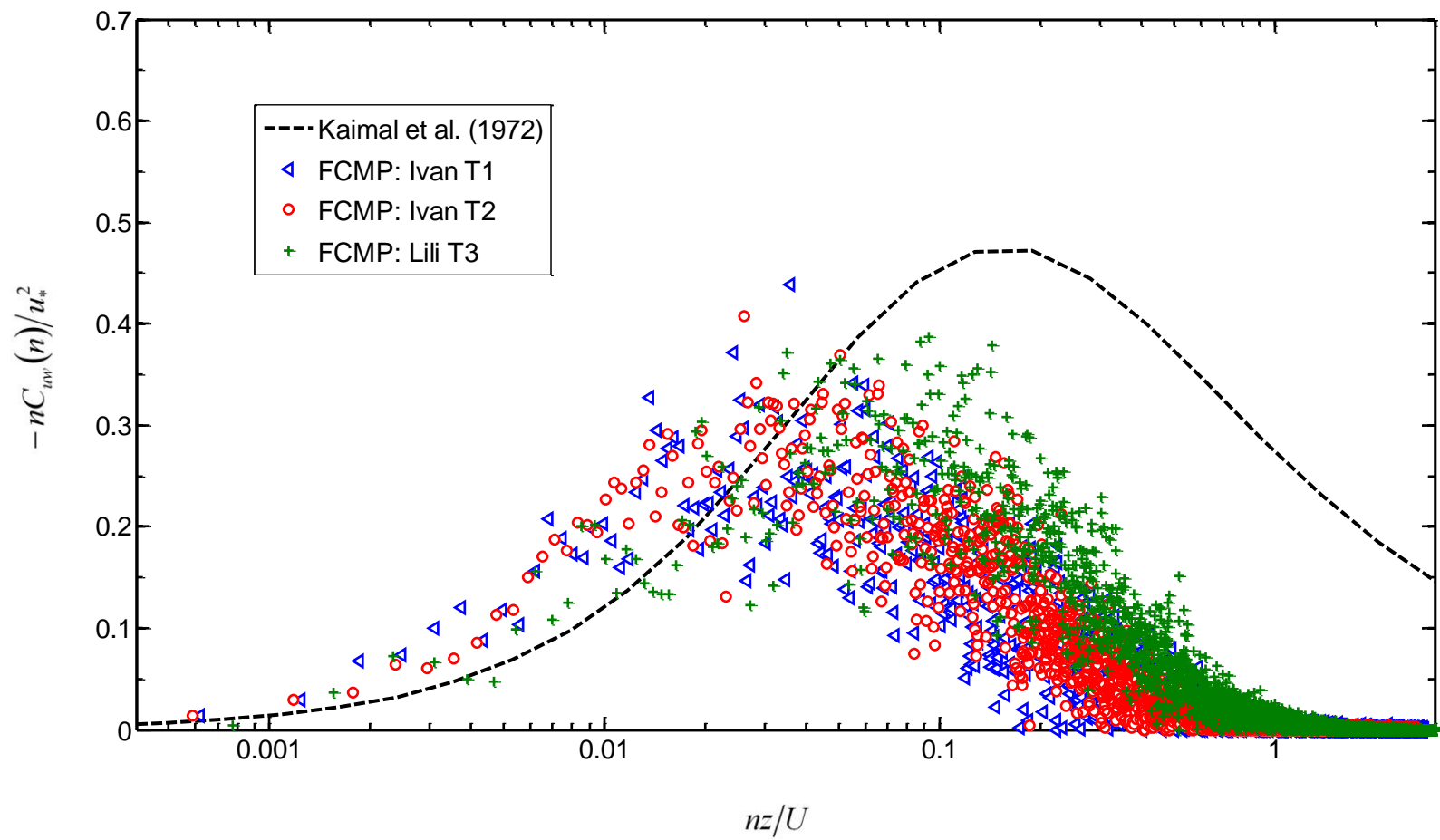


Figure 11. (a) Longitudinal wind spectra estimation and comparison at 10 m elevation; (b) Lateral wind spectra estimation and comparison at 10 m elevation; (c) Vertical wind spectra estimation and comparison at 10 m elevation.

Figure 12.  $u-w$  co-spectra comparison at 10 m elevation

## **V. WALL OF WIND**

### **Abstract**

This chapter presents information on the 6-fan Phase II Wall of Wind (WoW) in its current stage of development, that is, without flow management devices such as grids, flaps, or special fan controls. The objective was to test current wind speed measurement capabilities with a view to applying them at a later stage when flow management devices will be developed for the WoW. This section describes the WoW, the system control as developed at this stage, and the data acquisition system. Measurement results will be presented in a future report, with a view to comparing flows obtained without and with the benefit of flow management devices currently being developed.

### **1. Wall of Wind Facility**

The Wall of Wind (WoW) apparatus, created by the International Hurricane Research Center (IHRC) at Florida International University (FIU), is a new research facility aimed at simulating hurricane wind and rain impinging on low-rise structures at full scale. It allows engineers and scientists to study hurricane-induced effects on buildings, building components, and materials, and help to improve construction methods.

The WoW facility started from the Phase I with a 2-fan prototype and a water injection system simulating the wind-driven rain, which was used to develop and improve larger and more sophisticated testing apparatus. Phase I has successfully tested several structures including light commercial roofs, barrel-tile roofs, Florida Power & Light utilities, and a real house in Sweetwater City of Miami (Figure 1).

The current 6-fan WoW Phase II (Figure 2) is funded by Renaissance Reinsurance (RenaissanceRe) Holdings Ltd., one of the largest global catastrophe re-insurers. Measuring 16 ft tall by 24 ft wide, the WoW Phase II is large enough to engulf a single-story residence. It has been utilized in an evaluation of techniques for the mitigation of wind effects on roofs (Blessing, 2007).

The WoW will be further expanded to Phase III with a 24-fan array located in a large metal building being constructed at the Florida International University Engineering Campus. The Phase III facility will generate up to a Saffir-Simpson Category 5 (Table 1) hurricane-force winds, with rain and flying debris. Two-story testing structures can be mounted on a turntable to study their response to hurricane winds from different directions.

## **2. System Control and Data Acquisition**

This dissertation uses 10 Hz resolution velocity measurements of flow produced by the 6-fan WoW Phase II apparatus. The apparatus consists of a 2 by 3 array of Chevy 502 carburetor engines driving airboat propeller shafts. The propellers increase the air flow through the system. Each engine is mounted in a steel rectangular frame measuring 8 ft by 8 ft, which is connected to an octagonal-shaped diffuser. The diffuser section helps to minimize dead zones in the WoW flow.

The six WoW engines were controlled using LabView software developed by PrimeTest Automation. A Hightech HSR 5995 servo attached to the throttle was used to control the revolution rate for each WoW engine.

For efficient measurement and for safety in strong wind situations, a Unistrut frame was constructed, as shown in Fig. 3. The Unistrut frame was 24 ft wide by 16 ft high and had a depth of 9 ft from the edge of the diffuser section. Four wind monitors were housed on the frame in a square configuration with 8 ft sides and could be moved in 3 dimensions.

The RM Young model 05103V wind monitor measured the WoW-produced winds. The wind speed sensor is a four blade helicoid propeller. Propeller rotation produces an AC sine wave voltage signal with frequency directly proportional to the wind speed. The wind monitor records wind speed and direction with a range of 1-100 m/s (2.24 to 224 mph) and 0 - 360 °, respectively. All wind monitors were wired to the LabView data acquisition system for data collection.

To study the WoW-produced wind characteristics and turbulence structure and their variability, the experiment in this study consisted of two different runs (named Run I and Run II). Wind measurements were taken with engines running at 3000 rpm and 3600 rpm.

For *Run I*, all engines ran at 3000 rpm. The lower two wind monitors and upper two wind monitors were at 2 ft and 10 ft elevation, respectively. The wind monitor located in the middle of the WoW flow with 10 ft elevation was named WM 1. The wind monitor located at 10 ft elevation with a distance of 8 ft from the middle of the WoW flow was named WM 2. The wind monitor located in the middle of the WoW flow with 2 ft elevation was named WM 3. The wind monitor located at 2 ft elevation with a distance of 8 ft from the middle of the WoW flow was named WM 4, as shown in Fig. 4.

For *Run II*, the Unistrut frame was moved 4 ft higher than Run I and all engines ran at 3000 rpm. The lower two wind monitors and upper two wind monitors were located at

6 ft and 14 ft elevation, respectively. Two upper wind monitors at 14 ft elevation were named WM 1' and WM 2'. The WM 1' was placed in the middle of the WoW flow and the WoW 2' was placed at 8 ft away from the middle of the WoW flow. Two lower wind monitors at 6 ft elevation were named WM 3' and WM 4'. The WM 3' was placed in the middle of the WoW flow and the WM 4' was placed at 8 ft away from the middle of the WoW flow, as shown in Fig. 4.

Each run was processed as a 601 seconds record consisting of 6010 data points. The runs are summarized below: *Run I*: Engines ran at 3000 rpm, bottom two WMs at 2 ft elevation, upper two WMs at 10 ft elevation; *Run II*: Engines ran at 3000 rpm, bottom two WMs at 6 ft elevation, upper two WMs at 14 ft elevation;

Only horizontal winds (the longitudinal and the lateral wind components) were measured by the wind monitors (WM). Future WoW wind measurement systems will measure horizontal wind speeds and directions, and vertical wind speeds at various heights.

### **3. Program Development and Example**

A MATLAB program has been developed and tested to systematically analyze Wall of Wind (WoW) data, which will make it possible to perform analyses of baseline characteristics of flow obtained in the WoW. This program can be used in future research to compare WoW data with FCMP data, as gust and turbulence generator systems and other flow management devices will be used to create WoW flows that match as closely as possible real hurricane wind conditions.

Figure 8 presents normalized longitudinal power spectra as a function of reduced frequency  $f$  at 2 ft and 10 ft elevations. The velocity variance was used to normalize power spectral densities, that is, the normalized longitudinal power spectra is  $nS_{uu}(n)/\sigma_u^2$ . The observational height  $z$  and mean wind speed  $U$  at height  $z$  were used to normalize the frequency  $n$ , that is, the reduced frequency is  $f = nz/U$ .

The values of normalized power spectra are comparable for WoW longitudinal wind components at 2 ft and 10 ft elevation, respectively. Estimated longitudinal power spectra obtained by the WoW were compared to the Tieleman spectrum (Tieleman, 1995) over flat, smooth and uniform (FSU) terrain, as shown in Fig. 5.

#### **4. Conclusions**

A WoW wind field measurement system was successfully put in place and tested for future application to flows created without and with the benefit of flow management devices to be developed in the future. A program has been developed and tested to systematically analyze Wall of Wind (WoW) data. This program can be used in future research to compare WoW data with FCMP data, as gust and turbulence generator systems and other flow management devices will be used to create WoW flows that match as closely as possible real hurricane wind conditions.

## Appendix A. Basic Formulas

### (1) Surface roughness length

The surface roughness length  $z_0$  can be estimated by:

$$z_0 = \exp\left(\ln z - \sqrt{\beta} \cdot \kappa / TI_u\right) \quad (\text{A-1})$$

where  $\kappa = 0.4$  is the von Karman constant;  $\sqrt{\beta} = \sigma_u / u_*$  is the ratio of the standard deviation ( $\sigma_u$ ) of longitudinal wind component to the friction velocity ( $u_*$ );  $TI_u$  is the longitudinal turbulence intensity defined as:

$$TI_u = \sigma_u / U_z \quad (\text{A-2})$$

where  $U_z$  is the longitudinal mean wind speed at the measurement height  $z$ .

The friction velocity  $u_*$  is defined as:

$$u_* = \left( \overline{u'w'^2} + \overline{v'w'^2} \right)^{1/4} \quad (\text{A-3})$$

where  $u'$ ,  $v'$ , and  $w'$  are the longitudinal, lateral, and vertical wind fluctuation components, respectively.

### (2) Drag Coefficient

The drag coefficient,  $C_D$ , is commonly used to describe the aerodynamic properties of wind-terrain interaction. It is defined as

$$C_D = (u_* / u_z)^2 \quad (\text{A-4})$$

The drag coefficient  $C_D$  and surface roughness length  $z_0$  are interchangeable descriptions of surface terrain properties, that is:

$$z_0 = z \exp\left(-\kappa/\sqrt{C_D}\right) \quad (\text{A-5})$$

### (3) Gust Factor

The gust factor for the record of length  $T$  is defined as:

$$GF(T, t) = u_{\max}(T, t)/U(T) \quad (\text{A-6})$$

where  $u_{\max}$  is the maximum value of the wind speeds averaged over the intervals of length  $t$ , and  $U$  is the mean wind speed averaged over the time period  $T$ .

### (4) Turbulence Intensity

The longitudinal, later and vertical turbulence intensities ( $TI_u$ ,  $TI_v$ ,  $TI_w$ ) are defined as:

$$TI_a = \sigma_a/U_z, \quad (a = u, v, w) \quad (\text{A-7})$$

where  $\sigma_u$ ,  $\sigma_v$ ,  $\sigma_w$  are the standard deviation of longitudinal, later, and vertical wind components, respectively.

### (5) Integral Length Scales

The longitudinal and lateral integral length scale are defined by

$$L_a^x = U \int_0^\infty \rho_{aa}(\tau) d\tau, \quad (a = u, v, w) \quad (\text{A-8a})$$

$$L_a^y = V \int_0^\infty \rho_{aa}(\tau) d\tau, \quad (a = u, v, w) \quad (\text{A-8b})$$

$$L_a^z = W \int_0^\infty \rho_{aa}(\tau) d\tau, \quad (a = u, v, w) \quad (\text{A-8c})$$

where  $U$ ,  $V$ ,  $W$  are the mean values of the longitudinal, lateral and vertical wind component, respectively.  $\tau$  is the time lag value in seconds and  $\rho_{aa}$  ( $a = u, v, w$ ) are the autocorrelation coefficient functions of the various wind velocity components. For example, the  $\rho_{uu}$  is defined as

$$\rho_{uu}(\tau) = \frac{E[\{u(t) - U\}\{u(t + \tau) - U\}]}{\sigma_u^2} \quad (\text{A-9})$$

where  $E[\phi(t)]$  is the expected value of the stationary random process  $\{\phi(t)\}$ .

#### (6) Power Spectra and Co-Spectra: Estimation and Variability

For real-valued stationary signals, power spectra and co-spectra functions describe the power distributions of the various fluctuating velocity components in the frequency domain. The power spectral density function,  $S_{aa}$  ( $a = u, v, w$ ), is defined so that the total energy associated with the fluctuating velocity component over the frequency range can be represented by:

$$\sigma_{aa}^2 = \int_0^{\infty} S_{aa}(n) dn, \quad (a = u, v, w) \quad (\text{A-10})$$

where  $n$  is the frequency in Hz.

The power spectral density  $S_{aa}$  can be estimated from the correlation (covariance) function (and vice versa) using a Fourier transform (Bendat and Piersol, 2000), that is:

$$S_{aa}(n) = 2 \int_0^{\infty} R_{aa}(\tau) e^{-i2\pi n\tau} d\tau \quad (\text{A-10})$$

where  $e^{ix} = \cos(x) + i\sin(x)$ ,  $i = \sqrt{-1}$ , and the correlation (covariance) function  $R_{aa}$  is defined as:

$$R_{aa}(\tau) = E[a(t)a(t + \tau)], \quad (a = u, v, w) \quad (\text{A-11})$$

## **Appendix B. Time Histories of the Wind from WoW Experiments**

This appendix contains 10 min time histories of wind speed and wind directions obtained from WoW experiments, as shown in Figs A-1 through A-4.

## **Table Captions**

Table 1. Approximate relationship between wind speeds in ASCE 7 and Saffir-Simpson Hurricane Scale

## **Figure Captions**

Figure 1. Two-fan Wall of Wind test on a Sweetwater home in Miami

Figure 2. Six-fan Wall of Wind

Figure 3. Wind measurement system for WoW

Figure 4. Locations of wind monitors

Figure 5. WoW longitudinal wind spectra

Figure A-1. Wind speeds of WoW Run I

Figure A-2. Wind directions of WoW Run I

Figure A-3. Wind speeds of WoW Run II

Figure A-4. Wind directions of WoW Run II

## References

- Bendat J. S., and Piersol A. G., 2000: Random data analysis and measurement procedures (3rd Edition). John Wiley & Sons.
- Blessing, C. M., 2007. Mitigation of Roof Uplift through Vortex Suppression Techniques, Master thesis, Florida International University.
- Gan Chowdhury, A., Simiu, E., Lin, J., Leatherman, S. P., 2007. Wall Wind FIU, Newsletter of American Association for Wind Engineering, October, 1-6.
- Leatherman, S. P., Gan Chowdhury, A., Robertson, C. J., 2007. Wall of Wind Full-Scale, Destructive Testing of Coastal Houses and Hurricane Damage Mitigation, Journal of Coastal Research, 23 (5), 1211-1217.

Table 1. Approximate relationship between wind speeds in ASCE 7 and Saffir-Simpson Hurricane Scale

Saffir-Simpson Hurricane Category	Sustained wind speed over water <sup>a</sup>		Gust wind speed over water <sup>b</sup>		Gust wind speed over land <sup>c</sup>	
	mph	m/s	mph	m/s	mph	m/s
1	74-95	33.1-42.5	91-116	40.7-51.9	82-108	36.7-48.3
2	96-110	42.6-49.2	117-140	52.0-62.6	109-130	48.4-58.1
3	111-130	49.3-58.1	141-165	62.7-73.8	131-156	58.2-69.7
4	131-155	58.2-69.3	166-195	73.9-87.2	157-191	69.8-85.4
5	>155	>69.3	>195	>87.2	>191	>85.4

<sup>a</sup> 1-minute average wind speed at 33 ft (10 m) above open water.

<sup>b</sup> 3-second gust wind speed at 33 ft (10 m) above open water.

<sup>c</sup> 3-second gust wind speed at 33 ft (10 m) above ground in Exposure Category C.



Figure 1. Two-fan Wall of Wind test on a Sweetwater home in Miami



Figure 2. Six-fan Wall of Wind



Figure 3. Wind measurement system for WoW

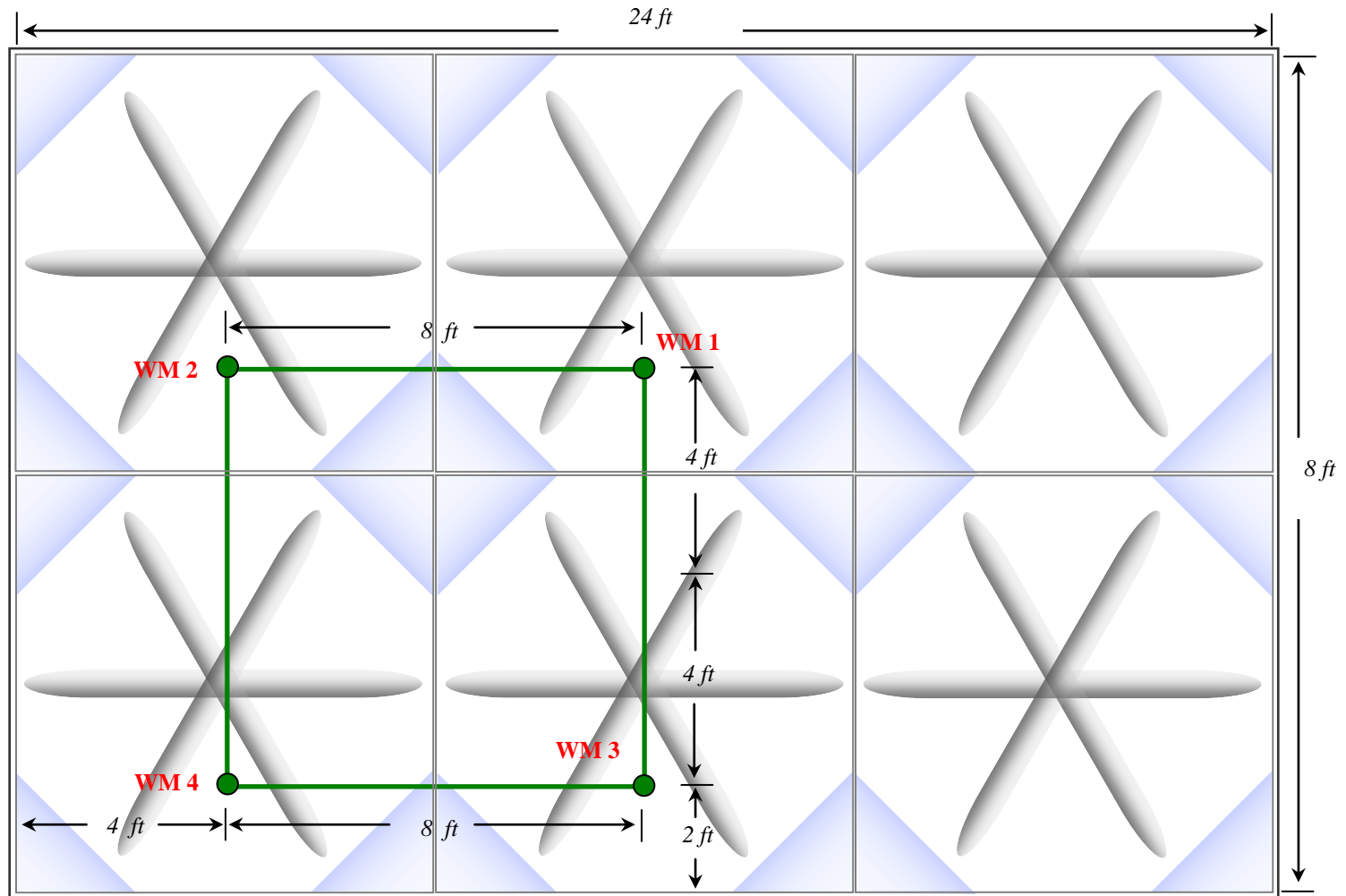


Figure 4. Locations of wind monitors

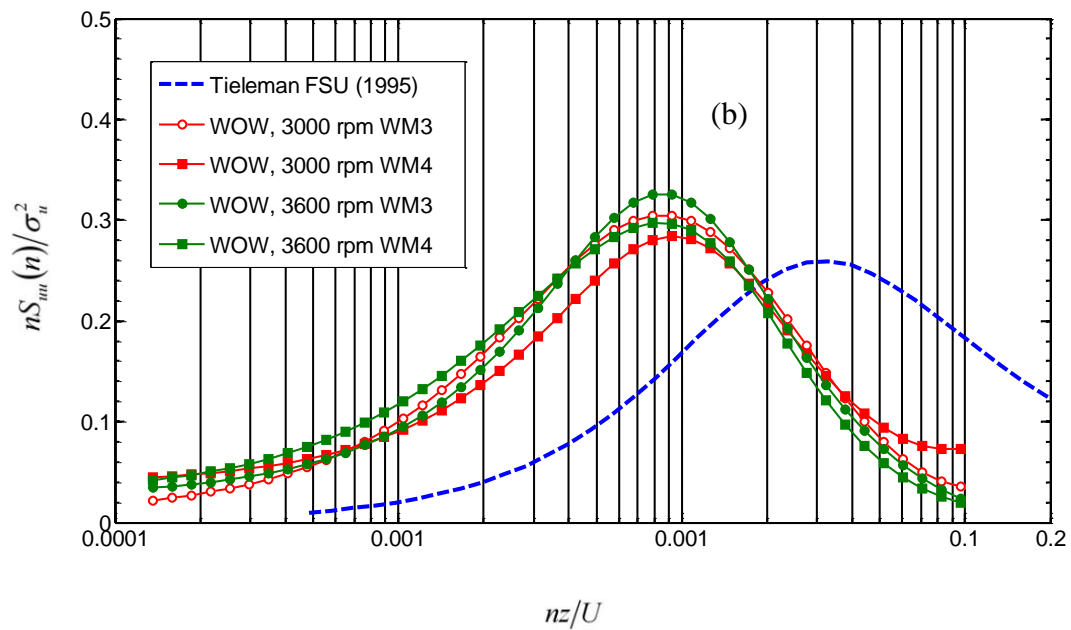
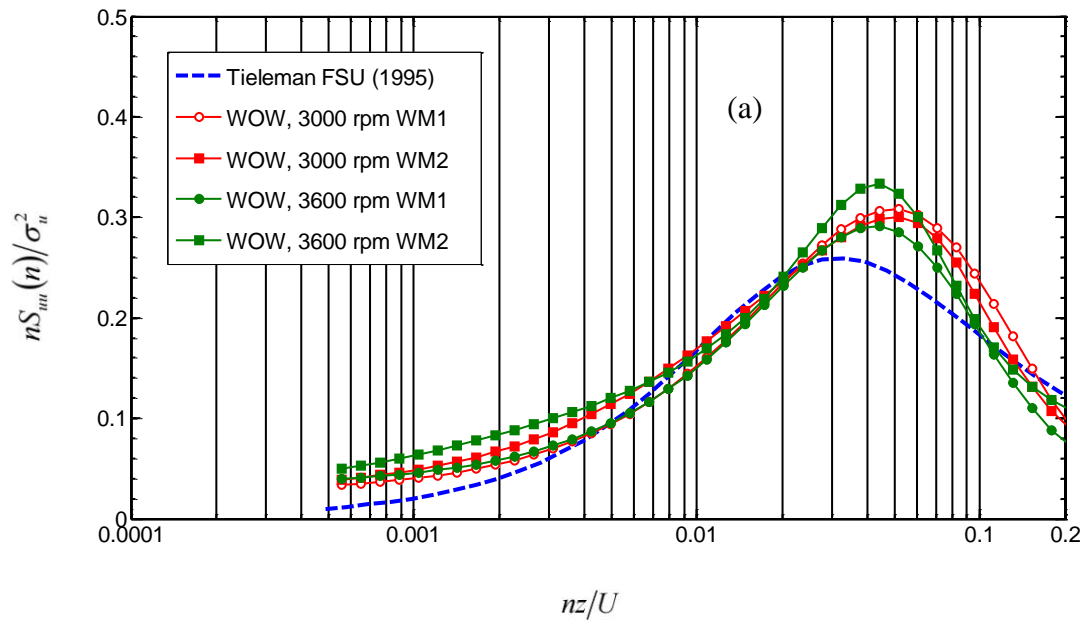


Figure 5. WoW longitudinal wind spectra

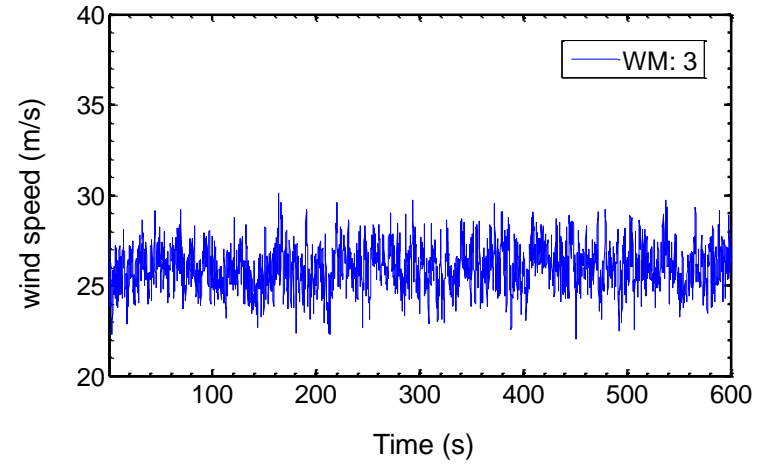
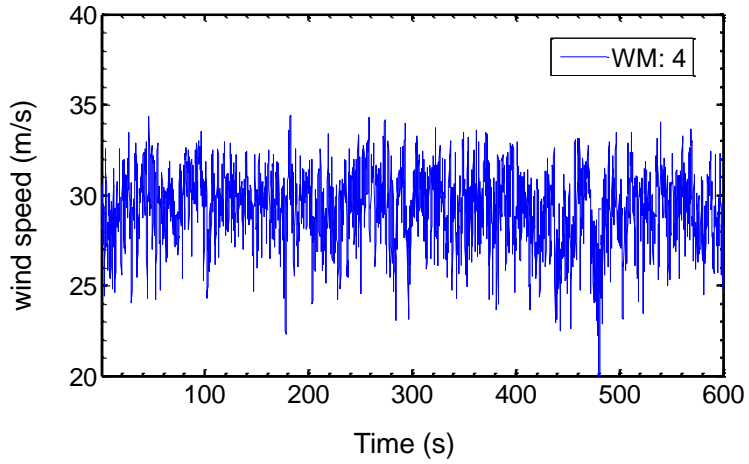
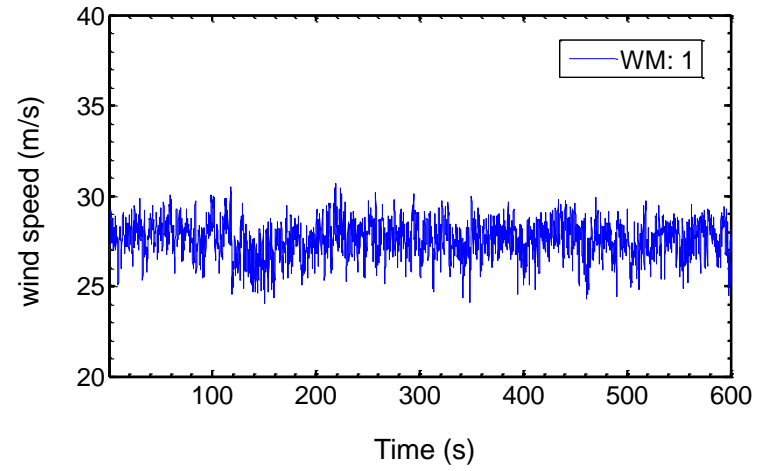
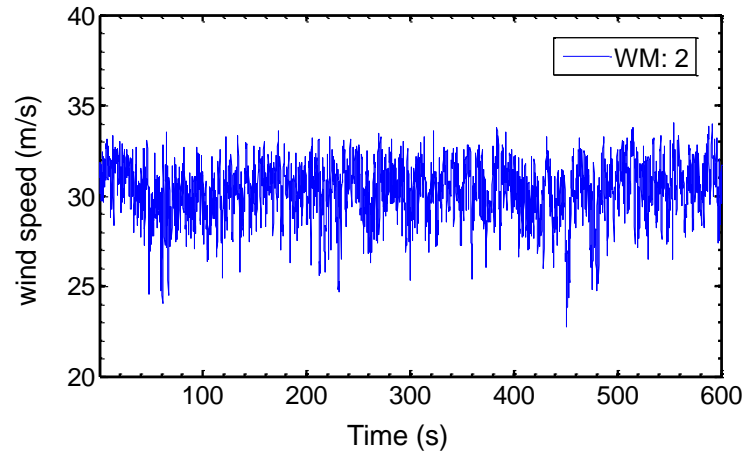


Figure A-1. Wind speeds of WoW Run I (engine revolution rate of 3000 RPM, wind monitor elevation of 2 ft and 10 ft)

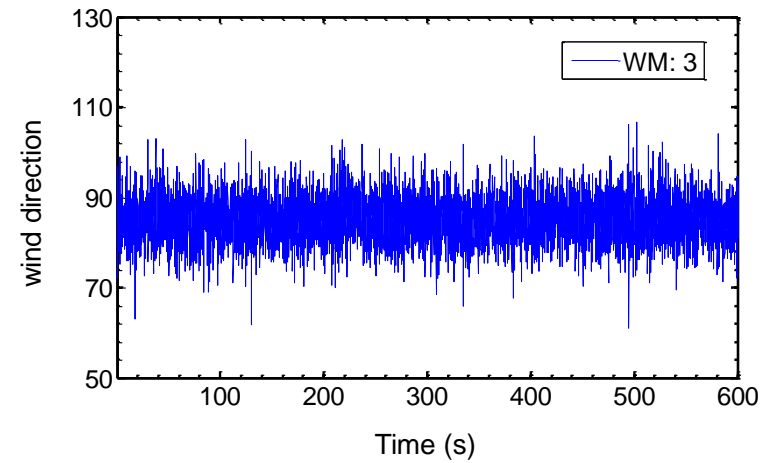
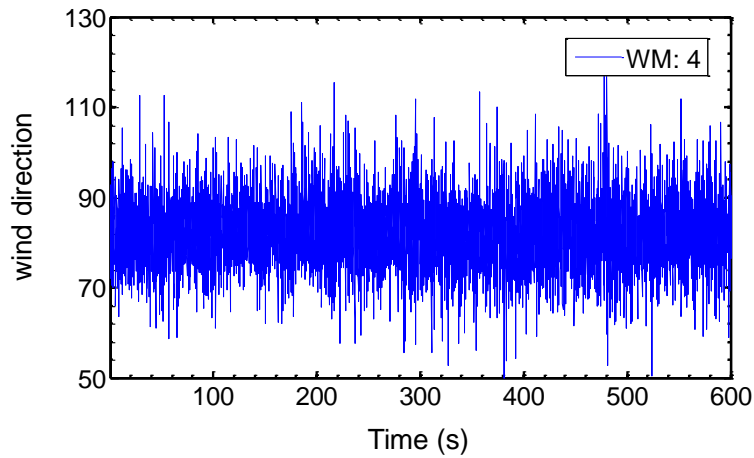
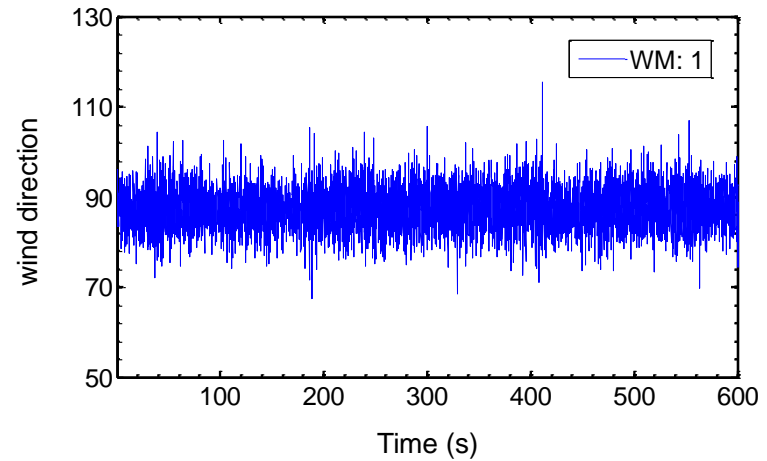
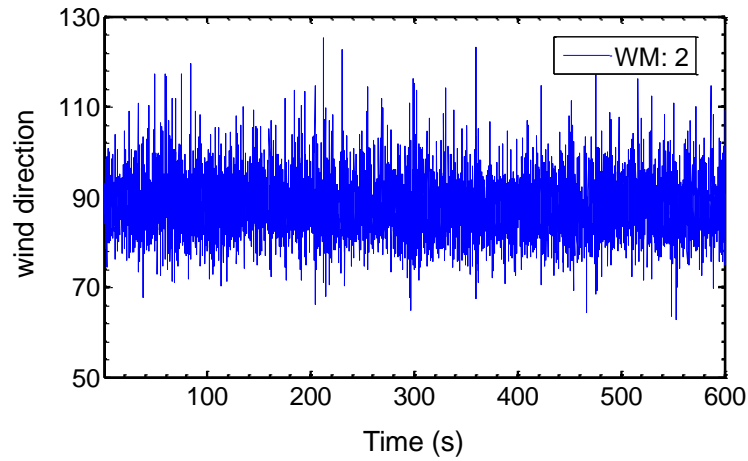


Figure A-2. Wind directions of WoW Run I (engine revolution rate of 3000 RPM, wind monitor elevation of 2 ft and 10 ft)

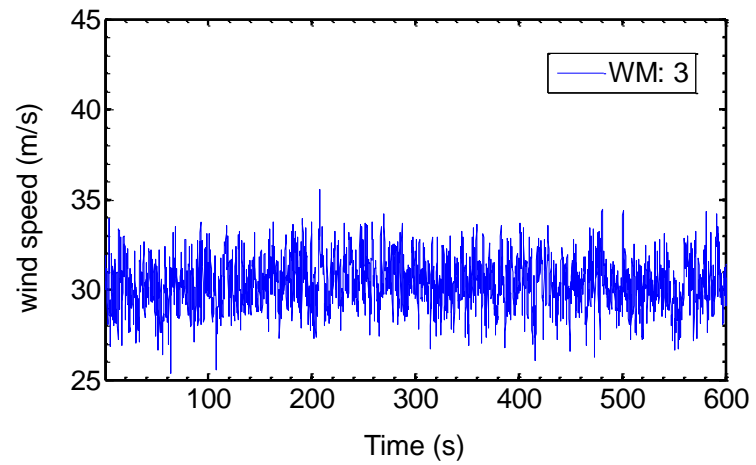
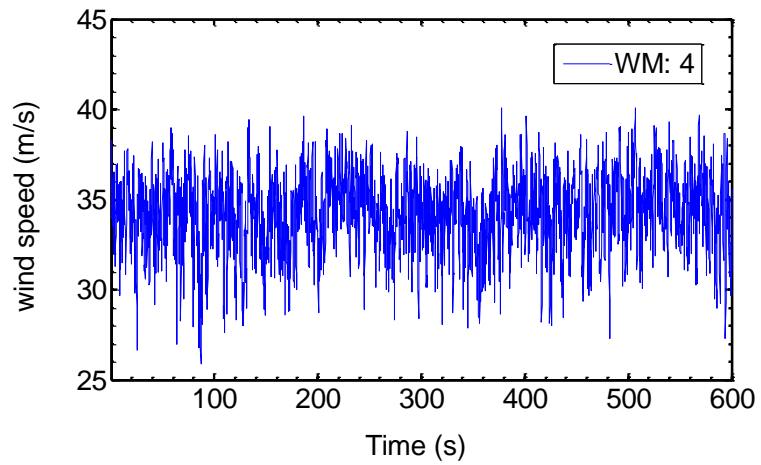
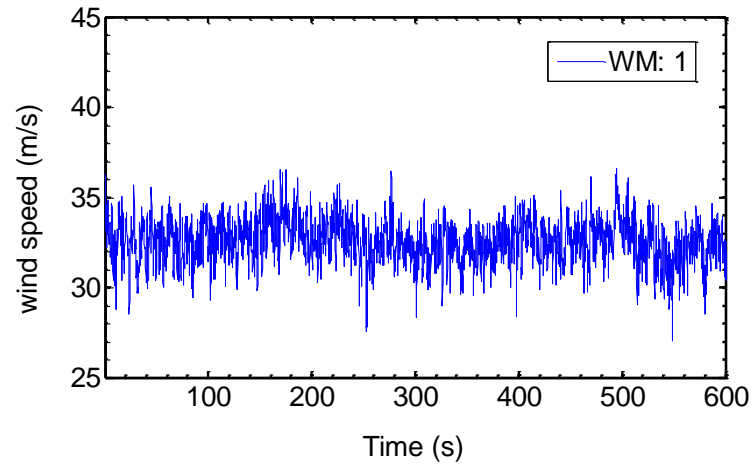
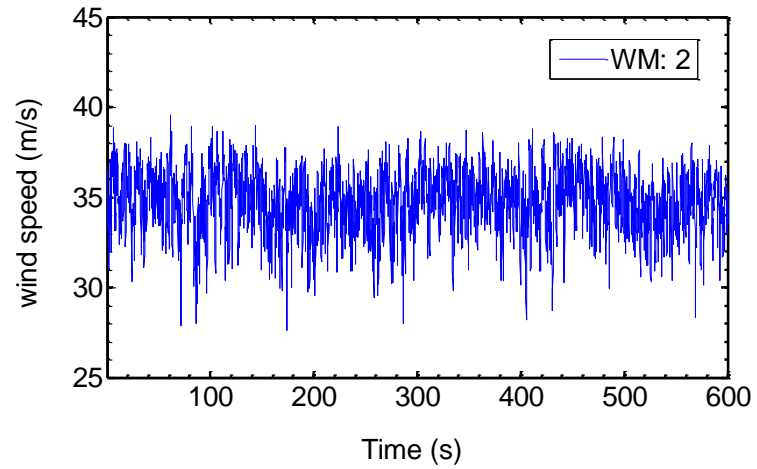


Figure A-3. Wind speeds of WoW Run II (engine revolution rate of 3600 RPM, wind monitor elevation of 2 ft and 10 ft)

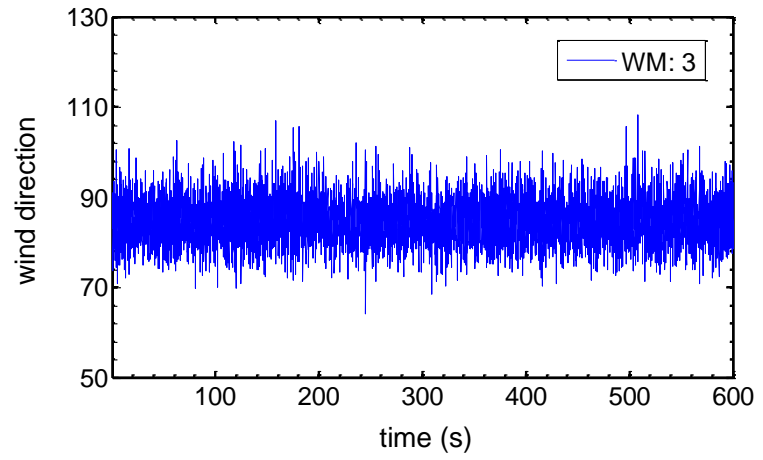
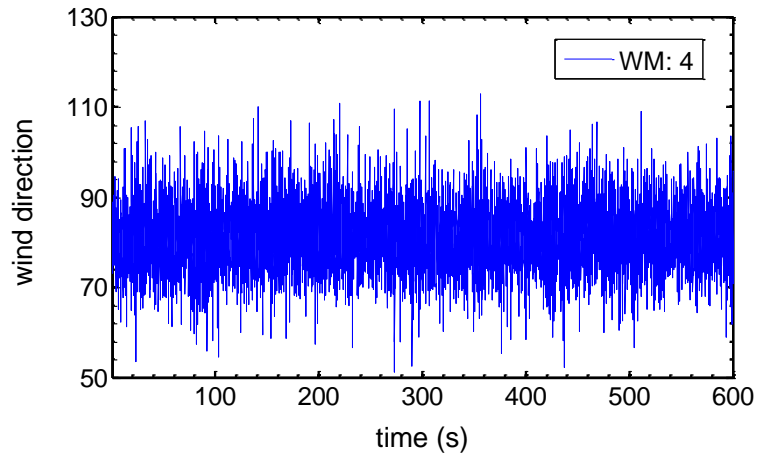
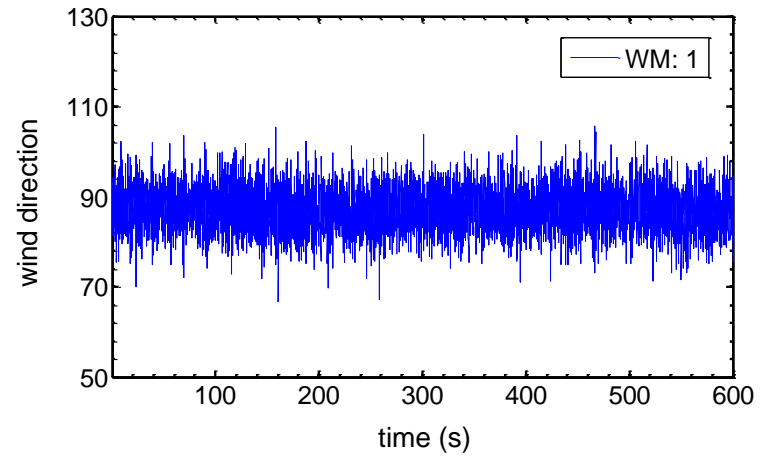
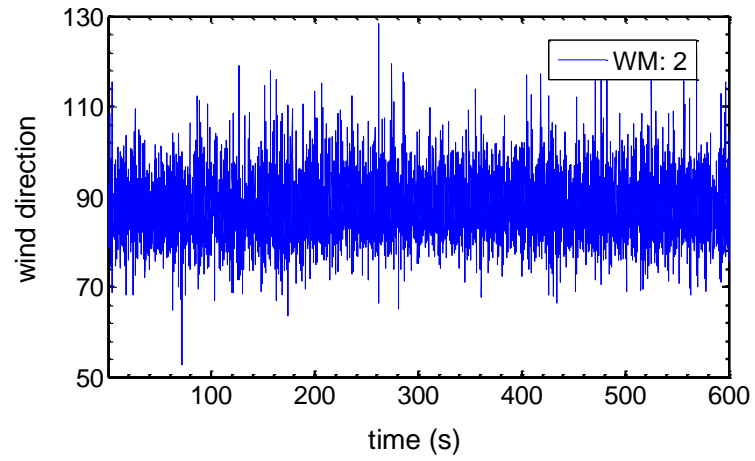


Figure A-4. Wind directions of WoW Run II (engine revolution rate of 3600 RPM, wind monitor elevation of 2 ft and 10 ft)

## VI. GENERAL CONCLUSIONS AND FUTURE WORK

### 1. General Conclusions

Using surface wind measurements collected by FCMP towers during hurricane passages over coastal areas, this study has presented comparisons of various methods for estimating surface roughness lengths for the non-homogenous coastal terrains, as well as estimates of gust factors, turbulence intensity, power spectra and co-spectra, and turbulence integral length scales for hurricane winds over coastal areas under neutral stratification conditions. Limited measurements and analyses of WoW-produced flow in the absence of flow management devices such as grids, flaps, and fan controls have also been presented.

#### (1) Methods for estimating surface roughness lengths

Surface roughness lengths as obtained for directionally non-homogeneous coastal terrains by using the *Turbulence-Intensity* Method and the *Hybrid* Method show good agreement both in magnitude and trend. They yield values of the surface roughness consistent with values obtained for similar roughness conditions in other micrometeorological studies and are therefore judged to be adequate for surface roughness length estimation.

*Friction-Velocity* Method results are comparable to the results obtained from the two above-mentioned methods, except for some higher values resulting from its application to Isabel T2 and Floyd T3. These results suggest that the Friction Velocity Method can experience errors that do not occur in the Turbulence-Intensity Method or the Hybrid Method.

The *Profile* Method results are comparable to the results obtained from other methods (*Turbulence-Intensity* Method, *Hybrid* Method, and *Friction-Velocity* Method) for the airport terrain for Jeanne T3. However, the *Profile* Method yielded unreasonably high values of roughness lengths for Isabel T2 and Floyd T3. This shows the sensitivity of the Profile Method to the quality of measured wind data and that a small wind measurement error may result in a large error in the estimation of the surface roughness length.

Estimates based on the *Gust-Factor* Method were significantly larger than those obtained by the other methods and exhibited wide scatter.

## (2) Gust factors and turbulence intensities for surface hurricane wind flows

For 10 m elevation over open exposure terrain the Durst model yields lower gust factors than those based on the FCMP data for gust durations less than 20 s, and closely matches the estimated gust factor curve for gust durations larger than 20 s.

For open terrain and  $0.008 \text{ m} \leq z_0 \leq 0.03 \text{ m}$ , the Kraye-Marshall (1992) model yields higher gust factors than those based on the FCMP data, particularly for gust durations less than 100 seconds. However, for open terrain and  $0.03 \text{ m} \leq z_0 \leq 0.06 \text{ m}$ , FCMP data yield higher gust factors than those obtained by Kraye-Marshall (1992), particularly for gust durations less than 10 s.

Estimated values of 5 s gust factor associated with hurricane winds based on FCMP data are higher than those associated with non-hurricane winds obtained from eight ASOS stations; for winds over roughness regime of  $0.008 \text{ m} \leq z_0 \leq 0.03 \text{ m}$ , hurricane wind gust factors can be more than 10 % higher than the non-hurricane gust factors.

Higher values of estimated gust factors are obtained for rougher terrain surfaces. Values of gust factors of hurricane winds at 5 m elevation were larger than those at 10 m elevation.

Current US codes standards and codes require the use of 3-s gust factors based on hourly mean wind speeds at 10 m elevation over open terrain. According to Durst (1960), that gust factor is about 1.52 for non-hurricane winds, while according to Krayner and Marshall (1992) it is about 1.66 for hurricane winds. The estimates based on the FCMP data yielded values of about 1.59 for hurricane winds over terrain with surface roughness lengths  $0.008 \text{ m} \leq z_0 \leq 0.03 \text{ m}$ , and 1.69 for hurricane winds over terrain with surface roughness lengths  $0.03 \text{ m} \leq z_0 \leq 0.06 \text{ m}$ . These values are underestimated owing to the properties of the anemometers used in the FMCP measurements. The underestimation was shown to be less than 4 %. The results obtained in this study therefore suggest that 3-s gust factors in the ASCE Standard 7 should be augmented with respect to the current values, obtained by Durst (1960) for non-hurricane winds.

Estimated values of turbulence intensities of longitudinal and vertical wind components increase as the terrain roughness increases. Results showed that  $TI_u > TI_v > TI_w$  for each roughness regime.

### (3) Length scales and power spectra for surface hurricane wind flows

Compared with spectral models proposed by other investigators for non-hurricane winds, the observed normalized power spectra of longitudinal, lateral and vertical hurricane wind components have significantly more energy at the lower frequencies. This result is in agreement with results obtained for one hurricane record by Schroeder and

Smith (2003), and is based on the analysis of six hurricane records, thereby establishing it on a firm basis. For  $u-w$  co-spectra, the observed co-spectral peaks and the corresponding reduced frequency are lower than the values obtained by Kaimal et al. (1972).

Estimates of the power spectra of longitudinal, lateral and vertical wind components over sea surface were higher than those over open terrain, while the  $u-w$  co-spectral values over the two surface regimes were comparable.

Estimates of the power spectra and the co-spectra of hurricane winds at 5 m elevation were larger than those at 10 m elevation, while estimates of power spectra and co-spectra are comparable over different wind speed regimes.

The longitudinal length scales increase with record length and elevation. The longitudinal length scales are lower over open terrain than over sea surface.

For the two three-record sets, the largest ratios of the variance of longitudinal velocity fluctuations to the square of friction velocity  $u_*$  were approximately 1.74 and 1.54 for water surface and open terrain, respectively; variabilities of power spectra were approximately commensurate with these ratios for all turbulent fluctuations. The ratios between largest and smallest estimated values of the integral turbulence scales at 10 m elevation were about 1.6 for both water surface and open terrain.

#### (4) Measurement of WoW winds

A WoW wind field measurement system was successfully put in place and tested for future application to flows created without and with the benefit of flow management devices to be developed in the future.

## **2. Recommendations for Future Research**

Contributions of this study include: comparisons of various methods for estimating surface roughness lengths for the non-homogenous coastal terrains; the characterization of surface hurricane winds; and limited comparisons between WoW flow in the absence of flow management devices such as grids or flaps on the one hand and natural hurricane wind flows on the other.

While the research performed in this work has resulted in new knowledge that will be useful in future efforts to simulate hurricane winds in both numerical studies and in full-scale experimental facilities, future research is required to actually develop flow management devices capable of achieving WoW flows reasonably representative of surface hurricane winds.

VITA

BO YU

June 28, 1974      Born, Jiangxi, China

1996                B.S., Atmospheric Physics & Atmospheric Environment  
Lanzhou University, Lanzhou, China

1996-1999        Graduate Research Assistant, Environmental Quality Assessment &  
Research Center, Lanzhou, China

11/1998            Attended the Seventh China Atmospheric Environment Academic  
Conference, Beijing, China

1998                Excellent Graduate Student, Lanzhou University

1999                M.S., Atmospheric Physics & Atmospheric Environment Lanzhou  
University, Lanzhou, China

1999-2003        Environmental Engineer, China Meteorological Administration  
Beijing, China

10/2000            Deployment of the Meteorological Monitoring Network Servicing  
for China Three Gorges Project, a national project.

07/2002            Field survey of environmental quality in Zhalong Eco-environmental  
Protection Area, an international wetland in Heilongjiang Province,  
Heilongjiang, China

2003-2005        Graduate Research/Teaching Assistant  
Laboratory for Analytical Air Pollution Research  
Department of Civil & Environmental Engineering  
Florida International University, Miami, FL

2005                Student Member of American Society of Civil Engineers

2005-2007        Graduate Research Assistant  
Laboratory for Wind Engineering Research  
International Hurricane Research Center (IHRC), Miami, FL

06/2007            Tower deployment training for Florida Coastal Monitoring Program  
(FCMP) in Gainesville, FL

2007                Associate Member of Sigma Xi - The Scientific Research Honor  
Society of North America